Microfluidic Sensing Platforms for Medicine and Diagnostics

Kiilerich-Pedersen, Katrine; Kledal, Thomas N; Rozlosnik, Noemi

Publication date:
2013

Document Version
Publisher's PDF, also known as Version of record

Microfluidic Sensing Platforms for Medicine and Diagnostics

PhD Thesis
DTU Nanotech
PolyMeDiag Group
April 2013

Supervisors

Noemi Rozlosnik
Thomas N Kledal

Katrine Kiilerich-Pedersen
katk@nanotech.dtu.dk

The frontpage image displays a snapshot of a human cell culture infected with virus.
Cells were immobilized on conductive polymer microelectrodes in a microfluidic system.

PhD Thesis

Microfluidic Sensing Platforms for Medicine and Diagnostics

Typeset using LaTeX

www.nanotech.dtu.dk/polymediag

Abstract

New and emerging infectious diseases pose a growing global challenge for patient diagnosis and treatment, and for public health responses. Biosensors are one of the fastest growing technologies for *in vitro* diagnostics, and the sophisticated microsystems offer exciting opportunities for decentralized clinical applications in medicine and diagnostics. In this PhD project, low cost electrochemical plastic sensors for basic research, diagnosis of viral infections or drug discovery were developed and evaluated.

In the developed biosensor chip, early signs of virus infection in cell culture could be detected electrically using a cell based biosensing platform. The system responded for the infection of human cells within a few hours. This is a highly competitive time frame compared to viral culture, which is still the golden standard for laboratory diagnosis of viral infections.

The biosensing platform was adapted to selectively fish out virions from body fluid by aptamer functionalization. The intact virus particles were captured by immobilized aptamer probes on conductive polymer electrodes, allowing fast and easy electrical detection. The sensor responded rapidly, and showed high sensitivity and specificity. Influenza virus in saliva specimen was detectable within fifteen minutes at a clinically relevant concentration. The device has potential for miniaturization into a cost effective field ready point of care diagnostic system, where the majority of established techniques fail to function outside the specialized laboratory.

Microfluidic cell migration devices, imitating *in vivo* conditions were developed with success, improving the *in vitro* experimental setup for basic research and drug discovery.

Polymer biosensors have reached a new level of maturity, and pathogen detection could benefit from the integration of electrical sensors into low cost plastic microdevices pioneering point of care testing. The presented biosensing platforms have potential for scaling up towards high throughput screening, and are adaptable to other applications in medicine and diagnostics, and other fields.

Resumé

Infektiøse sygdomme udgør en stadig større global udfordring når det kommer til diagnostik, behandling og offentlig sundhedspolitik. Biosensorer er en af de hurtigst voksende teknologier indenfor *in vitro* diagnostik. De sofistikerede mikrosystemer åbner op for spændende decentraliserede kliniske anvendelsesmuligheder i medicin og diagnostik. Billige elektrokemiske plastiksensorer til grundforskning, diagnostik af virusinfektioner og opdagelse af nye lægemidler blev udviklet og evalueret i dette ph.d. projekt.

Med en udviklet biosensor chip kunne tidlige tegn på virusinfektion måles elektrisk i cellekultur. Systemet registrerede en infektion i humane celler indenfor et par timer. Dette er en betydelig tidsbesparelse i forhold til traditionel viruskultur, som stadig er den gyldne standard i laboratoriet til diagnosticering af virusinfektioner.

Biosensorplatformen blev tilpasset til selektivt at fiske intakte viruspartikler fra kropsvæske ved hjælp af overfladefunktionalisering med aptamerer. Viruspartiklerne bandt til aptamer prober, der var immobiliserede på ledende polymerelektroder, og interaktionen kunne hurtigt og let måles elektrisk. Sensoren svarede hurtigt og udviste høj sensitivitet og specificitet. Klinisk relevante koncentrationer af influenzavirus i spytprøver blev påvist indenfor femten minutter. Apparatet kan potentielt udformes til et omkostningseffektivt diagnostisk point of care system til brug i felten - et sted hvor de fleste etablerede teknikker fejler.

Mikrofluide cellemigrationsplatforme - der imiterer *in vivo* forhold - blev udviklet med succes. De kan forbedre den eksperimentelle *in vitro* forsøgsopsætning til grundforskning og opdagelse af nye lægemidler.

Plastic biosensorer har nået et nyt niveau og medicinsk diagnostik kan drage fordel af integrering af elektriske sensorer i billige plastik mikrosystemer til påvisning af patogener, og bane vejen for point of care undersøgelser. De præsenterede platforme kan potentielt masseproduceres og let tilpasses andre opgaver indenfor området.

Preface

This thesis is presented to fulfill the criteria for obtaining a PhD degree from the Technical University of Denmark (DTU). The PhD project was conducted at DTU Nanotech, Department of Micro- and Nanotechnology, from May 2009 until April 2013 and was funded by the Danish Research Council for Technology and Production Sciences and DTU.

The project was supervised by Associate Professor Noemi Rozlosnik, leader of the Polymer Microsystems for Medical Diagnostics (PolyMeDiag) group, DTU Nanotech, and co-supervised by Thomas N. Kledal, Head of Virology at the National Veterinary Institute, DTU.

Thesis contents are based on results described within peer reviewed publications as well as unpublished material.

The reader of this thesis is expected to have basic knowledge within biosensors, cell biology and virology, and have some familiarity with microfluidics.

Acknowledgements

Several people have helped and inspired me during the project for which I would like to express my gratitude.

I would like to thank my supervisors - Noemi Rozlosnik and Thomas Kledal - for leading me through the project, giving me the freedom to follow my own ideas and always having the ability to push me in the right direction.

I would like to acknowledge former and present members of the PolyMeDiag group. It has been a pleasure and I appreciate your constructive criticism, ideas and our discussions - both humorous and serious. A special thanks to PhD student Solène Cherré for helping with virus experiments during my pregnancy.

During my PhD project, I co-supervised master students Dorota Kwasny and Louise Laursen, and bachelor student Maja Knudsen - it has been an inspiring process.

Furthermore, I would like to express my appreciation to colleagues at DTU Nanotech for expert guidance and patience during the years, and for providing an excellent working environment.

Contents

List of Figures

List of Abbreviations

The abbreviations used in this thesis are explained in the following. New abbreviations have only been adopted where they contribute to readability or clarity; otherwise terms commonly found in the literature have been used.

Abbreviation	Description
2D	Two-dimensional
3D	Three-dimensional
AIDS	Acquired Immunodeficiency Syndrome
AFM	Atomic force microscopy
AC	Alternate current
BSA	Bovine serum albumin
CCL2	Chemokine (C-C motif) ligand 2
COC	Cyclic olefin copolymer
CMV	Cytomegalovirus
cpe	Cytopathic effect
DC	Direct current
DMEM	Dulbecco's Modified Eagle's Medium
DNA	Deoxyribonucleic acid
DTU	Danmarks Tekniske Universitet/ Technical University of Denmark
EDC	1-ethyl-3-(3-dimethylaminopropyl)carbodiimide
EDOT	3,4-Ethylenedioxythiophene
EIS	Electrochemical impedance spectroscopy
ELISA	Enzyme linked immunosorbent assay
FBS	Fetal bovine serum
FET	Field effect transistor
HA	Hemagglutinin
HFF	Human foreskin fibroblast
HIV	Human immunodeficiency virus

hpi	hours post infection
ISO	International Organization for Standardization
LAPS	Light addressable potentiometric sensors
LED	Light emitting diodes
MEMS	Micro electro mechanical systems
MES	2-(N-morpholino)ethanesulfonic acid
MOI	Multiplicity of infection
NaBIS	Nano Bio Integrated Systems
NHS	N-hydroxysuccinimide
PBS	Phosphate buffered saline
POC	Point of care
PC	Polycarbonate
PCR	Polymerase chain reaction
PDMS	Poly(dimethylsiloxane)
PEDOT	Poly(3,4-ethylenedioxy thiophene)
PEDOT-OH	Hydroxymethyl PEDOT
PEG-DA	polyethylene diacrylate
pfu	plaque forming units
PIPAAm	Poly(N-isopropylacrylamide)
PMMA	Poly(methyl methacrylate)
PPy	Polypyrrole
PS	Penicillin-streptomycin
R&D	Research and Development
RNA	Ribonucleic acid
RPMI	Roswell Park Memorial Institute
RT-PCR	Reverse transcription PCR
SARS	Severe Acute Respiratory Syndrome
SICM	Scanning ion conductance microscopy
ssDNA	single stranded DNA
TsO	Tosylate
UV	Ultraviolet
VCAM-1	Vascular cell adhesion molecule-1
VLA4	Integrin alpha4beta1 (Very Late Antigen 4)
WHO	World Health Organisation

Chapter 1

Introduction

In modern medicine and diagnostics, interdisciplinarity is becoming increasingly important. This project combined research at the interface between nanotechnology, biology and medicine, which are important and strong scientific fields in Denmark.

With a background in biomedical engineering, a fascination of cellular mechanisms, and experience in microfluidic devices for cell migration studies, I was very determined on exploring the combination of the nano- and polymer technology with electrical sensing techniques to conduct cellular and virological studies. My goal was to improve the understanding of fundamental biological mechanisms and build a foundation for novel and innovative - and immensely useful - detection devices for application in medicine and diagnostics.

The demand in the field of medical diagnostics for simple, cost efficient and disposable devices is growing, among others attributable to infectious disease being an increasing cause of morbidity and mortality worldwide. Current diagnostic techniques are inadequate; labour intensive, expensive, and associated with slow turnaround. Therefore, the main goal of the PhD project was to develop an impedance based sensor for medical diagnostics of viral infections to remedy these shortcomings. Impedance based biosensors have lately been recognized for their high sensitivity, specificity and simplicity, and fast response time. Evidence point at early identification of emerging pathogens as a key to control and confine spread of infectious diseases, hence impedance based biosensors have the potential to become important diagnostic tools with point of care application.

1.1 Outline

The content of this thesis is based on a selection of published and unpublished work performed during the three year period of my PhD studies. Motivation for the project and relevant concepts are covered in Chapters 1 and 2. The core results of the project are presented in manuscripts and papers listed in Section 1.2 and included in Chapter 3

and Chapters 5–7. These chapters are structured with a short introduction to the article, and a concluding remark subsequent to the article. Selected side projects are collected in Chapter 4 and Chapter 8. A review of the project is given in Chapter 9, and the the PhD project is summarized in Chapter 10, with conclusions and outlook.

Chapter 2: Basic Concepts
Short general introduction to relevant background subjects.

Chapter 3: Aptamer Based Biosensor
Electrical detection of intact virus particles.
The work is presented in the form of a publication.

Chapter 4: Nanowire Based Biosensor
Electrical sensing of single cells.
Preliminary results are presented.

Chapter 5: Cell Based Biosensor: Review
Review of cell based biosensors.
The work is presented in the form of a publication.

Chapter 6: Cell Based Biosensor: Detection of Virus
Electrical and visual detection of the immediate cellular response to virus challenge.
The work is presented in the form of a publication.

Chapter 7: Cell Migration in Microfluidic Device
On-chip cell migration assay for studies of leukocyte homing.
The work is presented in the form of a publication.

Chapter 8: Impedimetric Detection of Cell Migration
On-chip cell migration assay for studies of wound healing.
Preliminary results are presented.

Chapter 9: Project Review
Summary of PhD project with objective and goal.

Chapter 10: Conclusion and Perspectives
General conclusion.

1.2 Publications

The following lists summarize the scientific first and co-author work of the PhD study in terms of papers and manuscripts for peer reviewed journals and conference proceedings. Papers and manuscripts have status of either published or accepted.

1.2.1 Manuscripts and Papers for Peer Reviewed Journals

1. **K. Kiilerich-Pedersen**, J. Dapra, S. Cherre and N. Rozlosnik. *High Sensitivity Point-of-Care Device for Direct Virus Diagnostics*, Biosensors and Bioelectronics, accepted, April 2013.

2. G.M. Hjortø, **K. Kiilerich-Pedersen**, D. Selmeczi, T.N. Kledal, and N.B. Larsen. *The human CMV chemokine receptor US28 induces migration of cells on a CX3CL1-presenting surface*, Journal of General Virology, accepted, January 2013.

3. **K. Kiilerich-Pedersen** and N. Rozlosnik. *Cell Based biosensors: Electrical Sensing in Microfluidic Devices*, Diagnostics, 2(4):83-96, 2012.

4. J. Dapra, **K. Kiilerich-Pedersen**, N.O. Christiansen, C.R. Poulsen, and N. Rozlosnik. *Conductive Polymers in Medical Diagnostics*, Nanomedicine in Diagnostics, Science Publishers, Chapter 5, 2012.

5. **K. Kiilerich-Pedersen**, C.R. Poulsen, J. Dapra, N.O. Christiansen, and N. Rozlosnik. *Polymer Based Biosensors for Pathogen Diagnostics*, Environmental Biosensors, InTech, Chapter 9, 2011.

6. **K. Kiilerich-Pedersen**, C.R. Poulsen, T. Jain, and N. Rozlosnik. *Polymer based biosensor for rapid electrochemical detection of virus infection of human cells*, Biosensors and Bioelectronics, 28(1):386-392, 2011.

7. D. Kwasny, **K. Kiilerich-Pedersen**, J.L. Moresco, M. Dimaki, N. Rozlosnik, and W.E. Svendsen. *Microfluidic device to study cell transmigration under physiological shear stress conditions*, Biomedical Microdevices, 13(5):899-907, 2011.

1.2.2 Conferences

1. **K. Kiilerich-Pedersen** and N. Rozlosnik. *All polymer sensor for pathogen detection*, Oral Presentation, AnalytiX2013, Suzhou, China, 2013.

2. **K. Kiilerich-Pedersen**, C.R. Poulsen, T. Jain, and N. Rozlosnik. *Polymer Based Biosensor for Rapid Electrochemical Detection of Virus Infection in Human Cells*, Poster Presentation, CLINAM, Basel, Switzerland, 2012.

3. D. Kwasny, **K. Kiilerich-Pedersen**, J.L. Moresco, M. Dimaki, N. Rozlosnik, and W.E. Svendsen. *Microfluidic device as a novel cell transmigration assay*, Poster Presentation, NanoBioTech Conference, Montreux, Switzerland, 2011.

4. **K. Kiilerich-Hansen**, C.R. Poulsen and N. Rozlosnik. *Polymer Based Biosensor for Rapid Electrochemical Detection of Human Cytomegalovirus Infection in Human Fibroblast Cells*, Poster Presentation, ESF-UB Conference in Biomedicine: Nanomedicine: Reality Now and Soon, San Feliu, Spain, 2010.

5. N. Rozlosnik, **K. Kiilerich-Pedersen**, and J. Dapra. *Advances in Virus detection: Functionalized and Micropaterned Microfluidic Systems*, Poster Presentation, NanoMedicine 2010, Beijing, China, 2010.
6. **K. Kiilerich-Pedersen**, G.M. Hjortø, and T.N. Kledal. *Microfluidic Device for Studies of Haptotactic Cell Migration*, Poster Presentation, COMS, Copenhagen, Denmark, 2009.

Chapter 2

Basic Concepts

This chapter provides a general introduction to the main subjects of this thesis: Impedance based biosensors for medical diagnosis of acute viral disease. Emerging and re-emerging infectious diseases are introduced in Section 2.1 - they are a source of worry to the world population, because they may cause severe illness and death, and can spread very rapidly. Early and precise identification of flourishing pathogens is vital for proper disease management. Section 2.2 introduces the concept of point of care. It is an emerging field within medical diagnostics and disease monitoring, and the technological advancements in the biosensor technology have lately accelerated research and development in point of care. Impedance based biosensors are presented in Section 2.3, followed by a brief description of the microfluidic system employed in this PhD study in Section 2.4. Section 2.5 introduces the biosensors employed in this thesis, and the chapter is wrapped up in Section 2.6 with a concluding remark.

2.1 Emerging Diseases

Millions of people are dying every year from diseases that are well understood, preventable, and treatable [1]. Environmental changes and increased global travel to remote regions of the developing world have exposed people to disease vectors that had not previously been encountered. Remote regions with inadequate healthcare are not equipped to handle diseases that are well known and preventable in other parts of the world, and the developed world is not immune to the diseases endemic to these remote regions. Therefore disease diagnosis, treatment and surveillance in the developing countries is of worldwide public health interest. Diagnosis of infectious disease currently requires extensive laboratory facilities, leaving many people undiagnosed in developing areas of the world.

Emerging and re-emerging diseases, combined with the rapid spread of pathogens resistant to antibiotics and of disease-carrying insects resistant to insecticides are a daunting challenge to human health.

Studies show that pandemics of new strains of influenza and other emerging diseases are travelling faster and wider than ever before owing to the global travel and trade [2]. Novel diseases such as Ebola, Severe Acute Respiratory Syndrome (SARS), HIV/AIDS, and hepatitis C are still incurable. They represent a significant cause of suffering and death, and impose an enormous financial burden on society. Some older diseases have been effectively controlled by vaccination programs and antibiotics, whereas well known diseases such as malaria and tuberculosis are re-emerging in antimicrobial resistant forms [2]. Figure 2.1 provides a global overview of emerging and re-emerging infectious diseases.

Pathogens are ubiquitous in the human environment and can cause disease in humans and animals. Viruses are a unique class of infectious agents which are extremely small, contain only one type of nucleic acid and have an absolute dependence on living cells for replication. Due to the limited genomic composition, viruses need host cell organelles, enzymes and other macromolecules for multiplication - and the effects of multiplication range from minor changes in the metabolism to cytolysis. Like other pathogens, virus populations continually evolve. As an example, influenza virus is a segmented RNA virus, hence new subtypes emerge periodically as a result of point mutations and genetic reassortment [3]. Some new strains are harmless whereas others can be highly pathogenic to humans and animals, therefore influenza will continue to be a major concern around the globe.

The most common tools applied for pathogen detection are polymerase chain reaction, cell culture and immunology based assays. These methods are well established and characterized by high sensitivity and specificity, and in particular yield robust results when used in

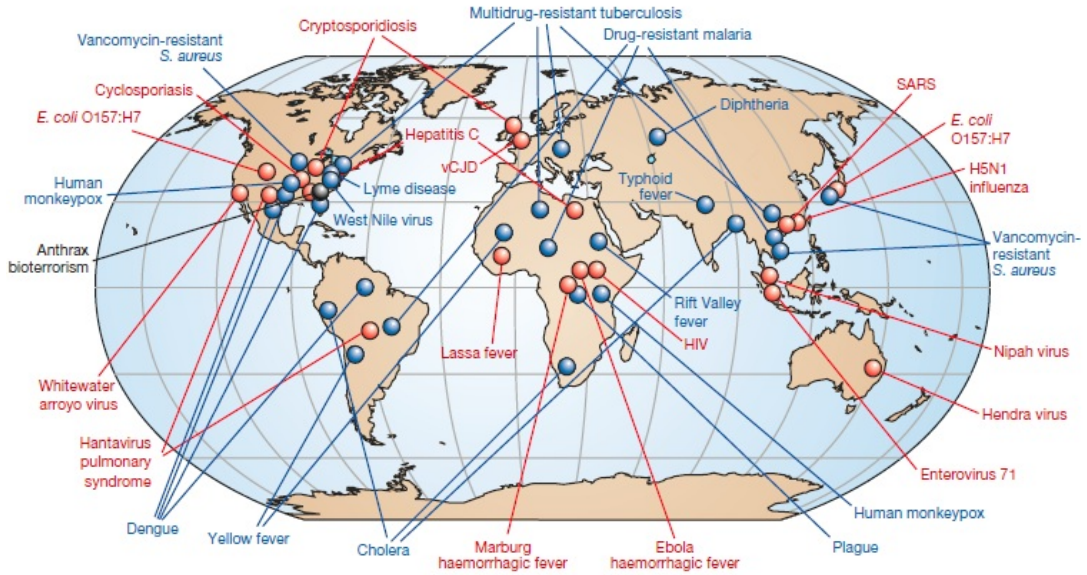

Figure 2.1: Global examples of emerging (red) and re-emerging (blue) infectious diseases. Adapted from [1].

combination [4]. Despite these qualities, the conventional techniques are labour intensive, expensive and associated with long turnover times. This is clearly insufficient, and efforts are being made in the development of new advanced tools for pathogen detection.

2.2 Point of Care

Point of care diagnostic systems are miniaturized devices designed to be inexpensive, portable, and field ready with high sensitivity and specificity. The concept of point of care testing was first introduced in the 1960's with urine sample analysis and glucose testing.

The new generation of point of care systems combines convenience and fast turnaround time with the reliability of laboratory testing, further driving the course towards patient side testing. The trend towards point of care diagnostics is an evolutionary change, where the decentralization of laboratory testing is an extension of the current laboratory services. Point of care systems could prevent unnecessary delays in critical therapeutic decisions, or provide more convenient patient management methods for both the healthcare provider and patient.

These systems could revolutionize healthcare in developing countries where the need for small and low cost medical solutions is ever increasing, and potentially reach populations in remote regions of the world where lack of infrastructure until now has hindered diagnosis and analysis of emerging infectious diseases.

2.3 Electrochemical Biosensors

Biosensors are analytical devices based on biological recognition elements, allowing for the development of point of care diagnostic tools by integrating them into closed microfluidic systems. The working principle of a biosensor is illustrated in Figure 2.2. Many different combinations of biological probes and transducing technologies have been developed and demonstrated throughout the years.

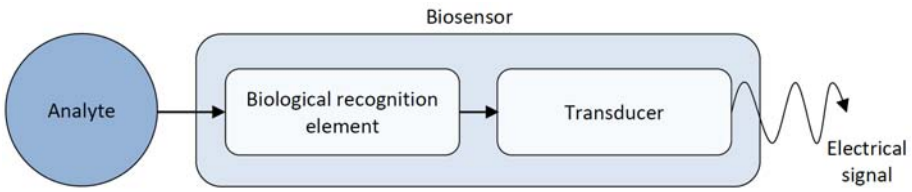

Figure 2.2: Schematic representation of a biosensor with the different components; analyte, biological recognition element, transducer, and the electrical signal originating from the biorecognition event.

Electrochemical biosensors constitute a large group of sensors transforming a chemical reaction or process into an electrical signal. Impedimetric biosensors belong to this class, and they have recently attracted attention for the high sensitivity, reliability and simplicity [5–10]. Moreover, impedimetric sensors are user friendly, cost effective and in many cases disposable, hence suitable for portable point of care systems. Miniaturization of electrochemical instrumentation to small pocket size devices has played an important role in the transition towards simplified testing for home usage.

2.3.1 Impedimetric Biosensors

Electrochemical impedance spectroscopy is a powerful tool for label free analysis of interfacial phenomena, providing detailed information on the changes in capacitance and resistance originating from biorecognition events at conductive surfaces. The impedance of a system is measured in real time by applying a small amplitude alternate current electric field, and the phase difference of the concomitant electrical potential that develops across it is measured. Since the impedance readout is an electrical signal, the risk of misinterpreting results is eliminated. Impedance signals can be correlated with standard levels, and quantification of data is attainable through calibration.

Impedance spectra are typically presented in the form of a Nyquist plot, where the imaginary component Z_{Im} is plotted against the real component Z_{Re} (Figure 2.3). The semicircle at the higher frequencies corresponds to the electron transfer limited processes, and the diffusion limited electrochemical processes at the lower frequencies are represented in the linear part of the spectrum. The frequency response of a system can be illustrated in a Bode plot (Figure 2.3).

The impedance technology is non invasive and enables analysis of small interfacial changes originating from a biorecognition event at an electrode surface. The technique is very

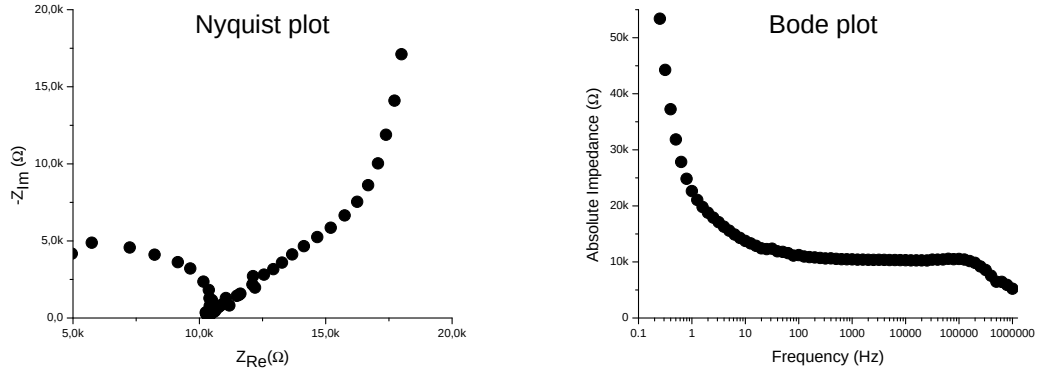

Figure 2.3: Examples of Nyquist and Bode plots. Z is the impedance.

sensitive and when combined in a microfluidic system, low concentrations of a target analyte is detectable.

Electrochemical sensors based on cells, antibodies or aptamers offer great selectivity and sensitivity for early diagnostics of cancer, autoimmune disorders or infectious diseases.

2.3.2 Note on Optical Detection

While impedimetric sensors are receiving much attention, there are other attractive transducing technologies with promising application in medicine and diagnostics.

Optical detection techniques - employing fluorescent markers or colored additive - comprise a category of biosensors with application within this field. Related methods are surface plasmon resonance and surface enhanced Raman spectroscopy. Applications for these techniques range from a simple laminar flow assay as found in pregnancy tests to high technological solution like DNA microarrays. Some argue that optical detection provide a higher sensitivity than electrochemical detection methods, however, the cost and complexity of optical sensors make them unattractive.

Cost efficiency is an important consideration in the development of biosensors. Microfabrication techniques have enabled downscaling of systems, leading to improved mixing rates and mass transport phenomena in microfluidic channels. As a results, analysis time and sample consumption have been significantly lowered, and so has the cost. Another benefit of low biological sample volumes is the increased safety associated with device handling.

2.4 Design of Biosensor

Polymer based microfluidic systems meet the requirements of disposable devices for low sample consumption, cost efficiency, reliability, and fast response time, which make the systems ideal for point of care analysis. Microfluidic channels offer a very controlled environment, providing a suitable platform for cellular studies or investigations of biochemical and biophysical events. An all polymer microsystem (Figure 2.4) was designed and fabricated in Topas® with interdigitated microelectrodes in conductive polymer PEDOT or PEDOT-OH doped with tosylate (PEDOT:TsO or PEDOT-OH:TsO). The fabrication process was continuously optimized; refer to Chapter 3 and Chapter 6 for detailed procedures.

In brief, top and bottom plastic parts were fabricated in Topas® by injection molding [11], while microchannels were defined in adhesive tape by laser ablation. Conductive polymer electrodes and electrical connection patches were either patterned in cleanroom using standard photolitographic processing techniques, or in a general laboratory by agarose stamping [12]. The final chip was bonded in a computer controlled press.

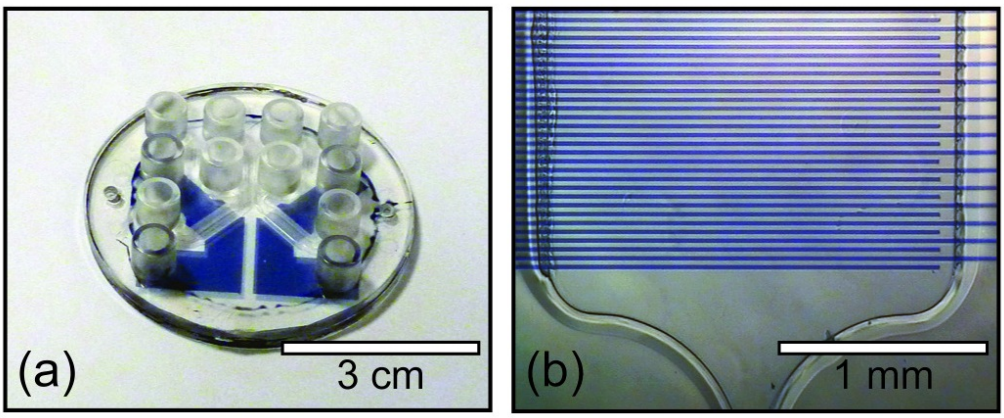

Figure 2.4: (a) All polymer microdevice with two functional channels fabricated in Topas® (transparent) and PEDOT:TsO (blue), (b) microchannel with an interdigitated microelectrode array. Adapted from [13].

2.4.1 Conductive Polymer Electrodes

There is an extensive pool of materials available when producing polymer based microfluidic systems. The conductive polymer PEDOT was selected for its high conductivity and environmental stability, biocompatibility, transparency to visible light and ease of processing [14]. Doping PEDOT with tosylate yields superior quality in phosphate buffers and high conductivity [15, 16].

Conductive polymers have the potential to replace metals and semiconductors as electrode materials; a long term stability of PEDOT has been demonstrated in aqueous solutions [17, 18]. Conductive polymers have the advantageous properties of inexpensive electrode fabrication and easy electrode functionalization [14]. This feature is of great importance in biosensor applications, where particles or cells are immobilized directly on the electrode surface.

The unique characteristics of PEDOT make the material particularly suited for use in biomedical devices and cell based assays. PEDOT is known for having great cell compatibility and is increasingly being used for handling, analyzing and culturing of living cells [19–25]. Here, PEDOT microelectrodes were employed in studies of cell development over time through impedance spectroscopy [13].

2.4.2 Cell Compatibility

Cells are very sensitive and respond immediately to environmental changes, thus it is of great importance that the cell compatibility of medical devices for both short and long term usage is evaluated. Material characteristics that affect cell compatibility are inertness, hydrophilicity and roughness. Materials used for the fabrication of microdevices

were investigated independently, and the compatibility of the all polymer microdevices were further evaluated by culturing human cells in chips for a week. The cells adhered and proliferated normally on Topas® and PEDOT:TsO, and no significant change in the morphology of cells could be observed during this period (Figure 2.5). The conducting polymer material PEDOT-OH:TsO also demonstrated excellent cell compatibility, similar to PEDOT:TsO [13].

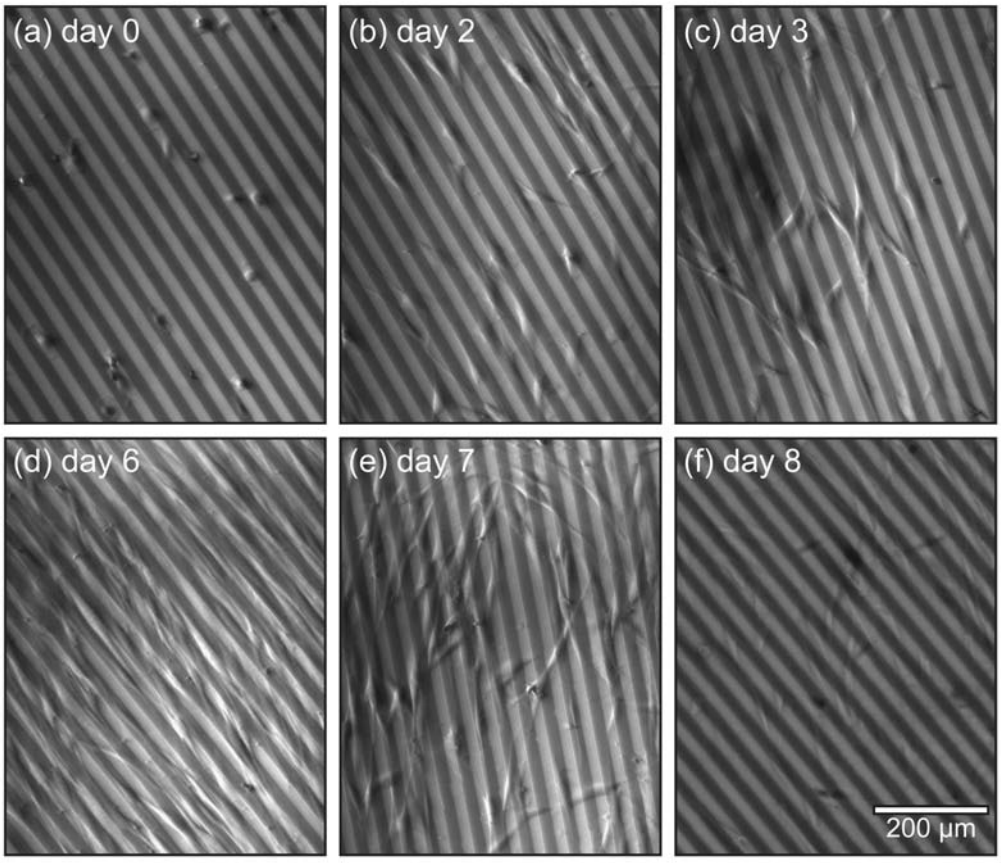

Figure 2.5: Cell compatibility of an all polymer microchip was evaluated by culturing human cells for a week. Cells were seeded on the conductive polymer microelectrodes in a microfluidic channel at low density. The cells adhered and proliferated normally on Topas® and PEDOT:TsO, and no significant change in the morphology of cells could be observed during the period. On the sixth day, cells were exposed to a flow at a high rate to decrease the number of cells. Adapted from [13].

2.5 Biosensors Used in This Thesis

Biosensors are composed of two elements; a sensor and a detector. Impedimetric sensors were introduced in Section 2.3.1; this mode of transduction was employed throughout the PhD project in combination with different sensing elements. The biosensors described in this thesis are classified according to the recognition elements, and the following sections provide shorts introductions to the different types of sensors.

2.5.1 Aptamer Based Biosensor

The use of aptamers as recognition elements in sensors is gaining increased popularity, and they are now recognized as substitutes for antibodies on the diagnostic front [27]. The short nucleotide sequences with specific binding capabilities are generated *in vitro* from a randomized pool of molecules by affinity and amplification processes [28]. Aptamers are generated with a high degree of control, giving a more consistent quality than antibodies, which are produced in a biological system, with a batch to batch variation and much

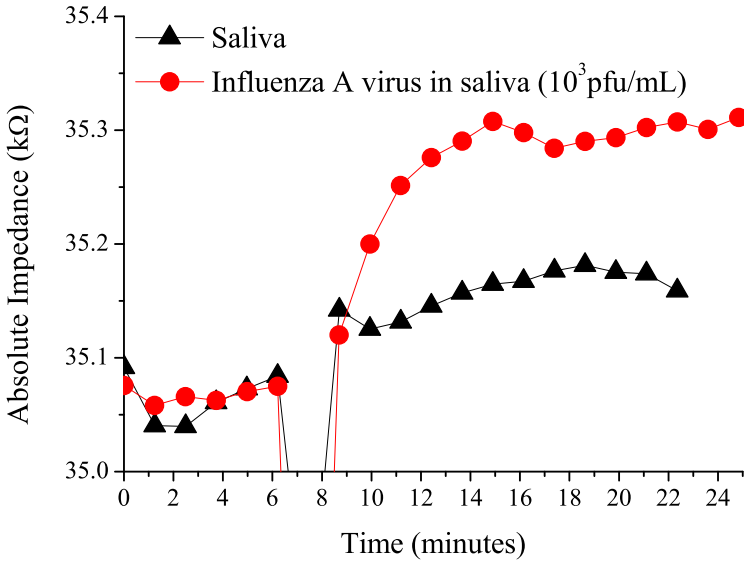

Figure 2.6: Example of an aptamer based biosensor for impedimetric detection of influenza virus in saliva. Aptamers with affinity for the virus were immobilized on conductive polymer microelectrodes, and a baseline in saliva was recorded. Sample was introduced around minute 7, and aptamer-virus complex formation induced an increase in the absolute impedance. Detection of influenza virus in saliva (circle, red trace) and control measurement in saliva (triangle, black trace). The outliers around minute 7 originate from the disturbances caused by sample injection. Adapted from [26].

shorter shelf life. Unlike most monoclonal antibodies, an aptamer binds highly specific to its target, and can be designed to discriminate between virus strains for a specific virus subtype, based on differences in the amino acid residues [27, 29].

Immobilization of aptamers on a microelectrode array provokes an increase in the impedance due to higher charge transfer resistance at the electrode/liquid interface, and the binding of target molecule to aptamers further cause an increase in the impedance (Figure 2.6). The complex formation perturbs the charged double layer at the interface, and the increased thickness and insulation of the surface gives rise to an increase in capacitance and resistance. Saturation is reached when the conductive surface is entirely covered with complexes.

An example of an aptamer based biosensor is given in Chapter 3.

2.5.2 Nanowire Based Biosensor

Nanostructures offer intriguing opportunities for developing novel biosensing platforms [31], and the field of silicon nanowires has been extensively investigated since the original paper was published more than a decade ago [32]. Nanowires have primarily been used as electrical detectors, in a simple design that allows for development of compact point of care devices. The large surface to volume ratio produces an extremely high sensitivity - ultimately a promise for single molecule detection. Although the technology is attractive, the cost is a challenge hindering full exploration of nanowire microdevices as biosensors in medicine and diagnostics [33]. Processing costs are significantly reduced with the use of conductive polymer nanowires [34–36] combined with a new and fast fabrication procedure exploiting the properties of self assembled peptide nanotubes [30].

Conductive polymer nanowires were fabricated by combining bottom up fabrication with standard cleanroom processing techniques. The conductive polymer was spun onto a substrate containing gold contact patches, and patterned into nanowires using self organizing

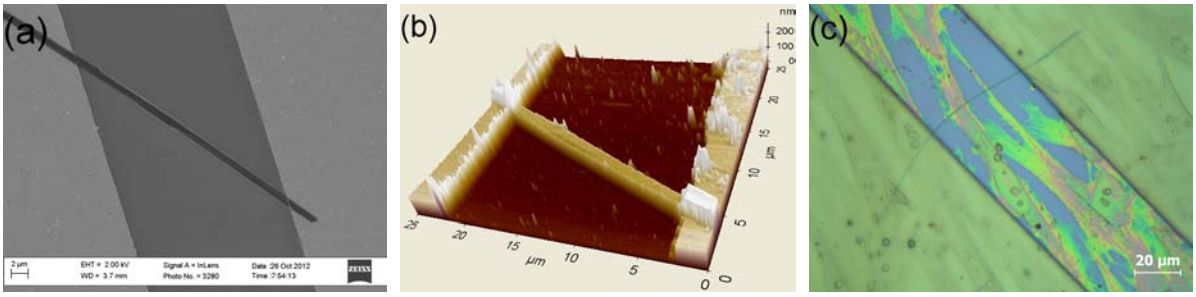

Figure 2.7: Conductive polymer (PEDOT-OH:TsO) nanowire; (a) scanning electron microscopy image of nanowire spanning between gold contact patches [30], (b) atomic force microscopy topography image of nanowire spanning between gold contact pads, and (c) microscopy image of human cell on a nanowire.

peptide nanotubes as dry etching mask. The nanotubes remained stable during etching, and were dissolved in water afterwards [30].

Figure 2.7 show a scanning electron microscopy image, an atomic force microscopy topography image, and a microscopy image of a conductive polymer (PEDOT-OH:TsO) nanowire spanning between gold contact pads, respectively. The surface roughness of the nanowire induces a larger surface to volume ratio than comparable flat nanowires and increases the sensitivity of measurements.

Single cell detection and analysis is essential for an accurate and profound comprehension of cell behaviour. Different assays for single cell analysis have been proposed [37–40], of which many require some sort of labeling. Silicon nanowire sensors were employed to detect the neuronal signal of a single neuron cell and muscle cell [31,41]. Due to alignment difficulties and low yield of production, only few cell detection studies have been conducted using silicon nanowires. Easy handling and processing of polymer nanowires make them suitable for single cell detection. In Figure 2.7(c), a living cell was immobilized on a conductive polymer nanowire in a microfluidic channel.

An example of a nanowire based biosensor is given in Chapter 4.

2.5.3 Cell Based Biosensor

Cell based biosensors are sophisticated devices, employing immobilized living cells as sensing elements. Cells are by nature very sensitive to changes in the environment, allowing for physiologically relevant studies of the cellular response to one or more compounds, or effects.

Among cell based assays, electrochemical impedance spectroscopy combined with microelectrode arrays provide a platform for label free detection of the cellular response to different drugs or pathogens [42, 43]. The interaction between a cell monolayer and the electrode surface can be monitored in real time by applying a small amplitude alternate current electric field. Cells are essentially non conducting at low frequencies and the cell membrane offers a significant barrier to current flow, so that the amplitude of the alternate current field is an indication of the cell volume or size [44]. Average alterations in the three dimensional shape of cells is then computed by integrating over a monolayer of hundreds or thousands of cells. The measured impedance reflects changes in the attachment and morphology of cells, and reaches its maximum when the electrode is completely covered [45, 46].

Impedance measured on cells cultured on microelectrodes is very sensitive to small changes in the cell membrane capacitance and resistance. These parameters are good indicators for the well being of cells at a given cell morphology. The real time detection of cell impedance gives an efficient and rapid technique for non invasive monitoring of the response of human cells in culture to the challenge of a virus infection [47, 48].

In general, viral infections can induce degenerative morphological changes in cell cultures;

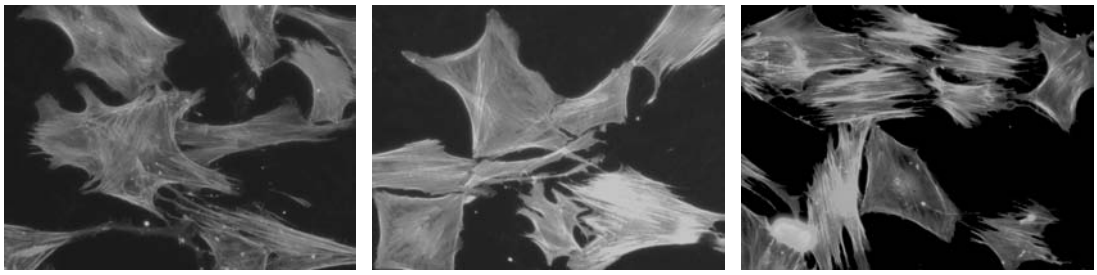

Figure 2.8: Actin cytoskeleton of human fibroblast cells stained with Phalloidin.

cell detachment from substrate, release of cell-cell adhesions, cell round up and eventually cell death. Beside the morphological effects, these changes in the cells produce a decline in the resistance and an increase in the capacitance in the impedance signal [47, 48].

Cell based biosensors are reviewed in Chapter 5, and an example of a cell based biosensor for virus detection is given in Chapter 6.

2.5.4 Cell Migration

Cell migration refer to the processes involving the translation of cells from one location to another. Cells migrate in response to multiple situations, and the mode of migration is highly cell type dependent. Immune cells are nimble, fast moving and rapid turning cells with a slightly disorganized cytoskeleton, whereas fibroblast cells - at the other end of the spectrum - have elaborated cytoskeleton structures and generally move slowly (Figure 2.8). Cells have different characteristics, and contribute to maintain homeostasis.

The process of cell migration plays a vital role in a variety of physiological and pathological processes. Wound repair and inflammation are examples of two homeostatic processes in the body that rely on the ability of cells to migrate. Neither of these processes would be possible if it were not for cell migration, and often they occur together.

An example of a microfluidic device for studies of leukocyte homing is given in Chapter 7, and preliminary work on a microfluidic system for electrical detection of wound healing is presented in Chapter 8.

2.6 Concluding Remarks

Design and development of biosensing platforms for medicine and diagnostics require a coordinated team work across several research fields. This chapter gave a general introduction to the basic concepts, and provided a context for the research results presented in the thesis.

Chapter 3

Aptamer Based Biosensor

3.1 Introduction

New and emerging infectious diseases pose a growing global challenge for patient diagnosis and treatment, and for public health responses. In the beginning of 2009, a novel influenza A (H1N1) virus of swine origin caused human infection and acute respiratory illness in Mexico. After spreading among persons in the United States and Canada, it spread globally, resulting in the first pandemic since 1968 with circulation outside the usual influenza season in the Northern Hemisphere. By March 2010, almost all countries had reported cases and many laboratory confirmed deaths had been reported to the World Health Organization (WHO) [49]. The 2009 influenza pandemic is an example of a zoonotic infection, and most emerging infectious disease events are caused by zoonotic pathogens.

There are different strategies to manage influenza infections and currently, vaccination is the primary method for preventing illness. Antiviral treatment is available for influenza infections, however treatment must be initiated within 36 -48 hours of onset of symptoms for it to be efficient [50].

The reference standards for laboratory confirmation of acute virus infection are molecular detection techniques or viral culture. Unfortunately, the results of these assays are generally not available within this narrow therapeutic window. Hence, there is a need for new diagnostic tools with high sensitivity that can deliver a result in a clinically relevant time frame.

The next generation of point of care devices are simple and inexpensive instruments allowing the untrained user to perform simple diagnostic analyses without the need for a specialized laboratory.

In this paper, we present a new fast and reliable point of care method for virus diagnostics, using influenza A virus as an example to demonstrate its usability. A low cost all polymer microfluidic system was fabricated in Topas® by injection molding and conductive polymer

(PEDOT-OH:TsO) microelectrodes were patterned by agarose stamping. The electrodes were functionalized with specific aptamers, and the microchip was exploited for real time and label free electrical detection of intact virus particles.

High Sensitivity Point-of-Care Device for Direct Virus Diagnostics

Katrine Kiilerich-Pedersen[a], Johannes Daprà[a], Solène Cherré[a], Noemi Rozlosnik[a,*]

[a]*Technical University of Denmark, Department of Micro- and Nanotechnology, Oersteds Plads 345 East, DK-2800 Kongens Lyngby, Denmark*

Abstract

Influenza infections are associated with high morbidity and mortality, carry the risk of pandemics, and pose a considerable economic burden worldwide. To improve the management of the illness, it is essential with accurate and fast point-of-care diagnostic tools for use in the field or at the patient's bedside. Conventional diagnostic methods are time consuming, expensive and requires specialized laboratory facilities. We present a highly sensitive, highly specific, and low cost platform to test for acute virus infections in less than 15 minutes, employing influenza A virus (H1N1) as an example of its usability. An all polymer microfluidic system with a functionalized conductive polymer (PEDOT-OH:TsO) microelectrode array was developed and exploited for label free and real time electrochemical detection of intact influenza A virus (H1N1) particles. DNA aptamers with affinity for influenza A virus (H1N1) were linked covalently to the conductive polymer microelectrodes in the microfluidic channel. Based on changes in the impedance when virions were captured by immobilized probes, we could detect clinically relevant concentrations of influenza A virus (H1N1) in saliva. This is a new, stable and very sensitive point-of-care platform for detection and diagnostics of intact virus particles.

Keywords: Conductive polymer, PEDOT-OH:TsO, electrochemical impedance spectroscopy (EIS), DNA aptamer, influenza A virus (H1N1), AFM, point-of-care (POC)

1. Introduction

Influenza infections are a major cause of morbidity and mortality, even though the vast majority of infections exhibit a self limited, acute illness. In the United States alone, influenza infections pose a considerable economic burden with more than 200,000 hospitalizations and an average of 36,000 deceased of influenza-related causes every year (Thompson et al., 2003, 2004). Influenza A virus has the potential to generate global pandemics, illustrated by the influenza A virus (H1N1) 2009 pandemic, which affected more than 214 countries and was responsible for more than 18,000 deaths (Taubenberger and Kash, 2010).

Early identification of influenza as the cause of a respiratory illness is important for optimal patient management by allowing timely administration of antiviral treatment if needed. Current antiviral treatments for influenza have been shown to be effective in reducing severity, duration of illness and complications, but they should be started within 48 hours after onset of symptoms (Nicholson et al.; Treanor et al., 2000).

The reference standards for laboratory confirmation of influenza virus infection are reverse transcription-polymerase chain reaction (RT-PCR), direct antigen detection through fluorescent antibody staining, or viral culture. Viral culture requires $3-10$ days, hence is not useful for patient management. Using the conventional immunofluorescence test to identify influenza antigens in clinical specimens produce a results in $2-4$ hours, however this test depends heavily on laboratory expertise.

Molecular biological techniques for genome detection are increasingly being used in clinical settings, and they can identify subtypes of the influenza A virus within $3-8$ hours in an advanced laboratory setup. RT-PCR and other molecular detection methods are attractive, because they have high sensitivity and specificity. However, these methods do not indicate the viability of virus or on-going viral replication, and moreover, these methods are expensive, time consuming and require well equipped laboratories and trained personnel. RT-PCR is also associated with multiple potential technical errors, including failed extractions and problems with PCR inhibition (Bustin and Mueller, 2005).

To improve the management of influenza infections and virus infections in general, it is essential to provide accurate and timely point-of-care (POC) diagnostic tools for use in general practice or at the patients bedside. Currently, there are a number of POC tests available on the market to diagnose influenza A virus (H1N1) in clinical specimens, unfortunately these tests have demonstrated poor sensitivity and specificity (Babin et al., 2011; Bai et al., 2012; Gavin and Thomson, 2004), and inconsistent accuracy (Harper et al., 2009; Chartrand et al., 2012).

To compete with and outmatch the conventional techniques in virus diagnostics, the new generation of POC sensing devices must fulfil high standards and be producible at reasonable cost (Price and Kricka, 2007). Polymer based microfluidic systems meet the requirements of disposable devices, low sample consumption, cost efficiency, reliability, and fast response time, hence making the systems ideal for POC analysis. By selecting conducting polymers as electrode materials, the additional advantageous properties of inexpensive electrode fabrication and easy electrode functionalization can be achieved (Rozlosnik,

*Corresponding author

Email address: noemi.rozlosnik@nanotech.dtu.dk (Noemi Rozlosnik)

2009).

Seasonal influenza A virus spread via respiratory secretions, and virus is shed in various specimens from the upper respiratory tract, such as nasal secretions or saliva specimens (Robinson et al., 2008). Nasal secretions are generally preferred due to high numbers of infected cells, which is important for conventional molecular diagnostic techniques. Saliva specimens are easily obtained but the virus concentration is lower (Robinson et al., 2008). However, utilizing a highly sensitive and highly specific POC device would neither require the presence of cells nor a high concentration of virus, consequently diagnosing influenza based on a saliva specimen would suddenly be doable.

We introduce a highly sensitive, highly specific, and very cheap method to test for acute virus infections in less than 15 minutes, using influenza A virus as an example. An all polymer microsystem with a functionalized conductive polymer (PEDOT-OH:TsO) microelectrode array was exploited for label free and real time electrochemical detection of intact influenza A virus (H1N1) particles. DNA aptamers with affinity for influenza A virus (H1N1) were linked covalently to the conductive polymer microelectrodes in the microfluidic channel. Based on changes in the electrical signal at the electrode surface when virus particles were captured by specific aptamers, we could detect clinically relevant concentrations of intact influenza A virus (H1N1). This is an new, stable and very sensitive platform for virus detection and diagnostics. In this system, intact virus is detected and quantified in its native configuration without destructing the particles, which is an advantage compared to RT-PCR.

2. Experimental Procedures

2.1. All polymer microsystem

The all polymer microfluidic device has previously been described (Kiilerich-Pedersen et al., 2011). In brief, top and bottom pieces were fabricated from the cyclic olefin copolymer TOPAS 5013L (TOPAS Advanced Polymers, Germany; $Tg \simeq 134\,^{\circ}\mathrm{C}$) by injection moulding (Victory 80/45 Tech, Engel, Germany). The top part contained access ports in standard luer lock size for fluid inlets, outlets and electrical connections. The second layer - microchannels and reservoirs - were defined in a 150 µm thick, pressure sensitive adhesive (PSA, ARcare 90106, Adhesive Research, USA) by laser ablation (Duo Laser CO_2 laser, Synrad Inc, USA). Electrodes and electrical connection patches in the third layer were patterned in the conductive polymers, poly(3,4-ethylenedioxythiophene) doped with tosylate (PEDOT:TsO) and ((2,3-dihydrothieno[3,4-b][1,4]-dioxin-2-yl)methanol) (PEDOT-OH:TsO) using agarose stamping, described in detail by Daprà et al. (Daprà et al., 2013). The final chip was assembled by thermal assisted bonding at 75 °C with 500 N force applied for 5 minutes in an in house build, LabView (National Instruments, USA) controlled press. In an assembled device, the volume of the microchannel was 100 µL.

2.2. Oligonucleotides

An oligonucleotide with the following sequence was used in this study: 5'AAT TAA CCC TCA CTA AAG GGC TGA GTC TCA AAA CCG CAA TAC ACT GGT TGT ATG GTC GAA TAA GTT AA-3 (A22 presented by Jeon et al. (2004)) (DNA Technology A/S, Denmark). The molecule was functionalized with an 5'-amino modified C_6 linker.

2.3. Virus

Influenza A virus (H1N1, strain A/PR/8/34, ATCC Cat. No. VR-1469; LOT:59252244) was aliquoted and stored at −80 °C.

2.4. Electrode Functionalization

Succinic acid was grafted onto surface hydroxymethyl groups with 0.1 M MES buffer (2-(N-morpholino)ethanesulfonic acid) at pH 4.0 supplemented with 50 mM 1-ethyl-3-(3-dimethylaminopropyl)carbodiimide (EDC) and 50 mM succinic anhydride for 20 minutes at room temperature. Following, the surface carboxylic acid groups were activated with 50 mM EDC and 40 mM NHS (N-hydroxy succinimide) in MES buffer (0.1 M, pH=4.0) for 5 minutes. The microchannel was washed with MES buffer (0.1 M, pH=4.0), and then the activated acid intermediate reacted with the 5'amino group of the aptamer at a concentration of 100 nM in water to form a stable amide bond. Reaction was allowed to proceed over night and then the microchannel was rinsed with PBS.

2.5. Electrochemical Measurements

Electrochemical impedance measurements were employed to detect influenza A virus (H1N1) in PBS or saliva. Electrochemical impedance measurements were recorded every 33 s in the frequency range from 0.2 Hz to 10 kHz with an amplitude of 10 mV in a two electrode setup. The optimal frequency for the analysis was found at 251 mHz. It was determined by the highest response to virus binding on electrodes, taking into consideration the best signal-to-noise ratio and the measurement time. This frequency was used for all analyses.

For characterization of the sensor, all measurements were carried out in stationary (no flow) conditions. A baseline was recorded in PBS (no analyte), and then increasing concentrations of influenza A virus (10-10^6 pfu/mL) in PBS were introduced every 20 minutes. Afterwards, the microchannel was rinsed with PBS and spectra were recorded for additional 20 minutes. The final step served as a control to ensure that virus was immobilized.

To test the usability of the sensor in a more realistic setting, saliva was spiked with influenza A virus (H1N1). A baseline was recorded in saliva diluted 1:10 in PBS. Saliva used for the initial baseline measurements had been boiled to prevent degradation of the ssDNA aptamer. Samples containing influenza A virus (H1N1) at a concentration of 10^3 pfu/mL in saliva diluted 1:10 in PBS were introduced at t=1 hour, and control measurements were conducted in saliva diluted 1:10 in PBS.

2.6. Atomic Force Microscopy (AFM) Imaging of Virus

TOPAS 5013L discs patterned with conductive polymer (PEDOT-OH:TsO) electrodes were employed for AFM examinations. Electrodes on discs were functionalized with ss-DNA A22 (except negative controls) according to the procedure described in Section 2.4, and virus at a concentration of 10^5 pfu/mL in PBS was allowed to bind for 20 minutes. Discs were then washed three times with PBS to remove residual virus, fixed in 2.5 % glutaraldehyde in PBS for 60 minutes at room temperature, and washed with PBS for 15 minutes at 4 °C. Samples were dehydrated by increasing concentrations of ethanol (30 -99 %) for 10 minutes at room temperature and allowed to air dry over night. AFM images were recorded with a XE150 (Park Systems, Korea) in tapping mode using non contact high frequency cantilever (BS-Tap300AI, Budget Sensors, Bulgaria) with a force constant of 40 N/m. Examinations were carried out in air at room temperature.

3. Results and Discussion

We present a new fast and reliable POC method for virus diagnostics, and employ influenza A virus (H1N1) as an example to demonstrate its usability. A low cost all polymer microfluidic system with functionalized interdigitated conductive polymer microelectrodes was exploited for real time and label free detection of intact virus particles.

3.1. Aptamers

Aptamers are nucleic acid ligands, generated in vitro from a randomized pool of molecules by affinity and amplification processes (**?**). DNA aptamers were employed in this study due to the advantageous properties over antibodies, and because aptamers are now recognized as substitutes for antibodies on the diagnostic front (Gopinath, 2007). Aptamers are generated with a high degree of control, giving a more consistent quality than antibodies, which are produced in a biological system, with a batch to batch variation and much shorter shelf life.

The applied ssDNA aptamer A22 with binding capacity to intact influenza A virus (H1N1) binds directly to the globular region of the influenza glycoprotein hemagglutinin (HA) (HA-(91-261)) (Jeon et al., 2004). Unlike most monoclonal antibodies, the aptamer A22 binds highly specific to its target, and can discriminate between virus strains within the influenza subtypes, based on differences in the amino acid residues (Gopinath, 2007).

The aptamers were covalently linked to conductive polymer microelectrodes with the 5'-amino modified C_6 linker, and a homogeneous distribution of aptamers on the microelectrode surface was achieved (see on Figure 4).

3.2. Impedimetric characterization of sensor

The immobilization of A22 aptamers on the electrodes provoked an increase in the impedance due to increased charge transfer resistance at the electrode/liquid interface.

The binding of the viruses to aptamers caused significant increase in the impedance already at very low concentrations. Washing the samples with PBS gave no significant change in the impedance signal, hence demonstrating that virus was bound to the aptamer.

Control experiments, where high concentrations of virus were reacted with a mismatching aptamer gave no changes in the impedance signal compared to the baseline (data not shown).

Figure 1 shows the electrochemical impedance spectroscopy (EIS) spectra of the impedimetric sensor presented in Nyquist plots from a typical experiment. The four traces refer to control measurement in PBS and influenza A virus (H1N1) in PBS at increasing concentrations; 10 pfu/mL, 10^2 pfu/mL and 10^5 pfu/mL, respectively. At low frequencies the impedance is dominated by mass transport of ions near the electrode surface, and thus considered to be the most sensitive range to investigate the binding event of a virus to an immobilized aptamer. Providing for the longer measurement time at low frequencies and signal-to-noise ratio, we found the optimal frequency for data analysis at 251 mHz, and this frequency was employed for all analyses.

Control measurements in PBS reflects the impedance of the conductive polymer microelectrode array with immobilized aptamers without virus. Viruses were captured by the aptamer probes when influenza A virus (H1N1) was introduced into the system, this was reflected by a gradual increase in the impedance for increasing concentrations of virus. In the Nyquist plot this is visualized by a shift to the right towards higher resistance.

The lowest concentration of virus tested in the experimental setup was 10 pfu/ml, which corresponds to introducing 1 - 2 pfu in the microfluidic system (volume $\leq 200\,\mu$L). A shift towards higher resistance was achieved at this dilution, indicating that the sensor has a high specificity and sensitivity. The change in resistance is more evident for the highest concentration of influenza A virus (H1N1) (10 pfu/mL), where numerous intact virus particles were captured by the immobilized aptamer probes (Figure 4).

The dynamic range of the sensor was evaluated by testing dilutions of influenza A virus (H1N1) in PBS (10 -10^6 pfu/mL). Figure 2 shows a typical impedance response displayed as the relative change in absolute impedance at frequency 251 mHz for increasing concentrations of virus. For every dilution of virus, the impedance was measured for 20 minutes, allowing the system to stabilize from the physical manipulation. Between every dilution the sample was washed with PBS to remove the unbound virus particles. When the system had stabilized, impedance data were collected (circa 20 values) and the mean was calculated and plotted. Error bars show the standard error of the mean.

The sensor demonstrated a broad dynamic range - from 10 pfu/mL to 10^6 pfu/mL. It begins to saturate at the highest concentrations of virus. The volume of the microfluidic channel (including inlet and outlet) in the microsystem is less than 200 μL, hence the sensor has very high sensitivity and can potentially detect $1-2$ pfu, i.e. one or two intact influenza A virus (H1N1) particles in PBS.

The broad dynamic range can be a useful feature in some

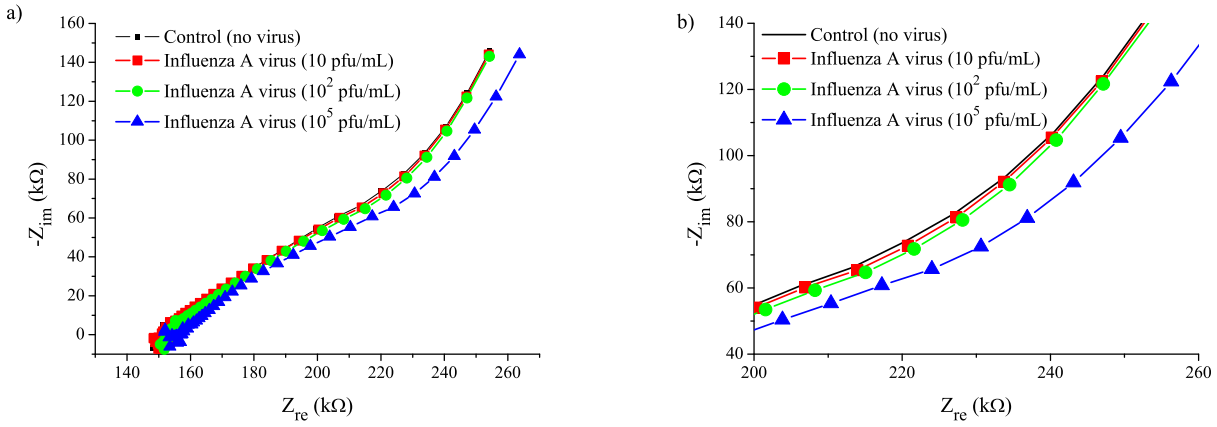

Figure 1: EIS spectra of the impedimetric sensor presented in Nyquist plots. (a) The full recoded range, and (b) zoom in lower frequency regime (2 Hz – 316 mHz). The black (line), red (square), green (circle) and blue traces (triangle) refer to (i) control measurement in PBS, (ii) influenza A virus (H1N1) at a concentration of 10 pfu/mL, (iii) influenza A virus (H1N1) at a concentration of 10^2 pfu/mL, and (iv) influenza A virus (H1N1) at a concentration of 10^5 pfu/mL, respectively.

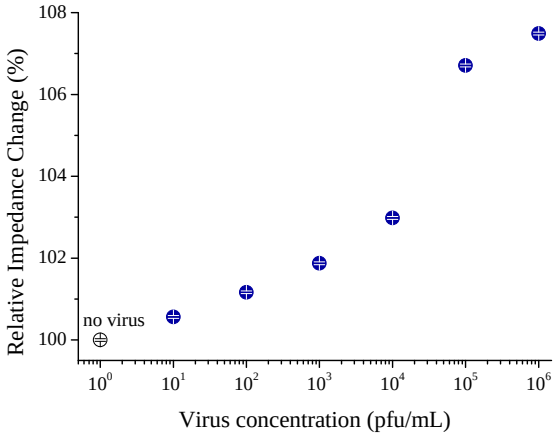

Figure 2: A typical impedance response at frequency 251 mHz for increasing concentrations of influenza A virus. The error bars display the standard error of the mean.

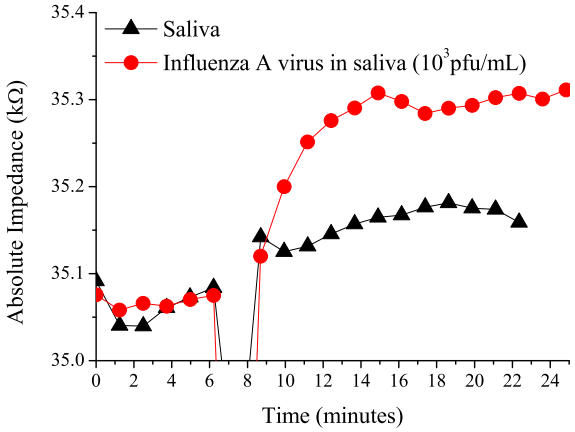

Figure 3: Electrochemical detection of influenza A virus at a concentration of 10^3 pfu/mL in saliva (circle, red trace) and control measurement in saliva (triangle, black trace). The system was stabilized with sterilized saliva and samples were injected at t = 7 minutes.

applications, but in clinical settings a simple yes/no answer is sufficient to diagnose an influenza virus infection.

To test the usability of the sensor in a realistic environment, saliva was diluted in PBS and spiked with influenza A virus (H1N1) at a concentration of 10^3 pfu/mL. Figure 3 shows the impedimetric detection of influenza A virus (H1N1) in saliva, with the absolute impedance displayed over time. A distinct increase in the measured impedance was observed immediately after injection of the sample. The control experiment remained unchanged, considering the slightly skewed baseline. The injection of sample at t = 7 minutes naturally caused a big disturbance in the system, hence the observed outliers. With the detection performance shown here, this sensor is a viable alternative to conventional diagnostic methods and rapid influenza POC tests.

Saliva is secreted by the salivary glands, and is easy obtained by untrained personnel, for example by a parent at home. Even so, employing saliva specimens to test for respiratory viruses such as influenza A virus is uncommon, because nasal secretions provide high concentrations of infected cells which is desirable for antigen detection (Robinson et al., 2008).

The profile of virus shedding for influenza A virus peaks on illness days 1 or 2 and then declines steadily, whereas the viral load varies from subtype to subtype (Suess et al., 2012; Cowling et al., 2010; Lau et al., 2010). For a number to relate to, patients with 2009 pandemic influenza A (H1N1) virus had a mean initial viral load in respiratory specimens of 10^8 copies/mL (To et al., 2010), which peaked soon after onset of clinical symptoms - in accordance with the profile of virus shedding - and then decreased gradually to a range of 10^5 copies/mL around day 5 (To et al., 2010).

Using this sensor, we could detect virus at a concentration of 10^3 pfu/mL in saliva diluted 1:10 in PBS, which is a rather

low estimate bearing in mind the microvolume of the system and the typical viral loads in clinical specimens (more than 100-fold higher). Controls, where a saliva specimen without influenza A virus (H1N1) was reacted with aptamer A22 gave no change in the absolute impedance signal compared to the baseline of saliva (Figure 3). Since saliva is composed of a variety of substances including, electrolytes, enzymes, antibacterial compounds and at times viruses, this result comply with previous studies demonstrating the high specificity of the aptamer A22. The result further comply with our finding, that influenza A virus (H1N1) failed to react with a mismatching aptamer.

The impedimetric sensor detects very low concentrations of virus within minutes and it does not require the presence of infected cells, consequently saliva specimens would be appropriate for analysis despite its lower concentration of viruses (Robinson et al., 2008). Moreover, there is evidence that influenza A virus (H5N1) - predicted by experts to be the next influenza pandemic - have higher concentrations of virus in the throat than the nasopharynx (Kandun et al., 2006).

In literature, several impedimetric sensors for rapid detection of influenza virus have been described, however, many are based on mono- or polyclonal antibodies, metal electrodes, need a label and require from 50 minutes to 2 hours to detect virus (Lum et al., 2012; Labib et al., 2012; Cheng et al., 2012; Wang et al., 2009). To the best of our knowledge, a device for sensing intact virus particles at clinically relevant concentrations in less than 15 minutes has not been reported before.

The biosensor has high sensitivity and selectivity for the tested target, which make it a promising platform for fast and reliable diagnostics of intact viruses. In a similar experimental setup, we have with success tested antibiotics in milk (Daprà et al., 2013), and combined with our newest results on influenza A virus (H1N1) we can conclude that larger targets will have a stronger effect on the impedance because it causes a greater disruption of the electrochemical environment near the electrode. Consequently, this sensor potentially could be used to diagnose any virus if a probe with high affinity for the target molecule is available.

3.3. Imaging Influenza Virus

Atomic Force Microscopy imaging have been conducted to prove the binding of viruses to the surface of the conductive polymer microelectrodes. We have shown that influenza A viruses with a size approx. 100 nm were successfully immobilised on the functionalized electectrodes. Figure 4 shows samples with and without immobilized aptamers reacted with infleunza A virus (H1N1). Small spherical objects were scattered on the electrode surface on the sample which was functionalized with the A22 aptamer, while there were no particles on the electrodes and on the substrate, where no aptamer probes were immobilized. The small, irregular indentations visible on both samples in the high resolution images could originate from the glutaraldehyde treatment used to fix the bound viruses and in the PEDOT-OH:TsO film .

4. Conclusion

In summary, we have developed a new POC platform virus diagnostics. The disposable all polymer microsystem is highly sensitive, highly specific, highly stable, and has a very competitive response time of less than 15 minutes. The sensor could directly detect clinically relevant concentrations of intact influenza A virus (H1N1) in saliva, and it displayed a broad dynamic range. We have used influenza A virus (H1N1) in saliva specimens as an example to demonstrate the usability of the biosensor, and this could be an alternative to current diagnostic techniques.

Acknowledgments

This work was supported by the Danish Research Council for Technology and Production Sciences and the Technical University of Denmark.

References

Thompson, W., Shay, D., Weintraub, E., Brammer, L., Cox, N., Anderson, L., Fukuda, K., 2003. JAMA journal of the American Medical Association 289, 179–186.

Thompson, W., Shay, D., Weintraub, E., Brammer, I., Bridges, C., Cox, N., Fukuda, K., 2004. JAMA journal of the American Medical Association 292, 1333–1340.

Taubenberger, J.K., Kash, J.C., 2010. Cell Host Microbe 7, 440–451.

Nicholson, K., Aoki, F., Osterhaus, A., Trottier, S., Carewicz, O., Mercier, C., Rode, A., Kinnersley, N., Ward, P., .

Treanor, J., Hayden, F., Vrooman, P., Barbarash, R., Bettis, R., Riff, D., Singh, S., Kinnersley, N., Ward, P., Mills, R., Grp, U.O.N.S., 2000. Journal of the American Medical Association 283, 1016–1024.

Bustin, S., Mueller, R., 2005. Clinical Science 109, 365–379.

Babin, S.M., Hsieh, Y.H., Rothman, R.E., Gaydos, C.A., 2011. Diagnostic Microbiology and Infectious Disease 69, 410–418.

Bai, H., Wang, R., Hargis, B., Lu, H., Li, Y., 2012. Sensors 12, 12506–12518.

Gavin, P.J., Thomson, R.B.J., 2004. Clinical and Applied Immunology Reviews 4, 151 – 172.

Harper, S.A., Bradley, J.S., Englund, J.A., File, T.M., Gravenstein, S., Hayden, F.G., McGeer, A.J., Neuzil, K.M., Pavia, A.T., Tapper, M.L., Uyeki, T.M., Zimmerman, R.K., 2009. Clinical Infectious Diseases 48, 1003–1032.

Chartrand, C., Leeflang, M.M.G., Minion, J., Brewer, T., Pai, M., 2012. Annuals of Internal Medicine 156, 500–U80.

Price, C.P., Kricka, L.J., 2007. Clinical Chemistry 53, 1665–1675.

Rozlosnik, N., 2009. Analytical and Bioanalytical Chemistry 395, 637–645.

Robinson, J.L., Lee, B.E., Kothapalli, S., Craig, W.R., Fox, J.D., 2008. Clinical Infectious Diseases 46, e61–e64.

Kiilerich-Pedersen, K., Poulsen, C.R., Jain, T., Rozlosnik, N., 2011. Biosensors & Bioelectronics 28, 386–392.

Daprà, J., Lauridsen, L.H., Nielsen, A.T., Rozlosnik, N., 2013. Biosensors & Bioelectronics 43, 315 – 320.

Jeon, S., Kayhan, B., Ben-Yedidia, T., Arnon, R., 2004. Journal of Biological Chemistry 279, 48410–48419.

Gopinath, S.C.B., 2007. Archives of Virology 152, 2137–2157.

Suess, T., Remschmidt, C., Schink, S.B., Schweiger, B., Heider, A., Milde, J., Nitsche, A., Schroeder, K., Doellinger, J., Braun, C., Haas, W., Krause, G., Buchholz, U., 2012. PLoS ONE 7.

Cowling, B.J., Chan, K.H., Fang, V.J., Lau, L.L., So, H.C., Fung, R.O., Ma, E.S., Kwong, A.S., Chan, C.W., Tsui, W.W., Ngai, H.Y., Chu, D.W., Lee, P.W., Chiu, M.C., Leung, G.M., Peiris, J.S., 2010. New England Journal of Medicine 362, 2175–2184.

Lau, L.L.H., Cowling, B.J., Fang, V.J., Chan, K.H., Lau, E.H.Y., Lipsitch, M., Cheng, C.K.Y., Houck, P.M., Uyeki, T.M., Peiris, J.S.M., Leung, G.M., 2010. Journal of Infectious Diseases 201, 1509–1516.

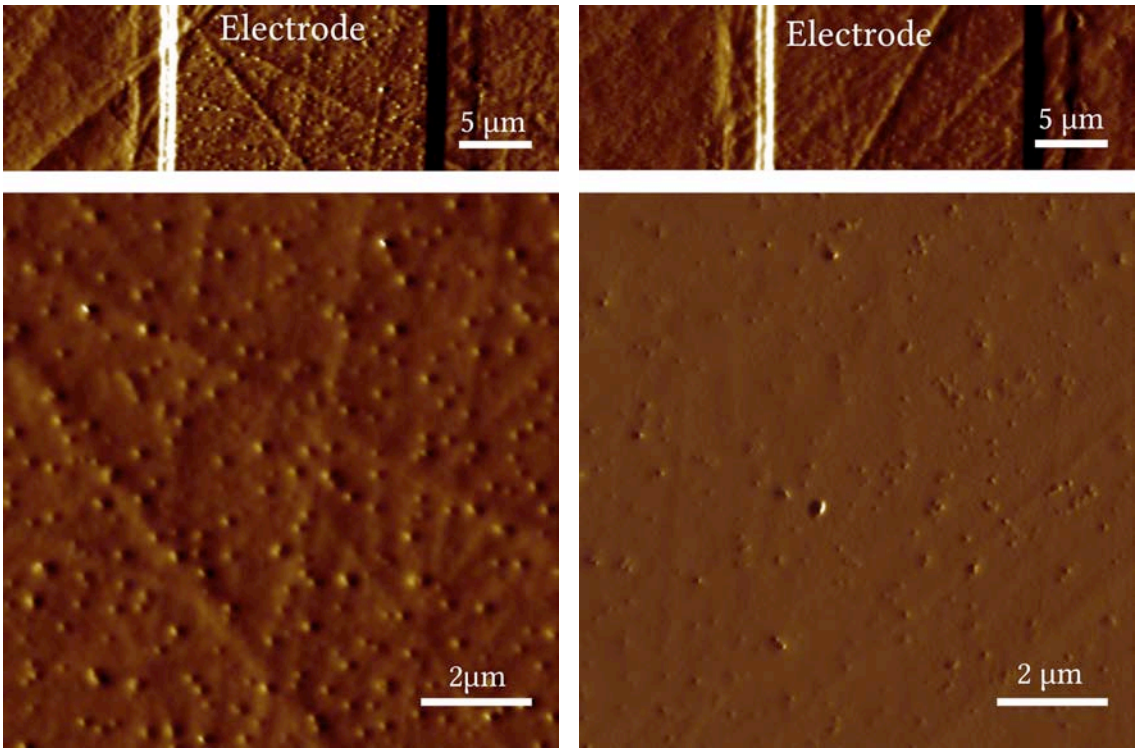

Figure 4: AFM images of stamped PEDOT-OH microelectrodes without and with aptamers. Influenza A virus (H1N1) particles captured by aptamer probes and control without aptamer, hence no virus.

To, K.K.W., Chan, K.H., Li, I.W.S., Tsang, T.Y., Tse, H., Chan, J.F.W., Hung, I.F.N., Lai, S.T., Leung, C.W., Kwan, Y.W., Lau, Y.L., Ng, T.K., Cheng, V.C.C., Peiris, J.S.M., Yuen, K.Y., 2010. Journal of Medical Virology 82, 1–7.

Kandun, I.N., Wibisono, H., Sedyaningsih, E.R., Yusharmen, Hadisoedarsuno, W., Purba, W., Santoso, H., Septiawati, C., Tresnaningsih, E., Heriyanto, B., Yuwono, D., Harun, S., Soeroso, S., Giriputra, S., Blair, P.J., Jeremijenko, A., Kosasih, H., Putnam, S.D., Samaan, G., Silitonga, M., Chan, K., Poon, L.L., Lim, W., Klimov, A., Lindstrom, S., Guan, Y., Donis, R., Katz, J., Cox, N., Peiris, M., Uyeki, T.M., 2006. New England Journal of Medicine 355, 2186–2194.

Lum, J., Wang, R., Lassiter, K., Srinivasan, B., Abi-Ghanem, D., Berghman, L., Hargis, B., Tung, S., Lu, H., Li, Y., 2012. Biosensors & Bioelectronics 38, 67 – 73.

Labib, M., Zamay, A.S., Muharemagic, D., Chechik, A.V., Bell, J.C., Berezoyski, M.V., 2012. Analytical Chemistry 84, 1813–1816.

Cheng, M.S., Ho, J.S., Tan, C.H., Wong, J.P.S., Ng, L.C., Toh, C.S., 2012. Analytica Chimica Acta 725, 74–80.

Wang, R., Wang, Y., Lassiter, K., Li, Y., Hargis, B., Tung, S., Berghman, L., Bottje, W., 2009. Talanta 79, 159–164.

3.2 Concluding Remarks

Electrochemical sensors play a significant role in the transition towards point of care diagnostic devices. The electrical systems are extremely useful for delivering the diagnostic information in a fast, simple, and low cost fashion in connection with compact analyzers.

The disposable all polymer microsystem presented here is highly sensitive, highly specific, highly stable, and has a very competitive response time of less than 15 minutes. The sensor could directly detect clinically relevant concentrations of intact influenza A virus (H1N1) in saliva, and it displayed a broad dynamic range. Saliva specimens spiked with influenza virus were used as an example to demonstrate the usability of the biosensor, and this could be an alternative to current diagnostic techniques.

There is room for improvements of the biosensor. The electrode material is very sensitive to many environmental factors, such as temperature and pH. Introducing a third electrode or measuring on two channels in parallel would allow for differential measurements where only the signal change caused by the biological recognition event would be registered. For mass production, standardization of electrode processing techniques would be required, since the micropatterning of electrodes by agarose stamping is currently a manual procedure.

This is a modular biosensor platform based on electrochemical impedimetric sensing. The microdevice can easily be modified by changing the biological receptors, offering a broad range of possible applications. To keep the costs and the environmental footprint low, the entire biosensor was designed in plastic; featuring a microfluidic channel and an electrode system fabricated from conductive polymers. Aptamers were used as recognition elements providing a more stable alternative to antibodies for easier handling and a longer shelf life. Moreover, aptamers have a much wider range of possible target molecules than antibodies.

The biosensor platform has successfully been adapted to different tasks and tested against three very different analytes: DNA hybridization (Johannes Dapra and Dorota Kwasny; manuscript in preparation), antibiotics [51] and influenza A virus. Throughout the experiments the sensors showed high sensitivity and were able to detect very low analyte concentrations in both buffered solutions, milk and saliva samples.

In summary, a novel biosensing platform was developed. Three prototypes of specialized sensors were tested and they performed very well under laboratory conditions. Together with some modifications and a suitable manufacturing solution this system has the potential for several marketable applications in the health care sector among others.

Chapter 4

Nanowire Based Biosensor

Nanowires still belong to the experimental world of laboratories, but they are predicted a great future in medicine and diagnostics. Early experiments have shown that nanowires are integrable as highly sensitive sensors in microdevices, and have the potential to push forward a change in the practise of medicine towards point of care testing.

The field of silicon nanowires has been studied for a decade now, and a major remaining challenge is processing costs. Recently, a new fabrication procedure was developed at DTU Nanotech, enabling fast and cost effective production of conductive polymer nanowires [30], allowing for effective utilization of nanowire microdevices as biosensors.

Our group just started working with conductive polymer nanowire microdevices as biosensors, and we are still at a learning stage.

This chapter presents our preliminary results. Section 4.1 gives a brief introduction to the new and easy fabrication procedure of conductive polymer nanowire devices. Preliminary studies with cells are presented in Section 4.2, and the work is summarized in Section 4.3.

4.1 Conductive Polymer Nanowires

Nanowires hold great promise for application in point of care devices for medicine and diagnostics, with potential for miniaturization and integration. It has now been more than ten years since the original paper on silicon nanowires was published, manifesting the potential of this new type of biosensor [32]. Silicon nanowire biosensors have been studied for detection of biological molecules as highly sensitive, label free and electrical tools. The advantageous diameter of nanowires - comparable to the size of biological species - makes them ideal for biosensing applications [52]. However, the main shortcoming of silicon nanowire devices are expensive and time consuming fabrication procedures, obstructing the development of disposable medical point of care systems.

Costs are lowered with the realization of nanowires in conductive polymer materials such as polyanaline [53,54] or PEDOT [34–36]. Nanowire devices have been demonstrated in applications, ranging from chemical gas and liquid sensor [55,56] to temperature sensors [57] and biosensors [33, 58, 59].

Processing time of nanowires is significantly reduced by the use of a self assembled peptide nanotube litography [30, 60]. The self organizing peptide nanotube structures were employed as a masking material for rapid, mild and low cost production of PEDOT-OH:TsO nanowires [30]. The new processing method was developed in the NaBIS group at DTU Nanotech.

The fabrication procedure was optimized to comply with studies of living cells and virus. In brief, the conductive polymer PEDOT-OH doped with tosylate was spun onto a wafer containing gold connection patches. Self organizing peptide nanotubes were then spin casted onto the surface of the wafer, and nanowires were patterned by a reactive ion etching procedure. The spinning forced the polymer nanotubes to align radially on the surface of the substrate, and ensured that conductive polymer nanowires were formed between gold contact patches. Finally, nanotubes were dissolved in water, and a SU-8 passivation layer was spun onto the surface. The entire fabrication procedure could be completed in half a day. Nanowire devices were designed and fabricated by Karsten Brandt Andersen and Nikolaj Ormstrup Christiansen, and the procedure is sketched in Figure 4.1.

A cell chamber was fabricated in polycarbonate, and the low cost microdevice was exploited for real time and label free electrochemical detection of living cells.

4.2 Cellular Studies

Sensing at a single cell level provides new opportunities in medical diagnostics. It is an emerging field, and has been recognized as a key technology for the elucidation of cellular functions, which are not accessible from bulk measurements on the population level. Single cell techniques let researchers track and catalogue the heterogeneity of cells to address fundamental questions regarding the biochemistry and functionality of individual cells, and what makes them different.

Many traditional cellular assays are based on the characterization of populations of cells, rather than single cell dynamics. Conclusions drawn from these studies may be misleading on a single cell level. Hence, single cell analysis has become a requirement in modern medicine. Current techniques include capillary electrophoresis and flow cytometry. These methods require the addition of fluorescent conjugates which could alter the original cellular functions [61], and the experimental procedure makes real time monitoring a challenge.

The presented microdevice is based on label free electrochemical detection, allowing for non invasive studies of single cell dynamics within a population of cells to preserve the natural cellular environment.

Electrochemical impedance spectroscopy is a sensitive technique for label free, non invasive studies of cells. By detecting minute changes in the cell membrane capacitance, it can provide relevant information about the functional status of a single living cell without disrupting the microenvironment. In general, impedance spectroscopy has gained popularity for its simplicity, sensitivity and opportunity for downscaling into portable point of care devices.

Impedance spectroscopy was used to measure the initial attachment and spreading of a single cell on a conductive polymer nanowire substrate. Control measurements were conducted in cell medium. Healthy fibroblast cells were seeded in the microdevice, and electrochemical impedance spectroscopy experimentation (no redox couple added) was carried out in a tightly controlled environment at 37 °C, 5 % CO_2. Impedance spectra were recorded every 33 s in the frequency range from 1 Hz to 10 KHz with an amplitude of 20 mV in a two electrode setup. The optimal frequency for the time dependent analysis was found at 1 Hz, and determined by the highest response to changes on the cells.

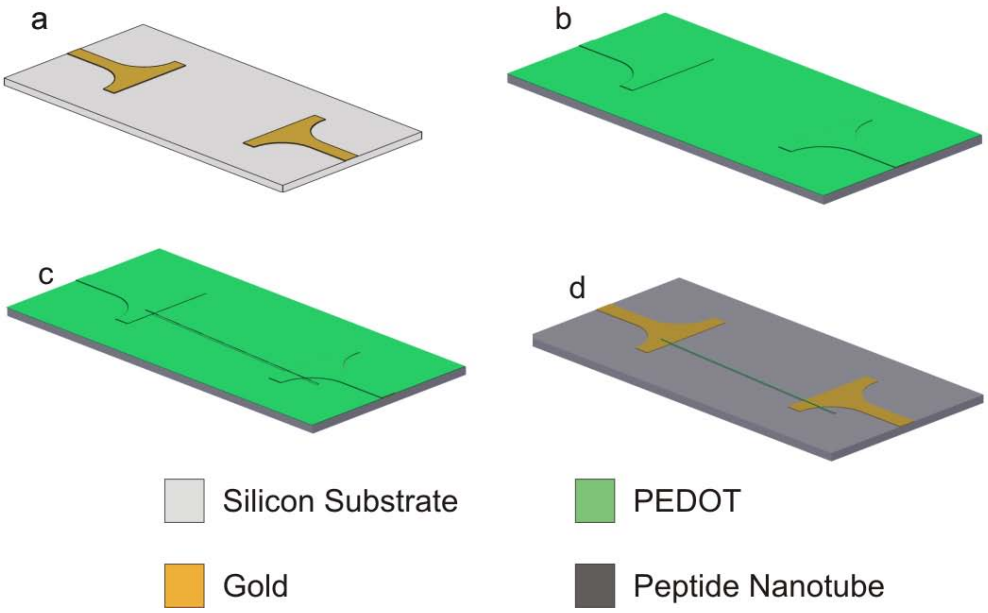

Figure 4.1: Fabrication of conductive polymer nanowires. (a) Gold electrodes were defined by a lift off procedure, (b) Conductive polymer was spin coated on the substrate, (c) self organizing peptide nanotubes were spin casted on the substrate (spinning ensured desired alignment), (d) conductive polymer nanowires were patterned by ion etching, and peptide nanotubes were dissolved in water. Finally, a passivation layer was applied by spin coating and patterned by standard photolitography. The entire process could be completed in half a day. Adapted from [30].

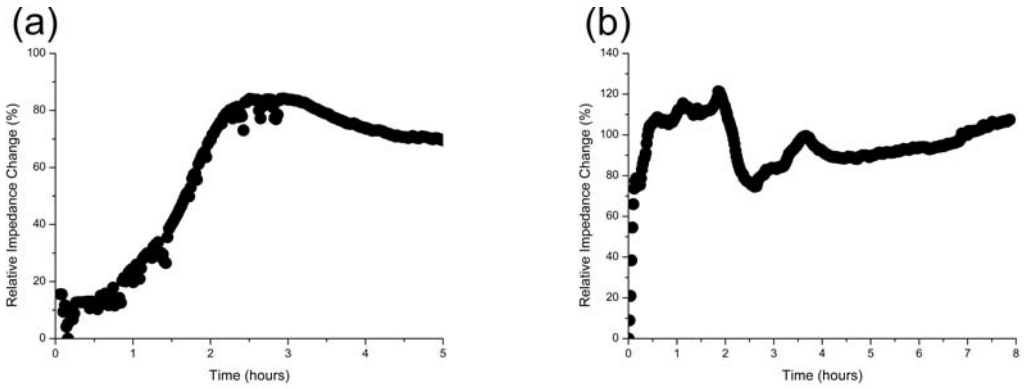

Figure 4.2: Electrochemical detection of single cell adhesion on conductive polymer (PEDOT-OH:TsO) nanowire. (a) and (b) display the relative impedance change at a frequency of 1 Hz from two independent measurements.

Single cell adhesion on a conductive polymer nanowire was monitored in real time, and Figure 4.2 shows the typical impedance changes at a frequency of 1 Hz. The initial attachment and spreading of a single cell was reflected by a gradual increase in the impedance until a plateau was reached after approximately 2.5 hours (Figure 4.2(a)). We have previously shown that the adhesion of a cell population follows a similar curve [13]. In Figure 4.2(b), the impedance increased rapidly, peaked within two hours, and then decreased slightly before reaching a plateau. The minor difference in the impedance change could result from the position of the cell on the wire. Other factors come into play, such as nanowire dimensions, cell morphology and cell motility. The microscopy image in Figure 4.3 display a nanowire spanning between gold contact patches. Atomic force microscopy images at higher resolution illustrate that a cell was immobilized on the wire (Figures 4.3(b)–(d)).

4.3 Concluding Remarks

The current fabrication procedure does not allow any control of the size and distribution of the nanowires. Moreover, the current microdevice design does not allow us to combine electrical measurements with video time lapse microscopy, complicating experimentation. This will be dealt with in the next prototype, where we plan to fabricate conductive polymer nanowires on a thin transparent sheet of Topas®.

Imaging of nanowires with human cells verified that alignment of a cell on the nanowire varied from experiment to experiment, therefore real time video time lapse microscopy is essential for proper data treatment.

The next step is to develop an improved prototype with nanowires fabricated on a transparent substrate, and study cell adhesion on nanowires by video time lapse microscopy

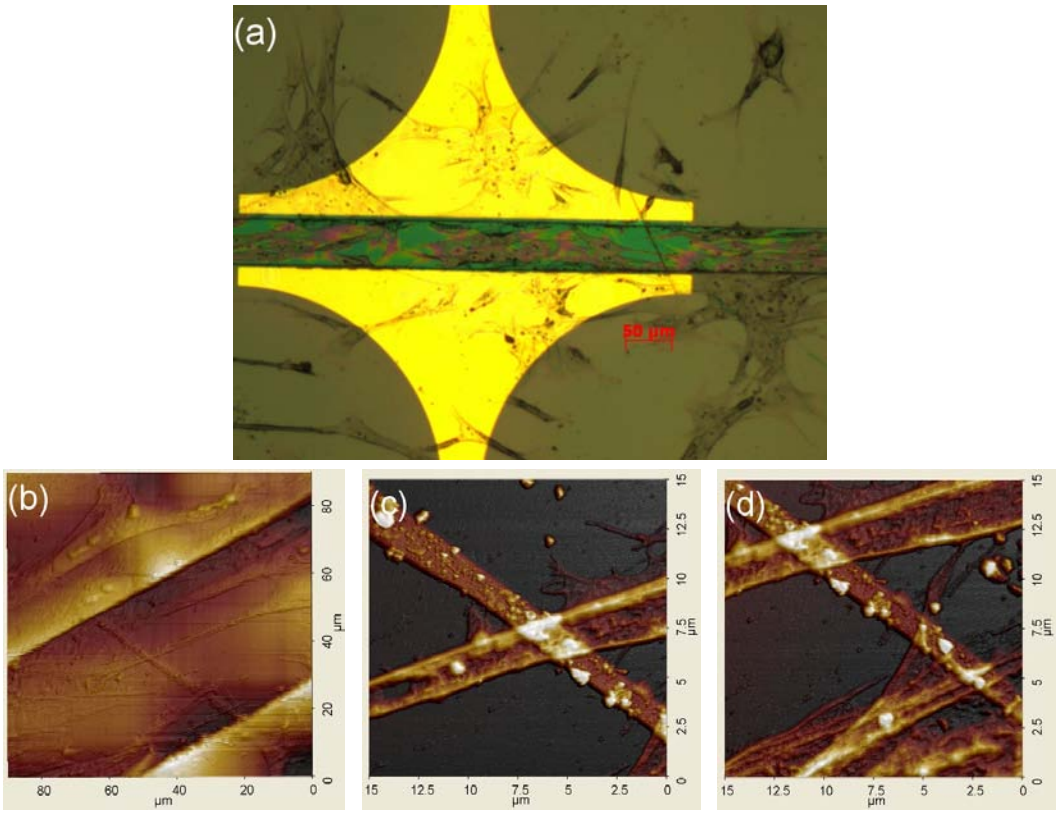

Figure 4.3: Cell on conductive polymer (PEDOT-OH:TsO) nanowire. (a) Microscopy image of nanowire spanning between gold contact patches, (b) atomic force microscopy topography image of cell on nanowire, (c) and (d) atomic force microscopy topography images of cell on nanowire at high magnification.

and electrochemical impedance spectroscopy. Subsequently, the early effects of virus or drug induced cell death of single cells in real time will be studied.

The cellular response to toxins or chemicals is usually measured as an average over a population of cells (refer to Chapter 6). By employing conductive polymer nanowires, the immediate response to a drug or virus could be detectable at single cell level in real time.

In another experimental setup the use of aptamer functionalized nanowires for direct detection of virus gave promising results, but further experiments are required. Electrical detection of single viruses in real time on conductive polymer nanowires have a possibility for large scale integration and potential for simultaneous detection of a large number of distinct viral threats at single virus level.

Chapter 5

Cell Based Biosensor *Review*

5.1 Introduction

Microfluidic systems for cell based biosensing provide advantageous opportunities in medicine and diagnostics [4]. Adapting living cells as recognition elements in a biosensor instead of material that has been extracted from living cells yields an attractive sensing platform, allowing for direct screening of biological active analytes. Cells are very sensitive to minor changes in the cellular microenvironment, hence cell based biosensors are sensitive and accurate tools for rapid detection of physiological effects.

Cell based biosensors are very versatile and have a wide range of applications, for example in drug discovery, personalized medicine and medical diagnostics.

Costs and risks involved in the development of pharmaceuticals continue to rise and stringent regulatory requirements are put in place, creating a need for technologies that can accelerate the process of drug discovery. Cell based biosensors provide a cost efficient platform for fast and accurate screening of known and unknown drug candidates.

The microenvironment in microfluidic devices is highly controllable; consequently conditions mimicking the natural cellular environment are achievable. This is an essential feature, making cell based biosensors ideal for the upcoming market in personalized medicine.

This chapter is concerned with cell based biosensors relevant to medical diagnostics. In this review article, microfluidic device considerations are covered, and three promising electrical transducing technologies facilitating real time analysis of cells are introduced. Short response time is important for application in point of care diagnostics, and live information concerning the state of cells allow for precise control in cell based biosensors. It will be a challenge to bring the sensors out of the laboratory, some potential applications are mentioned in the article.

Diagnostics **2012**, *2*, 83-96; doi:10.3390/diagnostics2040083

OPEN ACCESS

diagnostics

ISSN 2075-4418

www.mdpi.com/journal/diagnostics

Review

Cell-Based Biosensors: Electrical Sensing in Microfluidic Devices

Katrine Kiilerich-Pedersen and Noemi Rozlosnik *

Department of Micro- and Nanotechnology, Technical University of Denmark, Oersteds Plads 345 East, DK-2800 Kongens Lyngby, Denmark; E-Mail: katk@nanotech.dtu.dk

* Author to whom correspondence should be addressed; E-Mail: noemi.rozlosnik@nanotech.dtu.dk; Tel.: +45-4525-5691.

Received: 8 October 2012; in revised form: 13 November 2012 / Accepted: 3 December 2012 / Published: 6 December 2012

Abstract: Cell-based biosensors provide new horizons for medical diagnostics by adopting complex recognition elements such as mammalian cells in microfluidic devices that are simple, cost efficient and disposable. This combination renders possible a new range of applications in the fields of diagnostics and personalized medicine. The review looks at the most recent developments in cell-based biosensing microfluidic systems with electrical and electrochemical transduction, and relevance to medical diagnostics.

Keywords: biosensor; microfluidics; mammalian cells; electrochemical impedance spectroscopy; medical diagnostics

---

1. Introduction

Emerging pathogenic viruses or resistant bacteria in animals more frequently make the headlines than a decade ago. In a global community the outbreak of disease is a source of worry for the population, and the increased interest has indeed emphasized the need for new effective diagnostic screening solutions for point of care (POC) testing.

POC is an emerging field within medical diagnostics and disease monitoring, and eventually disease control. Integration of nanomaterials, microfluidics, automatic samplers, and transduction devices on a single chip provides many advantages for POC devices such as biosensors. Making use of specially designed microsystems [1], patients can be monitored continuously at bed side or at the general practitioner, and save precious time in commuting between home, doctor and hospital. The technological advancements in cell-based biosensors have accelerated the R&D in POC devices.

Conventional detection methods in medical diagnostics, such as polymerase chain reactions (PCR) and enzyme linked immunosorbent assays (ELISA), or whole animal testing are time consuming, labour intensive and expensive [2,3]. Accordingly, it is important to develop effective screening tools to detect, control and confine the spread of biohazards.

Cell-based biosensors—with living cells as the recognition element—are characterized by high sensitivity, selectivity and rapid response. They are very versatile and thus applicable in different fields such as food safety, environmental monitoring, drug screening and medical diagnostics. Cell-based biosensors are able to measure functional information and in this way help us to understand the cellular mechanisms behind particular diseases to improve the development of targeted treatment.

Cell-based biosensors can be constructed to detect the response of a single cell, a cell layer, or a network of cells. The mammalian cells are the most common recognition elements in the microsystems, allowing physiologically relevant studies of a cellular response to one or more compounds, or effects.

Several transducer methods are used for the recognition events including optical absorption and fluorescence, acoustic detection, surface plasmon resonance, electrical and electrochemical methods. Electrical signal detection can readily be integrated in biosensors and thus is an attractive alternative to other detection methods.

This review will focus on the recent developments of cell-based biosensing in microfluidic systems with electrical and electrochemical transduction that are relevant to medical diagnostics without aspiring to completeness. Readers interested in more general aspects of cell-based biosensors are directed to several other excellent review articles [4–8].

2. Device Considerations

For the new generation of POC diagnostics, sensors have to be producible at reasonable cost and fulfill high standards to outmatch the conventional techniques in medical diagnostics. Cell-based sensors are—by nature—very specific and sensitive giving a rapid response. Careful design considerations regarding the microfluidic channel network, electrode system, and selection of materials can further improve the microdevice significantly while maintaining them at low cost.

2.1. Microfluidic Systems

The microscale channels in a microfluidic device enable the use of extremely small volumes of expensive chemicals and low concentration of analyte. Since most of the bio- and chemical reactions are determined by diffusion of the molecules to the adequate places, the short distances in a microsystem permit the rapid detection by reducing the diffusion times. Both the mass and heat transport are faster in a microsystem, allowing a quasi-equilibrium state for the biochemical processes. A variety of microstructures can be used for optimization of transport processes, e.g., vortices, pillars, or herringbone.

A defined microfluidic environment is convenient for cellular studies because the physiological and electrical responses of single cells can be detected. All these desired properties of microfluidic devices are favourable in many biological and medical applications [9].

The majority of microfluidic cell culture systems are designed for adherent cells [10,11], as these are the dominant cell types used in biological studies. Besides, the handling and perfusion of fresh media

for culturing of adherent cell types is much easier. Recently, a cell culturing microfluidic reactor for culturing both adherent and non-adherent cells was presented. It allowed precise control of pH, oxygen, nutrition and temperature, and sustained the biochemical microenvironment of the cells, while supplying nutrients to the cells by diffusion controlled processes [12]. By producing miniature electrodes on the surface of the microchannels, electrical or electrochemical signals from the cells could be recorded in real time.

2.2. Materials for Fabrication

The choice of materials for fabrication of microfluidic devices is a very important factor. Since the 1990s, several studies have originated on interfacing materials with living cells, with the goal of detecting biocomponents or biological processes. The considerations include biocompatibility of the materials, transparency for microscopy, and wettability for aqueous liquid handling [13,14]. Initially, silicon and glass were the most attractive materials for microdevices due to well developed fabrication technologies for semiconductors and micro-electro-mechanical-systems (MEMS).

More recently, polymers have gained popularity, because both the polymer material and the polymer manufacturing techniques (injection molding and hot embossing, replica molding, casting) are inexpensive [15]. Several polymers have physical, mechanical, and chemical properties that meet the demands for biosensing, for example polydimethylsiloxane (PDMS), polymethylmethacrylate (PMMA), polyethylene diacrylate (PEG-DA), polycarbonate, cyclic olefin copolymers (COC).

PDMS is typically employed for prototyping because of its many excellent properties (including gas permeability, transparency, flexibility, and biocompatibility). The surface of native PDMS is hydrophobic, but can be made hydrophilic by surface modification with plasma, UV/ozone, or corona discharge. The oxidized surface remains hydrophilic if it stays in contact with water, and can be modified further by treatment with functionalized silanes [16]. PDMS seals reversibly to a variety of materials such as glass, hard plastic, silicon, flat metal, photoresist, and native PDMS.

Mass production of polymeric devices is commonly done by the injection moulding technique using COC [17,18], and only few polymers are suitable for production of microscale structures with injection molding. COC is a thermoplastic polymer with desirable physical and chemical properties, such as high optical transmittance, low water absorption, biocompatibility and high chemical stability in aqueous media, alkaline, acidic, and polar solvents. Hence, this material is particularly attractive for disposable, cost effective, reliable microfluidic devices with lab-on-a-chip applications.

The novel material Graphene has emerged as an attractive candidate for the biointerface [19,20]. Graphene is a two dimensional sheet of hybridized carbon atoms arranged in a honeycomb lattice, and it exhibits several superior and atypical properties owing to a unique combination of its crystallographic and electronic structure. Due to these properties, it can be a sensitive platform for interfacing with biological cells to detect intra- and extracellular phenomena, including cellular excretion and potential modulation of the cell membrane. Although these applications are lacking of maturity, cell interfaced graphene devices can open avenues for diagnostics and single cell analysis in the future [20].

2.3. Sensing Unit

A major cost factor in electrical and electrochemical sensors is the sensing unit. Electrodes are typically made in a noble metal, involving extensive production steps and cleanroom facilities. Afterwards, surface treatments with a bio- or biocompatible material are required to attain biocompatibility with living cells. For cell-based applications the surface of the metal electrodes can be covered with an extracellular matrix protein to improve cell adherence.

Conductive polymer electrodes present an alternative to noble metals. In addition to low material cost, electrode fabrication is inexpensive, and the electrodes are easily functionalized [21]. The use of conductive polymers as supporting materials in microfluidic systems is well established. However, the electronic sensing units in most microdevices are fabricated from metallic conductors such as platinum or gold.

Biocompatibility and functionalization of electrodes is of great importance in cell-based biosensor applications, where cells are immobilized directly on the electrode surface. The conductive polymer poly(3,4-ethylenedioxythiophene) (PEDOT) has high environmental stability, biocompatibility, transparency to visible light and ease of processing [21]. This polymer has shown high potential and superior quality [22,23], and it has been employed in several biosensor microdevices [24,25].

Figure 1. Electrochemical current response of microelectrodes for the presence of a single cell. The larger electrodes were incapable of resolving a single cell, whereas the use of small electrodes produced a clear change in the electrochemical impedance spectroscopy signal.

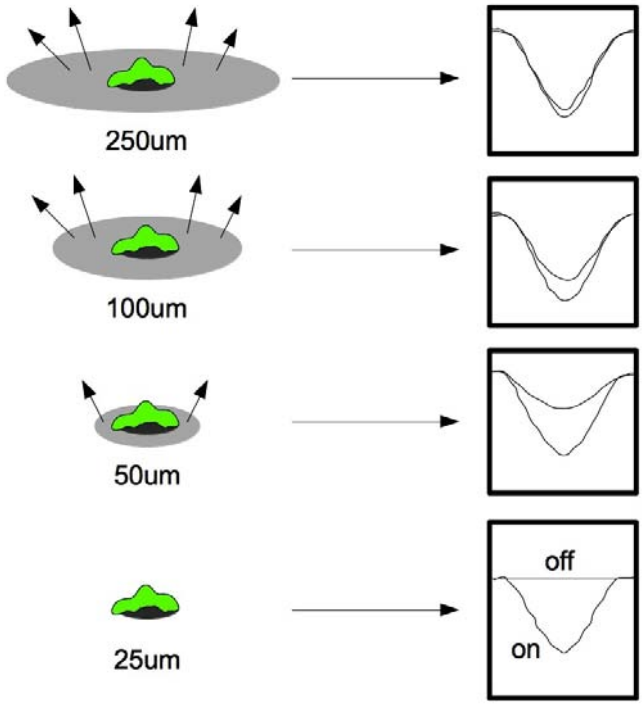

In general, the electrode design has major impact on the electrical readout, and the sensing unit should be designed and optimized in accordance with the application. The demands for studies of the dynamics of a cell culture on a conductive polymer interdigitated electrode array [25] are different than the demands for single cell investigations on an Au microelectrode array [26], or electrical characterization

of single cells on polysilicon wires [27,28]. Figure 1 illustrates the electrochemical current response of microelectrodes for the presence of a single cell, hence emphasizing the effect of electrode design on the electrical signal.

2.4. Microfluidic Design

Microfluidic technology is creating powerful tools for cell biologists to control the complete cellular microenvironment, leading to new questions and new discoveries [29].

For cellular analysis it is often necessary to culture the cells. The standard methods (e.g., culture flasks) do not represent a natural environment. Microfluidic culturing systems for adherent and non-adherent cells allow for precise control of the environment and diffusion based feeding, where important chemicals are not flushed away as it can be the case in conventional cell culture flasks [12].

At micrometer scale, we have a detailed understanding of fluid behaviour, which confers unique potential to microfluidic gradient generating methods. Laminar flow based micro gradient generation devices are used for diffusive mixing of two or more parallel laminar streams of different composition to generate molecular gradients. Gradients generated in these types of devices will maintain their shape in time and space at constant flow rate. The analysis of cell migration in different regions of both chemotactic and haptotactic gradients [30] is relevant for the improved understanding of among others wound healing, cell invasion, and tumour progression.

An intelligent microfluidic cell culture system allows precise control of cell adhesion by temperature changes [31]. The shear stress dependent cell detachment process was investigated in five individual microchannels, where surfaces were coated with the well known temperature responsive polymer Poly(N-isopropylacrylamide) (PIPAAm). To estimate the interaction between cells and the PIPAAm layer, the cells were exposed to a flow in the microchannels, and the shear stress generated by this flow was used as a key factor for cell detachment. The proposed device could be used to assess the possible interaction between the cells and the PIPAAm layer with a potential application in tissue engineering.

3. Principles of Transduction

The feasibility of sensors that can convert the cellular signals from living cells to electrical signals in real time depends especially on cost, usability, sensitivity, and specificity. Real time sensing provides live information regarding the state of the cells, allowing for precise control. This is of great importance in POC applications where rapid response is crucial, or in long term cytotoxicity studies. When cell viability has a relevance (rather than the cell count) real time sensing is advantageous. The three principles of transduction described here enable real time sensing.

3.1. Electrochemical Methods

Electrochemical sensors produce an electrical signal in response to an electrochemical reaction between an analyte and the surface. Direct electrochemical signal detection is preferable, because the use of a simple set of electrodes greatly reduces the complexity, size and costs—factors that are typically associated with other methods, such as optical detection.

Buchinger *et al.* have evaluated the chrono-amperometric detection method in a reporter gene assay based on the bacterial response in comparison with standardized methods [32]. It was shown that the chrono-amperometric detection—under optimized electrochemical conditions—is sufficiently sensitive with a limit of detection that is comparable to the respective ISO-standard.

Among cell-based assays, impedimetric sensors have attracted attention for the high sensitivity, reliability and simplicity [33–38]. Electrochemical impedance spectroscopy combined with microelectrode arrays provide a platform for label free detection of the cellular response to different drugs or pathogens [39,40]. The interaction between a cell monolayer and the electrode surface can be monitored in real time by applying a small amplitude alternate-current (AC) electric field. Cells are essentially non-conducting at low frequencies and the cell membrane offers a significant barrier to current flow, so that the impedance of the system is an indication of the cell volume or size [41]. Average alterations in the three dimensional shape of cells is then computed by integrating over a monolayer of hundreds or thousands of cells. The measured impedance reflects changes in the attachment and morphology of cells, and reaches its maximum when the electrode is completely covered [25,42,43].

3.2. Field Effect Devices

Field effect devices use an electric field to control the conductivity of a semiconducting material. The integration of living cells together with silicon field effect devices challenges a new generation of biosensors and bioelectronic devices. Among the variety of proposed concepts, the integration of living cells together with a silicon chip consisting of an array of (bio)chemical and/or electrophysiological transducers, based on a field-effect electrolyte/insulator/semiconductor system is one of the most attractive approaches. The cell/transistor hybrid is obtained by direct coupling of a single cell or cell system to the gate insulator of a field effect transistor (FET) (Figure 2). This system is very sensitive to any kind of electrical interaction at or nearby the gate insulator/electrolyte interface.

Figure 2. Cell/transistor hybrid. The open gate area of the FET is completely covered by one cell as indicated in the schematics (RE: reference electrode; VG: gate voltage; VDS: drain-source voltage; ID: drain current).

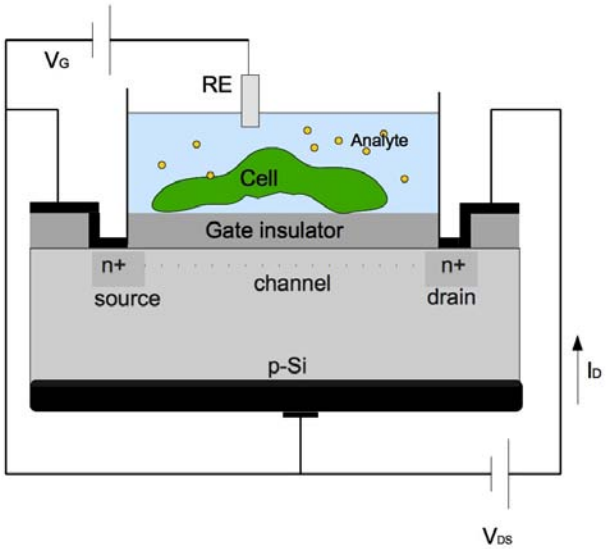

The state of a single cell or cell system can be monitored by means of various methods, such as (i) utilisation of the metabolism of cells like growth, toxicity, extracellular pH, redox potential, concentration of ions, *etc.*, (ii) utilisation of specific features of electrogenic cells, e.g., neuronal cells, or muscle cells by measuring the extracellular potentials [44,45].

3.3. Light Addressable Potentiometric Sensors

Light addressable potentiometric sensors (LAPS) use light to activate carriers in a semiconducting material. LAPS (Figure 3) are popular in chemical and biological applications, primarily because of high spatial resolution and because the measuring point can be selected by a scanning light beam [46].

Figure 3. Schematic set up of a LAPS device with living cells and light sources (RE: reference electrode; Vbias: bias voltage; Iph: generated photocurrent).

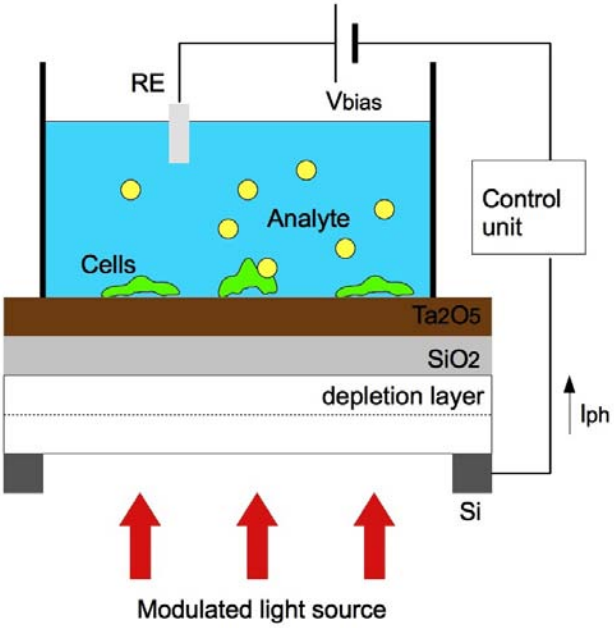

Electrochemical interactions between the transducer surface and the analyte generate surface potentials. They are then added to the applied DC bias voltage. To detect the gate insulator surface potential, the LAPS is illuminated with a modulated light source using laser beam or light emitting diodes (LED) in portable devices. The light source induces an AC photo current, which is measured as the sensor signal.

The light pointer in a LAPS device can be addressed at individual cells in culture, allowing for single cell analysis on chip. Although many cells are cultured on a chip surface, only the cell(s) in the illuminated area is interrogated.

4. Applications

Cell-based sensors are applicable in many areas of medical diagnostics, and have a large potential in the emphasized fields.

4.1. Pathogens and Toxins

Electrochemical impedance spectroscopy measured on cells cultured on a microelectrode array is very sensitive to small changes in the cell membrane capacitance and resistance (Figure 4). These parameters are good indicators for the well being of cells at a given cell morphology. The real time detection of cell impedance gives an efficient and rapid technique for non-invasive monitoring of the response of human cells in culture to the challenge of a virus infection [25,47,48], or a drug [49,50].

Figure 4. Cell-based biosensor. (**a**) All polymer microdevice with two functional channels fabricated in TOPAS (uncolored) and PEDOT:TsO (blue). (**b**) Healthy cells cultured on PEDOT:TsO microelectrodes in the biosensor.

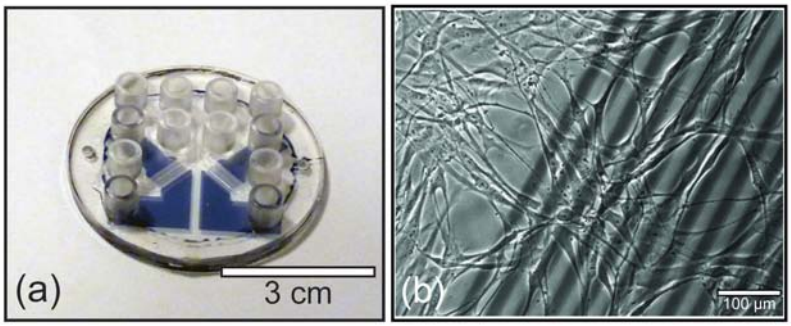

Cardiac cell-based biosensors have been used to study toxicity induced by a drug or heavy metal ions [51–53]. The toxic effects of ions lead to clear alterations in the action potential and were detectable within fifteen minutes [52].

4.2. Single Cell Analysis

Single cell analysis is of importance in certain aspects of medicine. Regeneration of neural tissue is very complex and requires multiple signals for axonal regrowth and functional recovery of damaged nerve tissue [54]. Microsystems allow cultures to be seeded at very high density in two or three dimensions to achieve cell-cell contact and generate an environment more anatomically similar to living tissue. Scaffolds of electrically conducting fibers immobilized with neural growth factor on PPy present multiple stimuli simultaneously and are attractive for neural cells, serving as a guidance and supporting neurite formation and outgrowth [55]. Understanding the complex signaling of neurites is a key in the process of understanding neurite migration and differentiation. A quantitative measure of cellular transmitter release by neuronal cells was measured by electrochemical techniques. The cells were trapped in a closed microchip close to a band of microelectrodes [56].

4.3. Drug Discovery

Cell-based biosensors with intact living cells as the sensor allow for screening of virtually any drug. Synchronization of the cell cycle by serum starvation is a common technique to enhance the cellular response [57].

Wound healing is complex process and it can be examined and accelerated in a biosensor [58].

Migration assays and invasion assays are well suited for drug screening by rapidly and quantitatively measuring cell movement and the ability to traverse physical barriers. The microfluidic technology presents an appealing strategy to control fluid flow necessary to generate gradients on a scale suitable for cellular migration studies. New gradient generating methods to study chemotactic [59–61] or haptotactic [62] cell migration are considered more advantageous than conventional methods such as the transwell assay [63]. A novel microfluidic migration device imitates the physiological conditions of cell transmigration (Figure 5) [64]. The principles of a shear flow chamber were combined with the transwell assay in a microfluidic system that closely resembles the natural environment of migrating immune cells. Microchannels were physically separated by a porous membrane, and the cells actively migrated towards a pore in response to a chemotactic gradient, similarly to extravasation from blood vessels to underlying tissue. In this work, the transmigrating cells were mapped using fluorescent imaging, but an electrode array could be implemented to count migrating immune cells by electrochemical impedance spectroscopy.

Figure 5. Microfluidic device for studies of chemotactic cell migration. The chip was fabricated in PMMA and contained separate channels for cells and chemoattractants. This type of assay has application in drug screening [64].

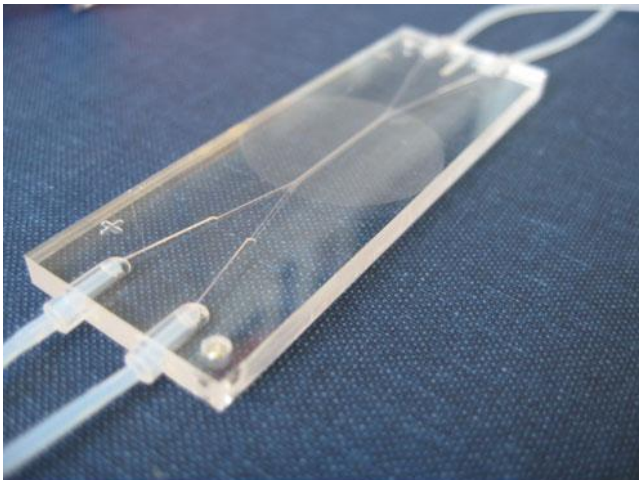

4.4. Cancer

Early-stage diagnosis of cancer is the critical factor for treatment and patient survival. Primary tumors can often be removed with advanced therapies and drugs. Unfortunately, many cancers are diagnosed after cancer cells have escaped from the primary tumor site, circulated with the blood stream to form secondary tumor sites throughout the body. Currently, invasion and metastases of tumors are the main reasons for patient mortality. The invasion properties of different cell lines were studied in a cell-based biosensor by electrical impedance spectroscopy [65]. New techniques are required for diagnosis and monitoring. Sensors with ultra-low detection limits can be targeted towards emerging cancer biomarkers (indicators of tumor growth), cancer cells in circulating blood (indicators of metastasis) and to determine drug effectiveness at various target sites. Precise counting of breast cancer cells was achieved on a gold microelectrode array via label free electrochemical impedance spectroscopy based detection at a single cell level [66,67].

5. Conclusion and Outlook

Elegant multidisciplinary research collaborations have provided new horizons for cell-based sensing in medical diagnostics. Lately, we have seen a wide variety of microsystem based sensors with many different clinical applications such as high throughput drug screening. Cell-based biosensors further have application in tissue engineering for regeneration of highly organized tissues facilitated by the patterning technologies. Some of the new cell-based biosensing systems will meet the requirements of high specificity and sensitivity, low cost, simplicity, and rapid readout—they raise the bar for sensors and qualify for point of care systems. There are limitations to cell-based biosensors such as shelf life, and it will be a challenge for researchers to bring the sensors out of the laboratory to be managed by untrained personnel. However, cell-based biosensors have a unique ability to simulate the physiological *in vivo* response, and will certainly continue to revolutionize sensing of pathogens and toxins in the near future.

Acknowledgements

This work was supported by the Danish Research Council for Technology and Production Sciences and the Technical University of Denmark.

References

1. Yan, M.; Huang, X.; Jia, Q.; Nadipalli, R.; Wang, T.; Shang, Y.; Yu, H.; Je, M.; Yeo, K. High-speed CMOS image sensor for high-throughput lensless microfluidic imaging system. *Proc. SPIE* **2012**, doi: 10.1117/12.911962.
2. Cheng, X.; Chen, G.; Rodriguez, W.R. Micro- and nanotechnology for viral detection. *Anal. Bioanal. Chem.* **2009**, *393*, 487–501.
3. Lazcka, O.; Del Campo, F.J.; Munoz, F.X. Pathogen detection: A perspective of traditional methods and biosensors. *Biosens. Bioelectron.* **2007**, *22*, 1205–1217.
4. Wang, P.; Xu, G.; Qin, L.; Xu, Y.; Li, R. Cell-based biosensors and its application in biomedicine. *Sens. Actuator. B Chem.* **2005**, *108*, 576–584.
5. Banerjee, P.; Bhunia, A.K. Mammalian cell-based biosensors for pathogens and toxins. *Trends Biotech.* **2009**, *27*, 179–188.
6. Pancrazio, J.; Whelan, J.; Borkholder, D.; Ma, W.; Stenger, D. Development and application of cell-based biosensors. *Ann. Biomed. Eng.* **1999**, *27*, 697–711.
7. Cheran, L.E.; Cheung, S.; Wang, X.; Thompson, M. Probing the bioelectrochemistry of living cells. *Electrochimi. Acta* **2008**, *53*, 6690–6697.
8. Ding, L.; Du, D.; Zhang, X.; Ju, H. Trends in Cell-Based Electrochemical Biosensors. *Curr. Med. Chem.* **2008**, *15*, 3160–3170.
9. Stott, S.L.; Hsu, C.H.; Tsukrov, D.I.; Yu, M.; Miyamoto, D.T.; Waltman, B.A.; Rothenberg, S.M.; Shah, A.M.; Smas, M.E.; Korir, G.K.; *et al.* Isolation of circulating tumor cells using a microvortex-generating herringbone-chip. *Proc. Natl. Acad. Sci. USA* **2010**, *107*, 18392–18397.

10. Rosenthal, A.; Macdonald, A.; Voldman, J. Cell patterning chip for controlling the stem cell microenvironment. *Biomaterials* **2007**, *28*, 3208–3216.
11. Kim, L.; Toh, Y.C.; Voldman, J.; Yu, H. A practical guide to microfluidic perfusion culture of adherent mammalian cells. *Lab Chip* **2007**, *7*, 681–694.
12. Svendsen, W.; Castillo-Len, J.; Lange, J.; Sasso, L.; Olsen, M.; Abaddi, M.; Andresen, L.; Levinsen, S.; Shah, P.; Vedarethinam, I.; Dimaki, M. Micro and nano-platforms for biological cell analysis. *Sens. Actuator. A Phys.* **2011**, *172*, 54–60.
13. Ng, J.; Gitlin, I.; Stroock, A.; Whitesides, G. Components for integrated poly(dimethylsiloxane) microfluidic systems. *Electrophoresis* **2002**, *23*, 3461–3473.
14. Wright, D.; Rajalingam, B.; Karp, J.M.; Selvarasah, S.; Ling, Y.; Yeh, J.; Langer, R.; Dokmeci, M.R.; Khademhosseini, A. Reusable, reversibly sealable parylene membranes for cell and protein patterning. *J. Biomed. Mater. Res. A* **2008**, *85A*, 530–538.
15. Becker, H.; Locascio, L. Polymer microfluidic devices. *Talanta* **2002**, *56*, 267–287.
16. Sia, S.; Whitesides, G. Microfluidic devices fabricated in poly(dimethylsiloxane) for biological studies. *Electrophoresis* **2003**, *24*, 3563–3576.
17. Utko, P.; Persson, F.; Kristensen, A.; Larsen, N.B. Injection molded nanofluidic chips: Fabrication method and functional tests using single-molecule DNA experiments. *Lab Chip* **2011**, *11*, 303–308.
18. Hansen, T.S.; Selmeczi, D.; Larsen, N.B. Fast prototyping of injection molded polymer microfluidic chips. *J. Micromech. Microeng.* **2010**, *20*, doi: 10.1088/0960-1317/20/1/015020.
19. He, Q.; Sudibya, H.G.; Yin, Z.; Wu, S.; Li, H.; Boey, F.; Huang, W.; Chen, P.; Zhang, H. Centimeter-long and large-scale micropatterns of reduced graphene oxide films: Fabrication and sensing applications. *ACS Nano* **2010**, *4*, 3201–3208.
20. Nguyen, P.; Berry, V. Graphene interfaced with biological cells: Opportunities and challenges. *J. Phys. Chem. Lett.* **2012**, *3*, 1024–1029.
21. Rozlosnik, N. New directions in medical biosensors employing poly(3,4-ethylenedioxy thiophene) derivative-based electrodes. *Anal. Bioanal. Chem.* **2009**, *395*, 637–645.
22. Balamurugan, A.; Chen, S.M. Poly(3,4-ethylenedioxythiophene-co-(5-amino-2-naphthalenesulfonic acid)) (PEDOT-PANS) film modified glassy carbon electrode for selective detection of dopamine in the presence of ascorbic acid and uric acid. *Anal. Chim. Acta* **2007**, *596*, 92–98.
23. Vasantha, V.S.; Chen, S.M. Electrocatalysis and simultaneous detection of dopamine and ascorbic acid using poly(3,4-ethylenedioxy)thiophene film modified electrodes. *J. Electroanal. Chem.* **2006**, *592*, 77–87.
24. Larsen, S.T.; Vreeland, R.F.; Heien, M.L.; Taboryski, R. Characterization of poly(3,4-ethylenedioxythiophene):tosylate conductive polymer microelectrodes for transmitter detection. *Analyst* **2012**, *137*, 1831–1836.
25. Kiilerich-Pedersen, K.; Poulsen, C.R.; Jain, T.; Rozlosnik, N. Polymer based biosensor for rapid electrochemical detection of virus infection of human cells. *Biosens. Bioelectron.* **2011**, *28*, 386–392.
26. Thein, M.; Asphahani, F.; Cheng, A.; Buckmaster, R.; Zhang, M.; Xu, J. Response characteristics of single-cell impedance sensors employed with surface-modified microelectrodes. *Biosens. Bioelectron.* **2010**, *25*, 1963–1969.

27. Wu, Y.L.; Hsu, P.Y.; Hsu, C.P.; Wang, C.C.; Lee, L.W.; Lin, J.J. Electrical characterization of single cells using polysilicon wire ion sensor in an isolation window. *Biomed. Microdevices* **2011**, *13*, 939–947.
28. Wu, Y.L.; Hsu, P.Y.; Hsu, C.P.; Lin, J.J. Detecting the effect of targeted anti-cancer medicines on single cancer cells using a poly-silicon wire ion sensor integrated with a confined sensitive window. *Biomed. Microdevices* **2012**, *14*, 839–848.
29. Velve-Casquillas, G.; Berre, M.L.; Piel, M.; Tran, P.T. Microfluidic tools for cell biological research. *Nano Today* **2010**, *5*, 28–47.
30. Barkefors, I.; Le Jan, S.; Jakobsson, L.; Hejll, E.; Carlson, G.; Johansson, H.; Jarvius, J.; Park, J.W.; Li Jeon, N.; Kreuger, J. Endothelial cell migration in stable gradients of vascular endothelial growth factor A and fibroblast growth factor 2. *J. Biol. Chem.* **2008**, *283*, 13905–13912.
31. Tang, Z.; Akiyama, Y.; Itoga, K.; Kobayashi, J.; Yamato, M.; Okano, T. Shear stress-dependent cell detachment from temperature-responsive cell culture surfaces in a microfluidic device. *Biomaterials* **2012**, *33*, 7405 – 7411.
32. Buchinger, S.; Grill, P.; Morosow, V.; Ben-Yoav, H.; Shacham-Diamand, Y.; Biran, A.; Pedahzur, R.; Belkin, S.; Reifferscheid, G. Evaluation of chrono-amperometric signal detection for the analysis of genotoxicity by a whole cell biosensor. *Anal. Chim. Acta* **2010**, *659*, 122–128.
33. Chen, J.; Zhang, J.; Yang, H.; Fu, F.; Chen, G. A strategy for development of electrochemical DNA biosensor based on site-specific DNA cleavage of restriction endonuclease. *Biosens. Bioelectron.* **2010**, *26*, 144–148.
34. Primiceri, E.; Chiriaco, M.S.; Ionescu, R.E.; D'Amone, E.; Cingolani, R.; Rinaldi, R.; Maruccio, G. Development of EIS cell chips and their application for cell analysis. *Microelectron. Eng.* **2009**, *86*, 1477–1480.
35. Diouani, M.F.; Helali, S.; Hafaid, I.; Hassen, W.M.; Snoussi, M.A.; Ghram, A.; Jaffrezic-Renault, N.; Abdelghani, A. Miniaturized biosensor for avian influenza virus detection. *Mater. Sci. Eng. C* **2008**, *28*, 580–583.
36. Hnaien, M.; Diouani, M.F.; Helali, S.; Hafaid, I.; Hassen, W.M.; Renault, N.J.; Ghram, A.; Abdelghani, A. Immobilization of specific antibody on SAM functionalized gold electrode for rabies virus detection by electrochemical impedance spectroscopy. *Biochem. Eng. J.* **2008**, *39*, 443–449.
37. Daniels, J.S.; Pourmand, N. Label-free impedance biosensors: Opportunities and challenges. *Electroanalysis* **2007**, *19*, 1239–1257.
38. Mathebula, N.S.; Pillay, J.; Toschi, G.; Verschoor, J.A.; Ozoemena, K.I. Recognition of anti-mycolic acid antibody at self-assembled mycolic acid antigens on a gold electrode: A potential impedimetric immunosensing platform for active tuberculosis. *Chem. Commun.* **2009**, doi: 10.1039/B905192A.
39. Arias, L.R.; Perry, C.A.; Yang, L. Real-time electrical impedance detection of cellular activities of oral cancer cells. *Biosens. Bioelectron.* **2010**, *25*, 2225–2231.
40. Ona, T.; Shibata, J. Advanced dynamic monitoring of cellular status using label-free and non-invasive cell-based sensing technology for the prediction of anticancer drug efficacy. *Anal. Bioanal. Chem.* **2010**, *398*, 2505–2533.

41. Cheung, K.; Gawad, S.; Renaud, P. Impedance spectroscopy flow cytometry: On-chip label-free cell differentiation. *Cytometry Part A* **2005**, *65A*, 124–132.
42. Giaever, I.; Keese, C.R. Use of electric-fields to monitor the dynamic aspect of cell behavior in tissue-culture. *IEEE Trans. Biomed. Eng.* **1986**, *33*, 242–247.
43. Keese, C.; Giaever, I. A biosensor that monitors cell morphology with electrical fields. *IEEE Eng. Med. Biol. Mag.* **1994**, *13*, 402–408.
44. Offenhausser, A.; Knoll, W. Cell-transistor hybrid systems and their potential applications. *Trends Biotech.* **2001**, *19*, 62–66.
45. Poghossian, A.; Ingebrandt, S.; Offenhusser, A.; Schning, M. Field-effect devices for detecting cellular signals. *Semin. Cell Dev. Biol.* **2009**, *20*, 41–48.
46. Schoening, M.J.; Poghossian, A. Bio FEDs (Field-Effect devices): State-of-the-art and new directions. *Electroanalysis* **2006**, *18*, 1893–1900.
47. McCoy, M.H.; Wang, E. Use of electric cell-substrate impedance sensing as a tool for quantifying cytopathic effect in influenza A virus infected MDCK cells in real-time. *J. Virol. Meth.* **2005**, *130*, 157–161.
48. Campbell, C.E.; Laane, M.M.; Haugarvoll, E.; Giaever, I. Monitoring viral-induced cell death using electric cell-substrate impedance sensing. *Biosens. Bioelectron.* **2007**, *23*, 536–542.
49. Arndt, S.; Seebach, J.; Psathaki, K.; Galla, H.J.; Wegener, J. Bioelectrical impedance assay to monitor changes in cell shape during apoptosis. *Biosens. Bioelectron.* **2004**, *19*, 583–594.
50. Solly, K.; Wang, X.; Xu, X.; Strulovici, B.; Zheng, W. Application of real-time cell electronic sensing (RT-CES) technology to cell-based assays. *ASSAY Drug Dev. Technol.* **2004**, *2*, 363–372.
51. Pancrazio, J.; Bey, P.; Cuttino, D.; Kusel, J.; Borkholder, D.; Shaffer, K.; Kovacs, G.; Stenger, D. Portable cell-based biosensor system for toxin detection. *Sens. Actuator. B Chem.* **1998**, *53*, 179–185.
52. Liu, Q.; Cai, H.; Xu, Y.; Xiao, L.; Yang, M.; Wang, P. Detection of heavy metal toxicity using cardiac cell-based biosensor. *Biosens. Bioelectron.* **2007**, *22*, 3224–3229.
53. Gray, S.A.; Kusel, J.K.; Shaffer, K.M.; Shubin, Y.S.; Stenger, D.A.; Pancrazio, J.J. Design and demonstration of an automated cell-based biosensor. *Biosens. Bioelectron.* **2001**, *16*, 535–542.
54. Schmidt, C.; Leach, J. Neural tissue engineering: Strategies for repair and regeneration. *Annu. Rev. Biomed. Eng.* **2003**, *5*, 293–347.
55. Lee, J.Y.; Bashur, C.A.; Milroy, C.A.; Forciniti, L.; Goldstein, A.S.; Schmidt, C.E. Nerve growth factor-immobilized electrically conducting fibrous scaffolds for potential use in neural engineering applications. *IEEE Trans. Nanobiosci.* **2012**, *11*, 15–21.
56. Larsen, S.; Matteucci, M.; Taboryski, R., Conductive Polymer Microelectrodes for On-Chip Measurement of Transmitter Release from Living Cells. In *Proceedings of Nanotech Conference and Expo 2012*, Santa Clara, CA, USA, 18–21 June 2012; Volume 2, pp. 302–305.
57. Migita, S.; Wada, K.I.; Taniguchi, A. Reproducible fashion of the HSP70B' promoter-induced cytotoxic response on a live cell-based biosensor by cell cycle synchronization. *Biotechnol. Bioeng.* **2010**, *107*, 561–565.
58. Nie, F.Q.; Yamada, M.; Kobayashi, J.; Yamato, M.; Kikuchi, A.; Okano, T. On-chip cell migration assay using microfluidic channels. *Biomaterials* **2007**, *28*, 4017–4022.

59. Liu, Y.; Sai, J.; Richmond, A.; Wikswo, J.P. Microfluidic switching system for analyzing chemotaxis responses of wortmannin-inhibited HL-60 cells. *Biomed. Microdevices* **2008**, *10*, 499–507.
60. Pihl, J.; Karlsson, M.; Chiu, D. Microfluidic technologies in drug discovery. *Drug Discov. Today* **2005**, *10*, 1377–1383.
61. Lin, F.; Butcher, E.C. T cell chemotaxis in a simple microfluidic device. *Lab Chip* **2006**, *6*, 1462–1469.
62. Georgescu, W.; Jourquin, J.; Estrada, L.; Anderson, A.R.A.; Quaranta, V.; Wikswo, J.P. Model-controlled hydrodynamic focusing to generate multiple overlapping gradients of surface-immobilized proteins in microfluidic devices. *Lab Chip* **2008**, *8*, 238–244.
63. Keenan, T.M.; Folch, A. Biomolecular gradients in cell culture systems. *Lab Chip* **2008**, *8*, 34–57.
64. Kwasny, D.; Kiilerich-Pedersen, K.; Moresco, J.; Dimaki, M.; Rozlosnik, N.; Svendsen, W.E. Microfluidic device to study cell transmigration under physiological shear stress conditions. *Biomed. Microdevices* **2011**, *13*, 899–907.
65. Yun, Y.H.; Eteshola, E.; Bhattacharya, A.; Dong, Z.; Shim, J.S.; Conforti, L.; Kim, D.; Schulz, M.J.; Ahn, C.H.; Watts, N. Tiny medicine: Nanomaterial-based biosensors. *Sensors* **2009**, *9*, 9275–9299.
66. Arya, S.K.; Lee, K.C.; Bin Dah'alan, D.; Daniel.; Rahman, A.R.A. Breast tumor cell detection at single cell resolution using an electrochemical impedance technique. *Lab Chip* **2012**, *12*, 2362–2368.
67. Chen, Y.; Wong, C.C.; Pui, T.S.; Nadipalli, R.; Weerasekera, R.; Chandran, J.; Yu, H.; Rahman, A.R. CMOS high density electrical impedance biosensor array for tumor cell detection. *Sens. Actuator. B Chem.* **2012**, *173*, 903–907.

5.2 Concluding Remarks

Biosensing platforms continue to gain ground i medicine and diagnostics, and the ongoing advances in cell biology and microtechnologies has contributed to the development of highly sophisticated cell based biosensors. These rapid *in vitro* screening platforms have a broad range of applications in industry and research, and having moral and ethics in mind - cellular platforms can to a certain extent replace animal based experiments.

Chapter 6

Cell Based Biosensor
Detection of Virus

6.1 Introduction

Personalized medicine and diagnostics are rapidly growing fields of research and general interest. Cell based biosensors employ living cells as sensing elements, and are important tools for individual patient care, providing information about cellular mechanisms for improved understanding of disease mechanisms, early diagnosis and targeted treatment.

By nature, cells are very selective and sensitive to small changes in the cell environment. Culturing cells on microelectrodes in microfluidic systems offer a high degree of control of the local cell environment, and precise analysis of cell development in response to stimulation by electrical detection methods. Compared to traditional cell culture dishes, microfluidic channels offer refined fluid control, low sample consumption and reduced interference, which is an advantage in many biological and medical applications [62].

The reference standards for laboratory confirmation of many virus infections are reverse transcription-polymerase chain reaction (RT-PCR) or viral culture. High sensitivity and specificity of RT-PCR makes it attractive, however the method lacks indication of the viability of virus or on-going viral replication, and moreover, it is expensive, time consuming and require well equipped laboratories and trained personnel. RT-PCR is also associated with multiple potential technical errors, including failed extractions and problems with PCR inhibition [63]. Viral culture is time consuming, and depending on the type of virus it may require a week or more to obtain the results.

In this paper, we present a biosensor for fast and sensitive detection of viral infections in cell culture. An all polymer microfluidic system was fabricated in Topas® by injection molding, and conductive polymer (PEDOT:TsO) microelectrodes were patterned using standard photolitographic processing techniques. Human cells were immobilized on the conductive polymer microelectrodes, and the effects of infection with human cytomegalovirus were studied by electrochemical impedance spectroscopy and video time lapse microscopy.

Biosensors and Bioelectronics 28 (2011) 386–392

Contents lists available at ScienceDirect

Biosensors and Bioelectronics

journal homepage: www.elsevier.com/locate/bios

Polymer based biosensor for rapid electrochemical detection of virus infection of human cells

Katrine Kiilerich-Pedersen[a], Claus R. Poulsen[a], Titoo Jain[b], Noemi Rozlosnik[a,*]

[a] Technical University of Denmark, Department of Micro- and Nanotechnology, Oersteds Plads 345 East, DK-2800 Kongens Lyngby, Denmark
[b] University of Copenhagen, Nano-Science Center and Department of Chemistry, Universitetsparken 5, DK-2100 Copenhagen, Denmark

ARTICLE INFO

Article history:
Received 11 May 2011
Received in revised form 18 July 2011
Accepted 21 July 2011
Available online 28 July 2011

Keywords:
Conductive polymer
PEDOT:TsO
Electrochemical impedance spectroscopy (EIS)
Human cytomegalovirus (CMV)
Human fibroblast cells
Atomic force microscopy (AFM)
Scanning ion conductance microscopy (SICM)

ABSTRACT

The demand in the field of medical diagnostics for simple, cost efficient and disposable devices is growing. Here, we present a label free, all-polymer electrochemical biosensor for detection of acute viral disease. The dynamics of a viral infection in human cell culture was investigated in a micro fluidic system on conductive polymer PEDOT:TsO microelectrodes by electrochemical impedance spectroscopy and video time lapse microscopy.

Employing this sensitive, real time electrochemical technique, we could measure the immediate cell response to cytomegalovirus, and detect an infection within 3 h, which is several hours before the cytopathic effect is apparent with conventional imaging techniques. Atomic force microscopy and scanning ion conductance microscopy imaging consolidate the electrochemical measurements by demonstrating early virus induced changes in cell morphology of apparent programmed cell death.

1. Introduction

In a global community, the outbreak of infectious diseases contributes to the fear of severe pandemics, and is a source of worry for the population. In recent years, emerging viruses have been a focus of attention (e.g. Dengue virus, West Nile virus, Influenza A virus) and has thus emphasized the need for new effective tools in medical diagnostics. Conventional diagnostic methods for detection of acute viral disease, such as polymerase chain reactions (PCR) and enzyme linked immunosorbent assays (ELISA) are time consuming, labour intensive and expensive (Cheng et al., 2009; Lazcka et al., 2007). Accordingly, it is important to develop effective point-of-care tools to detect, control and confine the spread of virulent diseases in the near future.

Recently, there has been great advancements in the biosensor technology, and in particular impedimetric sensors have attracted attention for the high sensitivity, reliability and simplicity (Chen et al., 2010; Primiceri et al., 2009; Diouani et al., 2008; Hnaien et al., 2008; Daniels and Pourmand, 2007; Mathebula et al., 2009).

Among cell based assays, electrochemical impedance spectroscopy combined with microelectrode arrays provides a platform for label free detection of the cellular response to different drugs or pathogens (Arias et al., 2010; Ona and Shibata, 2010). The interaction between a cell monolayer and the electrode surface can be monitored in real time by applying a small amplitude alternate-current (AC) electric field. Cells are essentially non conducting at low frequencies and the cell membrane offers a significant barrier to current flow, so that the amplitude of the AC field is an indication of the cell volume or size (Cheung et al., 2005). Average alterations in the three dimensional shape of cells is then computed by integrating over a monolayer of hundreds or thousands of cells. The measured impedance reflects changes in the attachment and morphology of cells, and reaches its maximum when the electrode is completely covered (Giaever and Keese, 1986; Keese and Giaever, 1994).

Electrochemical impedance spectroscopy (EIS) measured on cells cultured on a microelectrode array is very sensitive to small changes in the cell membrane capacitance and resistance. These parameters are good indicators for the well being of cells at a given cell morphology. The real time detection of cell impedance gives an efficient and rapid technique for non invasive monitoring of the response of human cells in culture to the challenge of a virus infection (McCoy and Wang, 2005; Campbell et al., 2007).

* Corresponding author.
E-mail addresses: noemi.rozlosnik@nanotech.dtu.dk, noro58@gmail.com (N. Rozlosnik).

0956-5663/$ – see front matter © 2011 Elsevier B.V. All rights reserved.
doi:10.1016/j.bios.2011.07.053

In general, viral infections can induce degenerative morphological changes in cell cultures; cell detachment from substrate, release of cell–cell adhesions, cell round up and eventually cell death. Beside the morphological effects, these changes in the cells produce a decline in the resistance and an increase in the capacitance in the impedance signal (McCoy and Wang, 2005; Campbell et al., 2007).

Polymer based microfluidic systems meet the requirements of disposable devices, low sample consumption, cost efficiency, reliability, and fast response time, which make the systems ideal for point-of-care analysis. By employing conductive polymers as electrode materials, the additional advantageous properties of inexpensive electrode fabrication and easy electrode functionalization can be achieved (Rozlosnik, 2009). This feature is of great importance in biosensor applications, where particles or cells are immobilized directly on the electrode surface.

In the present study, an all polymer microsystem with a PEDOT:TsO microelectrode array was developed and exploited for real time and label free electrochemical detection of the effect of human cytomegalovirus (CMV) on cells. In this work, we show that the novel biosensor technology demonstrates a fast and sensitive response to the small changes in the cell morphology induced by infectious agents, and thus presents a strongly competitive alternative to the current detection techniques opening a wide range of applications.

2. Experimental procedures

2.1. All polymer microdevice

The all polymer microfluidic device was composed of four layers (Fig. 1). Top and bottom pieces were fabricated from the cyclic olefin copolymer TOPAS 5013L (TOPAS Advanced Polymers, Germany; $T_g \simeq 134\,^{\circ}C$) by injection moulding (Victory 80/45 Tech, Engel, Germany). The top part contained access ports in standard luer lock size for fluid inlets, outlets and electrical connections. The second layer – microchannels and reservoirs – were defined in an 80 μm thick, pressure sensitive adhesive (PSA, ARcare 90106, Adhesive Research, USA) by laser ablation (Duo Lase CO_2 laser, Synrad Inc., USA). The electrodes in the third layer were made from a conductive polymer, poly(3,4-ethylenedioxythiophene) doped with tosylate (PEDOT:TsO). The EDOT monomer (Baytron M) and Fe(III)-tosylate (40% in butanol, Baytron C) were purchased from Bayer AG (Leverkusen, Germany). Conductive polymer coatings were fabricated using in situ polymerization of EDOT with Fe(III) tosylate as oxidation agent. This yields a highly conducting polymer (PEDOT:TsO) coating with a sheet resistance of ~100 Ω/sq (Hansen et al., 2010; Daugaard et al., 2008).

Electrodes and electrical connection patches were patterned in the PEDOT:TsO layer using standard photo lithographic processing techniques in the Danchip Cleanroom (Technical University of Denmark, Denmark).

The final chip was assembled by thermal assisted bonding at 55 °C with 55 kg force applied for 5 min in an in house build, LabView (National Instruments, USA) controlled press. Prior to the bonding step, top and bottom pieces with the patterned PEDOT:TsO electrode layer were cleaned in air plasma (50 W, 30 s; OEM-6AM-1B, ENI Power Systems, USA)

2.2. Cell culture

Human foreskin fibroblast (HFF; ATCC Cat. No. SCRC-1041; LOT: 58592555) cells were cultured in monolayers in a humidified incubator at 37 °C, 5% CO_2 in Dulbecco's modified Eagle's medium (DMEM, Invitrogen, Carlsbad, California, USA) supplemented with 10% Fetal Bovine Serum (FBS, F7524, Sigma, St. Louis, Missouri, USA), Penicillin 10,000 U/ml, and Streptomycin 10,000 μg/ml (PS, DE17-602E, Lonza, Basel, Switzerland). The cells were subcultured by trypsination for maintenance every third day, or at ~80–90% confluence.

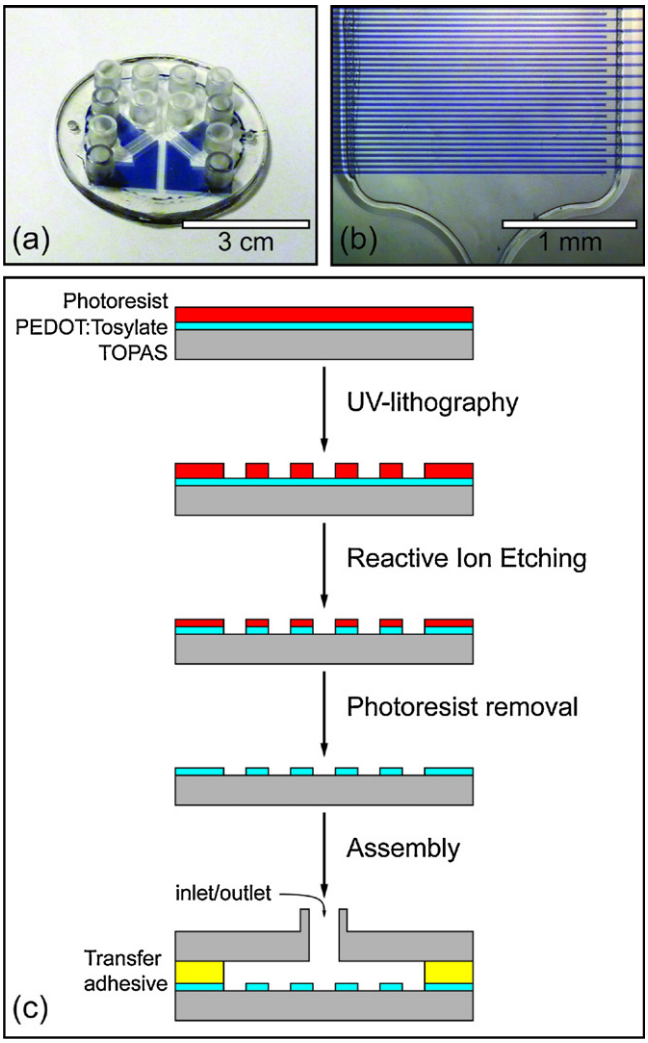

Fig. 1. Microdevice production: (a) Microdevice with two functional channels fabricated in TOPAS (uncolored) and PEDOT:TsO (blue), (b) microchannel with interdigitated microelectrode array, and (c) schematic representation of fabrication steps. (For interpretation of the references to color in this figure legend, the reader is referred to the web version of the article.)

2.3. Preparation of virus stock

Human CMV, (Towne strain; kindly provided by Thomas Kledal, Inagen ApS, Denmark) was employed as infectious agent against HFF cells. Human CMV is a ubiquitous β-herpesvirus that causes widespread, persistent infection in the human host. Virus was propagated and titered in HFFs, and infection of cells was performed in DMEM supplemented with 10% Nu Serum (355500, BD Biosciences), and 1% PS. Virus with a multiplicity of infection (MOI) of 0.01 was adsorbed for 2 h at 37 °C, overlaid with medium, and incubated for the required number of hours post infection (hpi). The cell medium was changed at 100% cytopathic effect, and virus was harvested two days later.

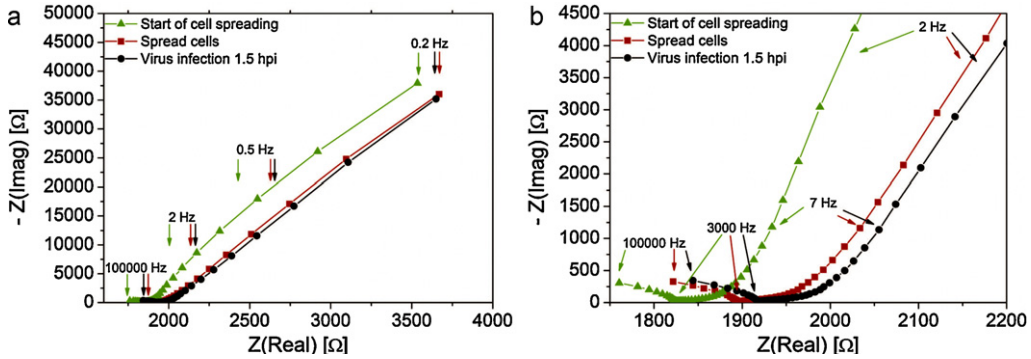

Fig. 2. EIS spectra of the impedimetric sensor presented in Nyquist plots. (a) The full recoded range, and (b) zoom in higher frequency regime. The green, red and black traces refer to (i) immediately before cells were seeded in the microchip, (ii) 14 h after cells seeding, and (iii) cells infected with human CMV, respectively. (For interpretation of the references to color in this figure legend, the reader is referred to the web version of the article.)

2.4. Virus purification

Medium from infected cell cultures was collected and centrifuged at 1260 × *g* for 10 min at 4 °C, and the virus was sedimented by centrifugation at 24, 336 × *g* for 1 h at 4 °C. The pelleted virus was resuspended in DMEM supplemented with 1% PS, layered over 20% sorbitol in Tris-buffered saline, and purified by centrifugation at 50, 228 × *g* over night at 4 °C. The pelleted virus was resuspended in DMEM supplemented with 1% PS, aliquoted, and stored at −80 °C. Virus titer was determined by plaque titration assay using methyl cellulose and crystal violet staining.

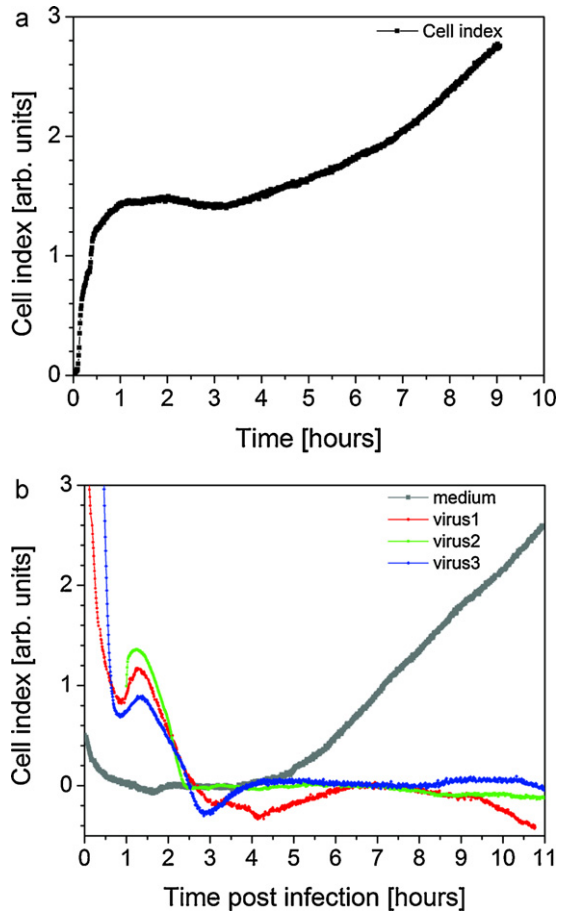

Fig. 3. Electrochemical detection of cell spreading and proliferation (a) and the effect of human CMV infection (b) on HFF cells cultured on PEDOT:TsO microelectrodes in the biosensor. The cell index – defined in Eq. (1) – was measured at a frequency of 2 Hz. The green, red and blue traces refer to three independent measurements on cells infected with human CMV at a MOI of 3 at $t = 0$. The grey trace refers to the measurement adding cell medium instead of virus containing solution at $t = 0$. (For interpretation of the references to color in this figure legend, the reader is referred to the web version of the article.)

2.5. EIS on cell culture

Healthy HFFs were seeded directly on a conductive polymer electrode surface in the micro channel of the chip (Fig. 1), and allowed to attach and spread on the substrate and acclimatize over night. EIS was used to monitor the electrical properties of the cell monolayer before and after the introduction of pathogen. The microchip was placed in a temperature controlled incubation chamber, and EIS experimentation (no redox couple added) was carried out in a tightly controlled environment at 37 °C.

Impedance spectra were recorded every 33 s in the frequency range from 0.2 Hz to 100 KHz with an amplitude of 10 mV in a two-electrode setup.

The optimal frequency for the time dependent analysis – determined by the highest response to changes on the cells – was found at 2 Hz (Fig. 2). This frequency was used for all analyses. We defined a cell index

$$\mathrm{CI} = (Z_{\mathrm{cell}}(t)Z_{\mathrm{cell}}(0) - 1) \cdot 100 \quad (1)$$

where $Z_{\mathrm{cell}}(0)$ and $Z_{\mathrm{cell}}(t)$ are the measured impedance on the chip at the beginning of the measurement and after a time t, respectively.

The cytopathic effect on cells was monitored in an inverted phase contrast microscope (Nikon Eclipse Ti-S/L100, Japan) with auto focusing controlled by dedicated software. A digital camera (VisiCam 3000, VWR) recorded time lapse movies with intervals of 15 min for 20 h. In the presented results, cells were inoculated with human CMV at an MOI of 3.

2.6. Imaging virus infected cells

HFFs were grown in petri dishes and infected with human CMV at a MOI of 5 in 1 ml. At given time points post infection (.5, 1, 1.5, 2, and 3 h), cells were washed twice with preheated infection medium to remove residual virus, fixed in 2% glutaraldehyde in Phosphate Buffered Saline (PBS; (1×), Lonza) for 60 min at room temperature, and washed with PBS for 15 min at 4 °C. Samples for investigations by scanning ion conductance microscopy (SICM) were stored in PBS at 4 °C. Fixed cell samples for atomic force microscopy (AFM) studies were dehydrated by increasing concentrations of ethanol (30–99%) for 3 min on a shaker at room temperature and freeze dried over night (Tojima et al., 1998; Kirk et al., 2009).

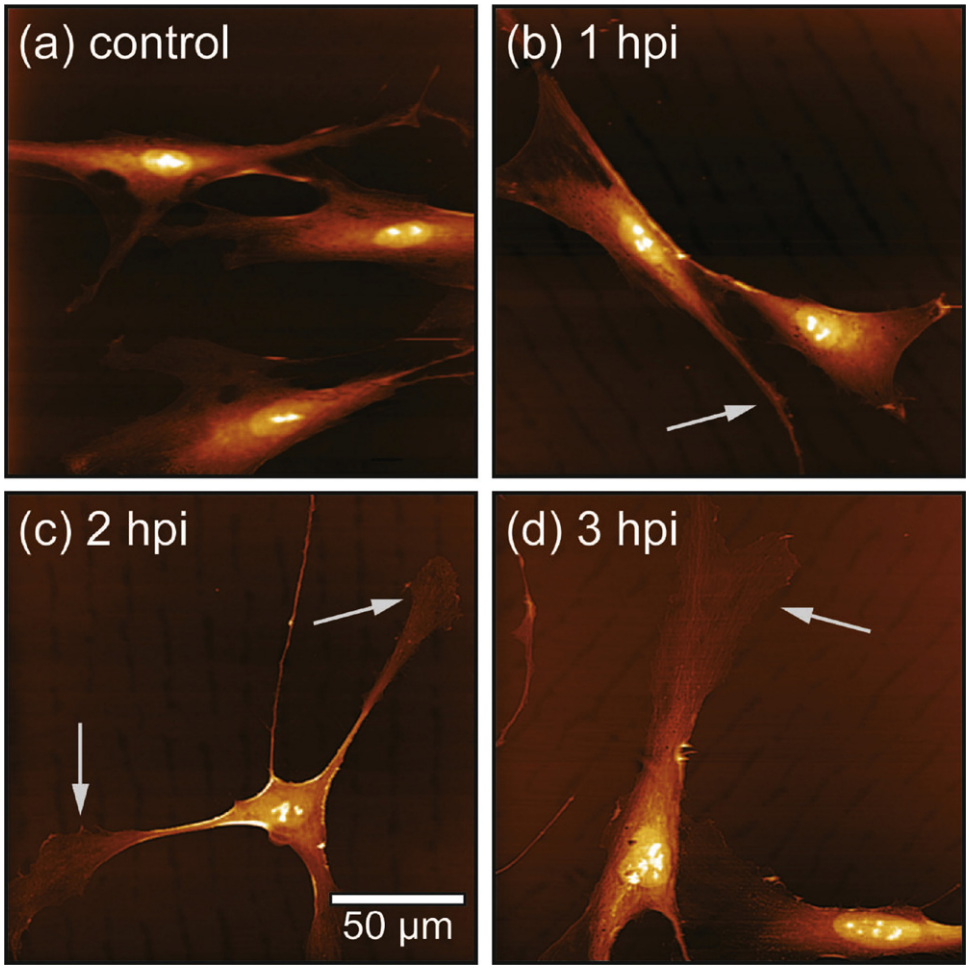

Fig. 4. AFM topography images of fixed HFF cells at different time points post infection with human CMV. Cell morphology was affected by virus, and arrows indicate some adverse cellular protrusions. (a) Control cell. (b) 1 hpi the cell has contracted and formed narrow filamentous projections. (c) 2 hpi the filamentous projections are beginning to spread-out. (d) 3 hpi the cell body has somewhat recovered its size and shape though adverse spread-out protrusions remain present. Enlargment of the nucleus and nuclear DNA fragmentation can be observed, which are the hallmarks of apoptosis.

2.7. AFM imaging

AFM images were recorded with a DME-SPM (Dualscope II, Denmark) in tapping mode using standard non contact high frequency cantilevers (TAP300Al, Budget Sensors) with a force constant of 40 N/m. AFM examinations were carried out in air at room temperature.

2.8. SICM imaging

SICM images were recorded with an XE-Bio system (Park Systems, Korea) in adaptive Approach-Retract-Scan (ARS) mode with borosilicate capillary glass pipettes (inner diameter of 80 nm). SICM examinations were carried out in PBS at room temperature.

3. Results and discussion

An all polymer microsystem was fabricated by injection moulding and standard photo lithographic processing techniques (Fig. 1), and exploited for label free, real time, electrochemical detection of infectious agents in human cell culture.

3.1. Microchip design considerations

The low cost microsystem was fabricated in TOPAS with interdigitated electrodes in the conductive polymer PEDOT:TsO. PEDOT was selected for its high environmental stability, biocompatibility, transparency to visible light and ease of processing (Rozlosnik, 2009). Before producing the all polymer microdevice, finite element method simulations (COMSOL Multiphysics 3.5) were made for optimizing the geometry of the conductive polymer electrodes and the microchannel shape (results are not shown). Microchannels offer refined fluid control, low sample consumption, and reduced interference, which is favorable in many biological and medical applications (Stott et al., 2010).

Although PEDOT:TsO is a redox system, this impedimetric sensor is based on the low frequency response (i.e. non faradaic region) with no additional electron-transfer mediators. Previous studies on impedimetric immunosensors have shown that this scheme is more amenable to biosensor applications (Berggren et al., 2001; Rickert et al., 1996), because the long term presence of a redox-couple reduces the activity of the enzymes (Rickert et al., 1996).

The biocompatibility of the all polymer biosensor chip was evaluated by culturing HFF cells in the chip for a week (see Fig. S1 in Supplemental Data available online). The cells adhered and proliferated normally on TOPAS and PEDOT:TsO, and no significant change in the morphology of cells could be observed during this period. On the other hand, the morphological changes on the virus infected cell culture could easily be observed on the samples in a time frame of 12–24 hpi (see Fig. S2 in Supplemental Data available online).

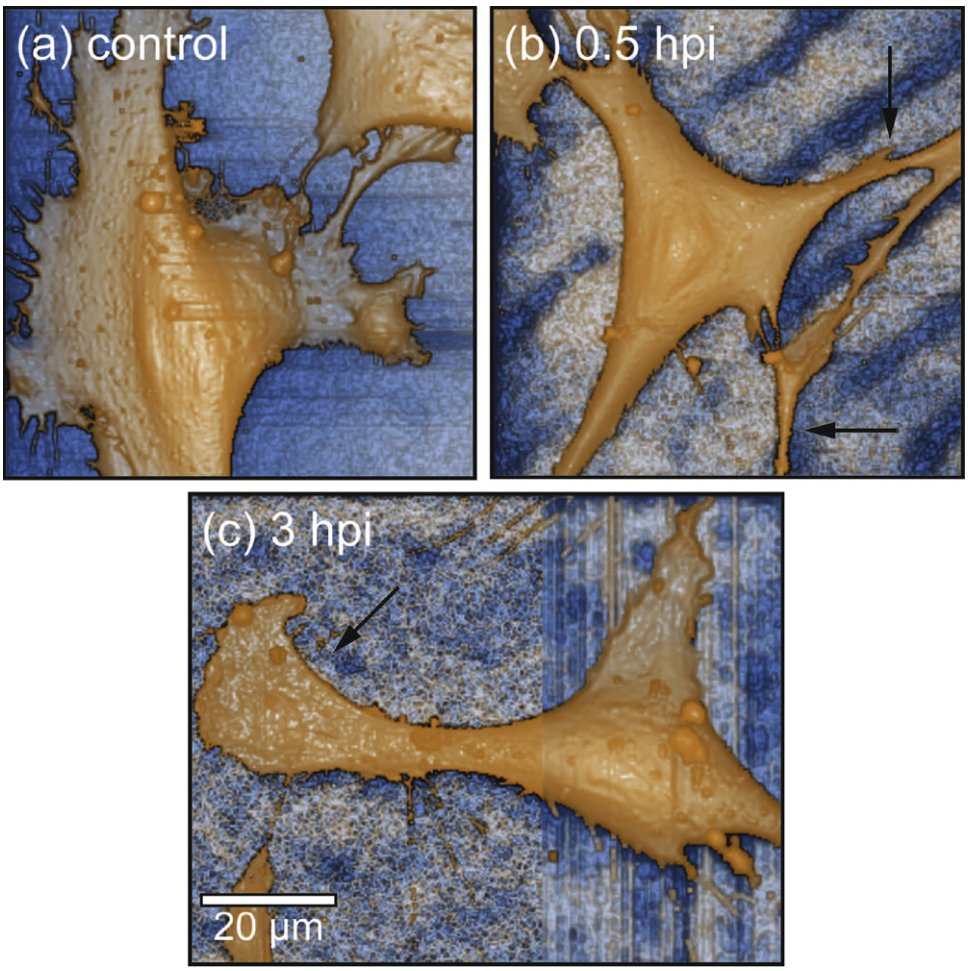

Fig. 5. SICM topography images of fixed HFF cells at different time points post infection with human CMV. Cell morphology was affected by virus, and arrows indicate some adverse cellular protrusions.(a) Control cell. (b) 30 min post infection the cell has contracted and formed narrow filamentous projections. (c) 3 hpi the cell body has recovered its size and shape though adverse spread-out protrusions remain present.

3.2. Electrochemical detection of virus

HFF cells were cultured in a monolayer on the conductive polymer substrate over night to allow the cells to get acclimatized before virus inoculation.

Fig. 2 shows the EIS spectra of the impedimetric sensor presented in Nyquist plots. The three traces refer to (i) immediately before cells were seeded in the microchip, (ii) 14 h after cells seeding, and (iii) cells infected with human CMV, respectively. The higher frequency regime (>3 kHz, semicircle) corresponds to the charge transfer at the electrode-solution interface (faradaic current) and is determined by the charge transfer resistance and the double layer capacitance, while the impedance at low frequencies is dominated by diffusion (i.e. mass transport of ions). Considering that the ion diffusion is expected to be much faster in the liquid solution than in a solid material, this part of the spectrum is anticipated to be the most sensitive for the changes on the electrode surface. At very low frequencies the measurement of one single point takes relatively long time, and the sensitivity is not improved significantly, therefore we have selected the highest reasonable frequency (i.e. 2 Hz).

The initial attachment and spreading of cells on the electrode surface was reflected by a gradual increase in the impedance until a plateau was reached (Fig. 3a), because the healthy cells act as an insulating layer on the electrode surface (Giaever and Keese, 1986) by blocking the diffusion of the ions to the electrodes. A second rise in the cell index is observed after 4 h, reflecting the proliferation of cells (Fig. 3a).

When the cells were infected with human CMV at a MOI of 3 at $t = 0$, the infection was detectable within 2 hpi – several hours before the cytopathic effect appeared. The immediate cell response to virus was mirrored by a drastic fluctuation in the impedance at low frequencies, and thus in the cell index (Fig. 3b). At 2 Hz, the absolute impedance peaked at around 1.5 hpi to reach a local maximum and then gradually decreased to a local minimum in the hours that followed, reflecting the inter- and intra-remodeling events caused by the virus. No sign of proliferation was observed on virus infected cells.

In control measurements, cell medium was added at $t = 0$ instead of virus containing medium. The absolute impedance decreased slightly to reach a plateau within 30 min after the physical manipulation. Over a period of 10 h, the absolute impedance increased in response to proliferation (Fig. 3b, grey trace).

In all cases, we observed a linear increase in the impedance signal (a drift) at all frequencies in the system. This drift arose most probably from swelling of the pressure sensitive adhesive, in which the microchannels were defined, and it was subtracted (as a base line) from each impedance curve.

To investigate the effect of the infection in microscopy, high resolution images of healthy and virus infected HFF cells were captured 1, 3 and 8 hpi with human CMV at high dose (MOI 10).

The early cellular changes were not observable in microscope (see Fig. S3 in Supplemental Data available online).

Video time lapse microscopy studies of cell cultures showed that the cytopathic effect of the virus manifested itself approximately 8–10 hpi depending on the MOI (see Virus-infected-cells.mp4 video file in Supplemental Data available online).

The application of EIS as a sensing tool for quantifying virus or drug induced cell death in cell cultures has previously been reported, e.g. cells infected with influenza A virus (McCoy and Wang, 2005), infectious pancreatic necrosis virus (Campbell et al., 2007) or infectious hematopoeitic necrosis virus (Campbell et al., 2007). In those studies, the terminal stages of cell death (lysis and detachment from substrate) were detected by EIS, rather than the early morphological features related to a virus infection. These changes are only detectable after many hours or even days, and they can also be imaged by phase contrast microcopy. In certain cases a clear spike in resistance was reported at the time of virus inoculation (McCoy and Wang, 2005; Campbell et al., 2007), however, we presume that this was attributed to physical manipulation and was not caused by the virus. In our measurements, the short term response to virus was directly monitored by the impedance changes, which allowed us to recognise the virus infection in the very early stage (Kukura et al., 2009; Seisenberger et al., 2001).

Cell survival and appearance of the cytopathic effect depend on the dilution of virus. Our preliminary impedimetric studies on cells infected with different dilutions of human CMV indicated that the change in the absolute impedance at 2 Hz was highly dependent on the amount of virus (data not shown). Our data implied that the initial peak shifted in time in response to virus dose. Further investigations are required to determine the exact concentration dependence.

3.3. Early morphological signs of apoptosis

Complementary imaging investigations were performed to understand the biology that gave rise to the drastic changes in impedance associated with virus infection.

AFM of fixed infected cells permit structural investigations of the cell surface at high resolution. Topography scans 1, 2, and 3 hpi (Fig. 4) demonstrate that the cytoskeleton organization is aberrantly rearranged within few hours post infection. During the initial phase of high dose infection (MOI of 5), the cells contract and filamentous projections occur, presumably in response to a calcium influx (Albrecht et al., 1983; Sharon-Friling et al., 2006). Around 3 hpi, the cell body recovers its size and shape, though adverse protrusions remain present. These distinct morphological features – in particular the changes in cell surface area – clarify the impedimetric changes caused by the virus infection.

The topography scans further indicate adverse nuclear morphology, which is a hallmark of apoptosis (Ghibelli et al., 1995; Gadaleta et al., 2002; Jurak et al., 2008). Some viruses have been reported to induce programmed cell death in the absence of viral replication, for instance triggered by the interaction with a cellular membrane receptor or entry and uncoating of the virion (Jan and Griffin, 1999).

AFM images were captured in air to obtain a high resolution, even though the drying process of the samples could influence the 3D cellular structure. Therefore, SICM images were captured in liquid to preserve the cellular structure.

SICM is an emerging non contact scanning tool based on ion currents through a micro pipette, providing true topography of soft samples (Boecker et al., 2007; Korchev et al., 1997). The technique has several advantages over AFM; an essential feature is that no imaging force is exerted on the sample. SICM images (Fig. 5) exhibit detailed information from the cell surface structure, and display fine structures, which are smeared out or not visible in the AFM image. Further, cell–cell interactions are more evident by SICM imaging than AFM imaging. Protrusions and cellular extensions are challenging to sight in the AFM image, however, the cytoskeleton is very detailed, an attribute to the direct mechanical contact during scanning (Rheinlaender et al., 2011). Therefore, the scans obtained by AFM and SICM imaging accentuate different morphological characteristics and thus complement each other.

4. Conclusion

In summary, we have developed a disposable polymer microsystem with PEDOT:TsO microelectrodes for rapid, label free, and real time electrochemical detection of infectious agents in human cell culture. We have demonstrated that an infection of HFF cells with human CMV causes drastic changes in the cell index within the first 3 hpi. Thus, the infection is detectable much faster than by conventional assays. To comprehend the cellular changes at this early stage in the infectious cycle, virus infected cells were examined by AFM and SICM imaging. Our investigations indicated the rearrangement of cytoskeleton organization and the early signs of apoptotic nuclei within 3 h post virus infection explaining the results of the impedance measurements. Compared to conventional inspection techniques, the use of inexpensive electrochemical biosensors (which is also suitable for mass production) can thus significantly reduce the time frame of virus diagnostics.

Acknowledgments

This work was supported by the Danish Research Council for Technology and Production Sciences and the Technical University of Denmark. The authors greatly acknowledge the technical assistance from Brian Choi and Anika Gruetzner in SICM imaging, and Park Systems Corp. and the Europe Demo. Lab. Center for providing the instrument to conduct the SICM research.

Appendix A. Supplementary Data

Supplementary data associated with this article can be found, in the online version, at doi:10.1016/j.bios.2011.07.053.

References

Albrecht, T., Speelman, D., Steinsland, O., 1983. Life Sciences 32, 2273–2278.
Arias, L.R., Perry, C.A., Yang, L., 2010. Biosensors & Bioelectronics 25, 2225–2231.
Berggren, C., Bjarnason, B., Johansson, G., 2001. Electroanalysis 13, 173–180.
Boecker, M., Anczykowski, B., Wegener, J., Schaeffer, T.E., 2007. Nanotechnology 18.
Campbell, C.E., Laane, M.M., Haugarvoll, E., Giaever, I., 2007. Biosensors & Bioelectronics 23, 536–542.
Chen, J., Zhang, J., Yang, H., Fu, F., Chen, G., 2010. Biosensors & Bioelectronics 26, 144–148.
Cheng, X., Chen, G., Rodriguez, W.R., 2009. Analytical and Bioanalytical Chemistry 393, 487–501.
Cheung, K., Gawad, S., Renaud, P., 2005. Cytometry Part A 65A, 124–132.
Daniels, J.S., Pourmand, N., 2007. Electroanalysis 19, 1239–1257.
Daugaard, A.E., Hvilsted, S., Hansen, T.S., Larsen, N.B., 2008. Macromolecules 41, 4321–4327.
Diouani, M.F., Helali, S., Hafaid, I., Hassen, W.M., Snoussi, M.A., Ghram, A., Jaffrezic-Renault, N., Abdelghani, A., 2008. Materials Science & Engineering C: Biomimetic and Supramolecular Systems 28, 580–583.
Gadaleta, P., Vacotto, M., Coulombie, F., 2002. Virus Research 86, 87–92.
Ghibelli, L., Maresca, V., Coppola, S., Gualandi, G., 1995. FEBS Letters 377, 9–14.
Giaever, I., Keese, C.R., 1986. IEEE Transactions on Biomedical Engineering 33, 242–247.
Hansen, T.S., Selmeczi, D., Larsen, N.B., 2010. Journal of Micromechanics and Microengineering 20.
Hnaien, M., Diouani, M.F., Helali, S., Hafaid, I., Hassen, W.M., Renault, N.J., Ghram, A., Abdelghani, A., 2008. Biochemical Engineering Journal 39, 443–449.
Jan, J.T., Griffin, D.E., 1999. Journal of Virology 73, 10296–10302.
Jurak, I., Schumacher, U., Simic, H., Voigt, S., Brunel, W., 2008. Journal of Virology 82, 4812–4822.
Keese, C., Giaever, I., 1994. IEEE Engineering in Medicine and Biology Magazine 13, 402–408.
Kirk, S.E., Skepper, J.N., Donald, A.M., 2009. Journal of Microscopy: Oxford 233, 205–224.

Korchev, Y., Bashford, C., Milovanovic, M., Vodyanoy, I., Lab, M., 1997. Biophysical Journal 73, 653–658.
Kukura, P., Ewers, H., Mueller, C., Renn, A., Helenius, A., Sandoghdar, V., 2009. Nature Methods 6, 923–U85.
Lazcka, O., Del Campo, F.J., Munoz, F.X., 2007. Biosensors & Bioelectronics 22, 1205–1217.
Mathebula, N.S., Pillay, J., Toschi, G., Verschoor, J.A., Ozoemena, K.I., 2009. Chemical Communications, 3345–3347.
McCoy, M.H., Wang, E., 2005. Journal of Virological Methods 130, 157–161.
Ona, T., Shibata, J., 2010. Analytical and Bioanalytical Chemistry 398, 2505–2533.
Primiceri, E., Chiriaco, M.S., Ionescu, R.E., D'Amone, E., Cingolani, R., Rinaldi, R., Maruccio, G., 2009. Microelectronic Engineering 86, 1477–1480.
Rheinlaender, J., Geisse, N.A., Proksch, R., Schaffer, T.E., 2011. Langmuir 27, 697–704.
Rickert, J., Gopel, W., Beck, W., Jung, G., Heiduschka, P., 1996. Biosensors & Bioelectronics 11, 757–768.
Rozlosnik, N., 2009. Analytical and Bioanalytical Chemistry 395, 637–645.
Seisenberger, G., Ried, M., Endress, T., Buning, H., Hallek, M., Brauchle, C., 2001. Science 294, 1929–1932.
Sharon-Friling, R., Goodhouse, J., Colberg-Poley, A.M., Shenk, T., 2006. Proceedings of the National Academy of Sciences of the United States of America 103, 19117–19122.
Stott, S.L., Hsu, C.H., Tsukrov, D.I., Yu, M., Miyamoto, D.T., Waltman, B.A., Rothenberg, S.M., Shah, A.M., Smas, M.E., Korir, G.K., Floyd Jr., F.P., Gilman, A.J., Lord, J.B., Winokur, D., Springer, S., Irimia, D., Nagrath, S., Sequist, L.V., Lee, R.J., Isselbacher, K.J., Maheswaran, S., Haber, D.A., Toner, M., 2010. Proceedings of the National Academy of Sciences of the United States of America 107, 18392–18397.
Tojima, T., Hatakeyama, D., Yamane, Y., Kawabata, K., Ushiki, T., Ogura, S., Abe, K., Ito, E., 1998. Japanese Journal of Applied Physics Part 1: Regular Papers Short Notes & Review Papers 37, 3855–3859.

Polymer Based Biosensor for Rapid Electrochemical Detection of Virus Infection of Human Cells

Katrine Kiilerich-Pedersen[a], Claus R. Poulsen[a], Titoo Jain[b], Noemi Rozlosnik[a,*]

[a] *Technical University of Denmark, Department of Micro- and Nanotechnology, Oersteds Plads 345 East, DK-2800 Kongens Lyngby, Denmark*
[b] *University of Copenhagen, Nano-Science Center and Department of Chemistry, Universitetsparken 5, DK-2100 Copenhagen, Denmark*

1. Supplementary Information

1.1. Cell Viability on Chip

The biocompatibility of the all polymer biosensor chip was evaluated by culturing HFF cells for a week. Cells were seeded on the conductive polymer microelectrode array in a microfluidic channel at low density. The cells adhered and proliferated normally on TOPAS and PEDOT:TsO, and no significant change in the morphology of cells could be observed during this period (Figure S1). On the other hand, the morphological changes on the virus infected cell culture could be observed on the samples in a time frame of $12 - 14$ hpi (Figure S2).

1.2. Video Time Lapse Microscopy Studies

HFF cells were seeded in Nunc 24-well plates and infected with human CMV (MOI 10) at $\sim$ 70 % confluence. PlasDIC images (20x, Zeiss) were captured every 15 minutes for 15 hours, and the experiment was performed in a humidified incubator at 37 °C, 5 % CO_2. The studies showed that the cytopathic effect of human CMV manifested itself around 8 hpi depending on the MOI (Figure S3).

*Corresponding author
Email address: noemi.rozlosnik@nanotech.dtu.dk (Noemi Rozlosnik)

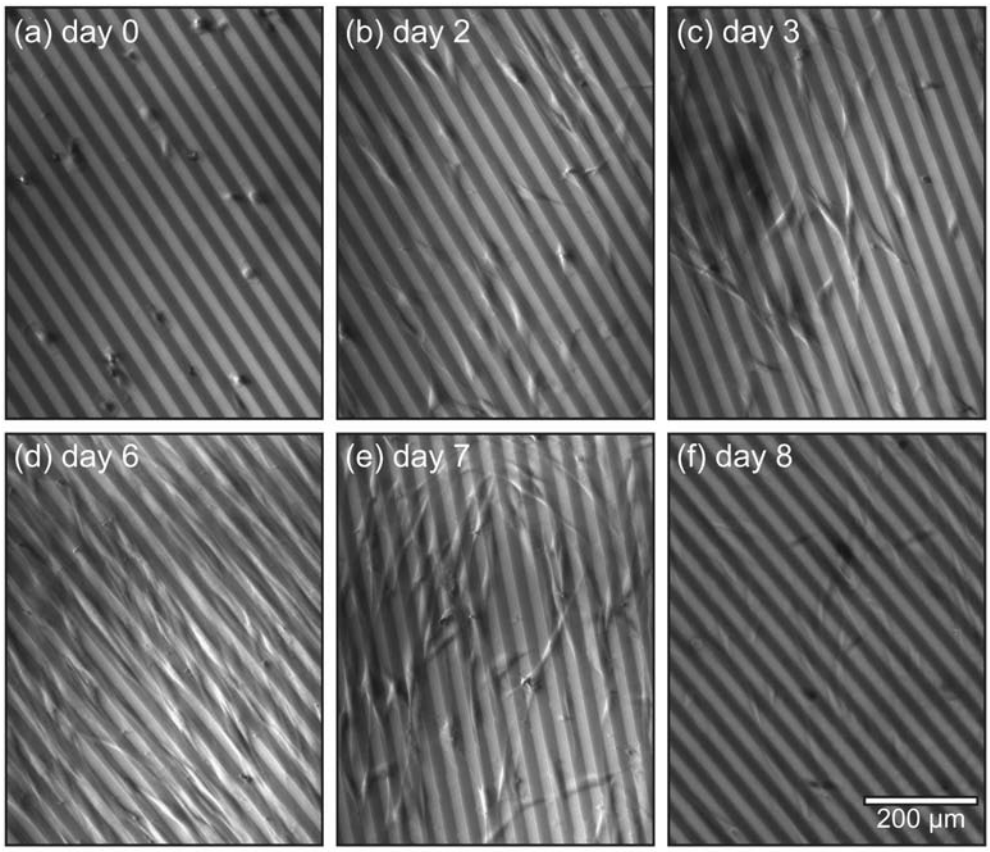

Figure S1: Cell viability on chip. HFF cells adhere, spread and proliferate on the conductive polymer electrode substrate in the microchip. On the sixth day, cells were exposed to flow at a high flow rate to decrease the number of cells.

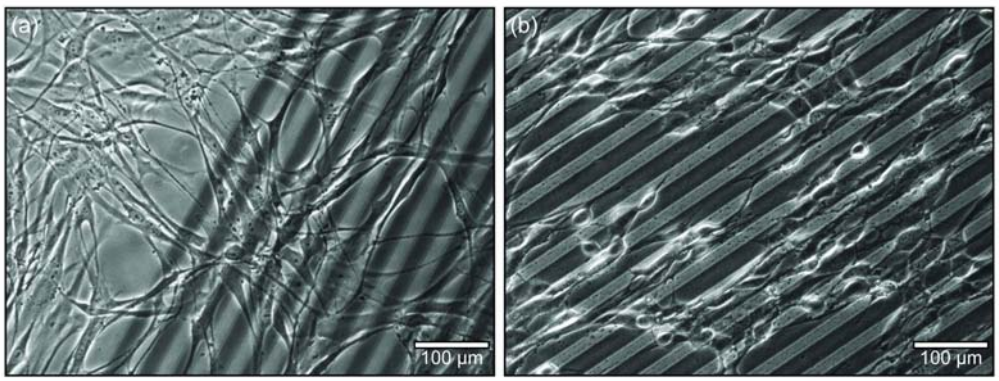

Figure S2: HFF cells cultured on PEDOT:TsO microelectrodes in the biosensor. (a) Healthy cells, and (b) cells infected with human CMV (MOI of 3, 24 hpi).

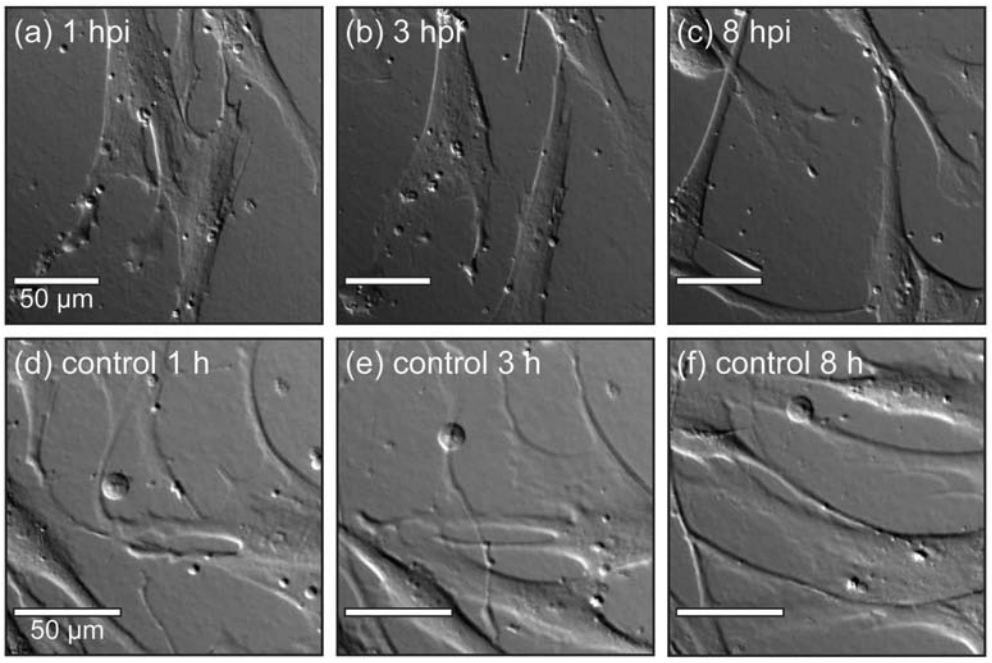

Figure S3: PlasDIC (20x) images of healthy and virus infected human foreskin fibroblast cells. Images were captured 1 , 3 and 8 hpi with human CMV at high dose (MOI 10). Video time lapse microscopy of cell cultures show that the cytopathic effect of the virus manifested itself around 8 hpi.

1.3. Virus Infection on Electrodes

A monolayer of HFF cells were infected with human CMV at an MOI of 3 at $t = 0$. Phase contrast images (10x, Zeiss) were captured every 20 minutes for 15 hours to monitor the morphological changed induced by the virus at a specific position in the micro channel. The cytopathic effect was apparent after around 8 hpi at this virus dose.

Enclosed movie (Virus-infected-cells.mpg4): HFF cells infected with human CMV at an MOI of 3.

6.2 Concluding Remarks

Electrochemical sensors have received major attention in biosensor development, because these low cost devices comprise a simple, sensitive and accurate platform for personalized medicine and diagnostics.

Electrochemical methods are very sensitive to small changes in the membrane capacitance of cells. By employing impedance spectroscopy, we could measure the immediate cell response to virus, and detect an infection with a herpes virus within three hours post infection, which is several hours before the cytopathic effect is apparent with conventional imaging techniques. In previous studies of drug- or virus induced cell death, the terminal stages of cell death rather than the early morphological signs related to the drug or virus were detected. Atomic force microscopy and scanning ion conductance microscopy imaging consolidated the electrochemical measurements by demonstrating early virus induced changes in cell morphology of apparent programmed cell death.

In its present design, the biosensor represents a competitive alternative to current laboratory based virus detection techniques in terms of sensitivity, response time, and cost.

With some modifications of the design to improve user friendliness and with optimized fabrication processes, we believe, that the novel all polymer biosensor platform has application in virus diagnostics or personalized medicine for drug testing to achieve targeted treatment.

Chapter 7

Cell Migration in Microfluidic Device

7.1 Introduction

Advanced polymer devices for improved cell handling, culturing and analyses are becoming increasingly important in modern medical research, diagnostics and therapy. Although, impressive research breakthroughs have been achieved with conventional cell culture dishes, the system far from resemble *in vivo* conditions, thus translation of data for clinical use is difficult and has to be done with delicacy.

Migration of cells - essential for all living organisms - is a key in the development of the immune system, influenced by many different factors in the blood and the surroundings. Some cells are said to be intrinsically motile, whereas other cells need at least a global stimulation with a chemoattractant to initiate movement [64]. A continuous redistribution of cells to different anatomic sites throughout the body is central to immune surveillance and host defence [65], and an in depth comprehension of the immune cell trafficking patterns is imperative to understanding the role of specific cells in disease processes and to devising rational therapeutic strategies.

Recruitment of leukocytes from the circulation into sites of injury or inflammation requires the coordinated action of cellular adhesion proteins and chemotactic factors, mediating sequential leukocytes rolling, triggering, adhesion, and extravasation to peripheral tissue (Figure 7.1) [66, 67]. The complexity of the cell environment makes it difficult to model *in vitro*, and the conventional cell migration assays are far from mimicking the natural conditions.

Microfluidics is an appealing strategy to control fluid flow necessary to generate gradients in a scale suitable for cellular studies. Novel gradient generating methods to study chemotactic [69–71] or haptotactic [72, 73] cell migration are considered more advantageous than the conventional methods [71, 74], such as the Boyden Chamber [75] or shear

flow chamber [76].

In this paper, we present a new assay for real time studies of cell transmigration. We developed a microfluidic device incorporating the principles of a traditional Boyden chamber and shear flow chamber. The system imitate the natural environment of immune cells by maintaining a stable and constant concentration gradient of chemoattractant, while introducing shear flow action on migrating cells.

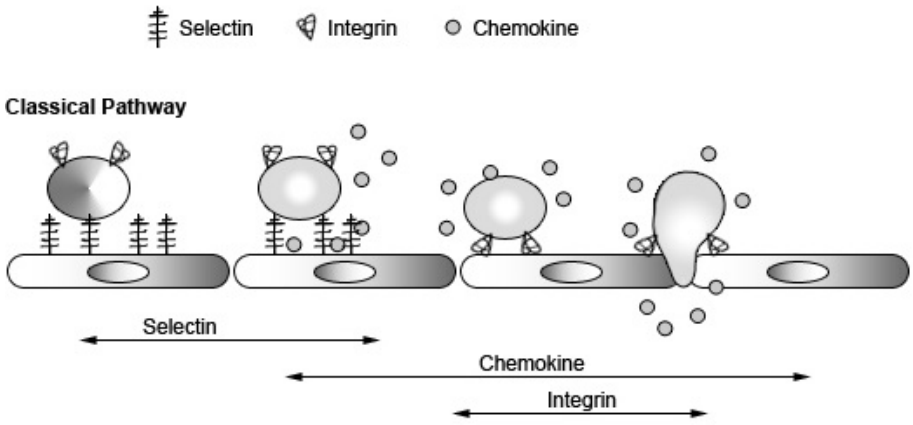

Figure 7.1: Schematic model of the classical pathway in the adhesion cascade. Leukocyte migration from the circulation into the peripheral tissue is a stepwise process. The first step involves transient, weak selectin-mediated binding. Chemokines that have been presented by glycosaminoglycans activate integrins on leukocytes, triggering firm adhesion between the leukocytes and endothelial cells. Finally, leukocytes migrate through the endothelial layer in response to a chemokine gradient. Modified from [68].

Biomed Microdevices (2011) 13:899–907
DOI 10.1007/s10544-011-9559-x

Microfluidic device to study cell transmigration under physiological shear stress conditions

Dorota Kwasny · Katrine Kiilerich-Pedersen · Jacob Moresco · Maria Dimaki · Noemi Rozlosnik · Winnie E. Svendsen

Published online: 8 July 2011

Abstract The development of new drug therapies relies on studies of cell transmigration in *in vitro* systems. Migration has traditionally been studied using two methods, the Boyden chamber and a shear flow chamber assay. Though, commonly applied in cell transmigration studies, they are far from imitating a natural migration process. Here we describe a novel *in vitro* cell transmigration microfluidic assay, which mimicks physiological shear flow conditions in blood vessels. The device was designed to incorporate the principles of both the Boyden chamber and the shear flow chamber assay, i.e. migration through the membrane under flow conditions. The 3D environment of migrating cells is imitated by injecting cell adhesion proteins to coat the membrane in the device. We tested the developed device with Jurkat cells migration towards medium supplemented with serum, and with chemokine induced lymphocytes migration. The applied continuous flow of cell suspension and chemoattractant ensures that the concentration gradient is maintained in time and space. The cell adhesion proteins used to enhance cell migration in the device were fibronectin and VCAM-1. We successfully observed a multistep transmigration process by means of the developed microfluidic migration assay. The presented device is inexpensive, easy to fabricate and disposable, having a potential to be applied in basic research as well as in the drug development process.

Keywords Cell migration · Microfluidic migration assay · Shear stress · Lymphocytes

D. Kwasny · K. Kiilerich-Pedersen · J. Moresco · M. Dimaki · N. Rozlosnik · W. E. Svendsen (✉)
Department of Micro- and Nanotechnology, Technical University of Denmark, Ørsteds Plads, 2800 Kgs. Lyngby, Denmark
e-mail: wisv@nanotech.dtu.dk

D. Kwasny
e-mail: dorota.kwasny@nanotech.dtu.dk

Present Address:
J. Moresco
Sunstone Capital A/S, Lautrupsgade 7, 5, 2100 Copenhagen, Denmark

1 Introduction

Cell migration plays an important role in a variety of physiological and pathological processes, such as angiogenesis, cancer metastasis, embryonic development, wound healing and inflammation. It is a complex process, essential for all living organisms, and it has been under investigation for many years (Finger et al. 1996; Lawrence et al. 1997; Guan 2005; Nie et al. 2007). Novel therapies and drug development rely on a proper understanding of the migration process.

Recruitment of leukocytes is central to immune surveillance and host defense (Nowak and Handford 2004). Trafficking from the circulation into sites of injury and inflammation requires the coordinated action of cellular adhesion proteins and chemotactic factors, mediating sequential leukocyte rolling, triggering and adhesion (Frow et al. 2004; Goldsby et al. 2006). Leukocytes circulating in postcapillary venules are pressed to vessel walls due to collisions with red blood cells, and extravasation into sites of inflammation is mediated by sequential adhesive interactions between surface receptors on leukocytes and their endothelial counterligands (Goldsby et al. 2006; Hamann and

Engelhardt 2005). The activation of leukocytes by ligands on endothelial cells occurs within seconds *in vivo* under blood flow (Butcher and Picker 1996). It is important to rapidly stop rolling cells because they have to react at the specific sites of chemokine stimulation (Campbell et al. 1998).

During extravasation from the vessels, receptors on the leukocyte surface detect an extracellular signal due to which the cell orients and starts to move directly towards a gradient of chemoattractant (Kay et al. 2008). Such guided movement was first described for the soil amoeba *Dictyostelium disoideum* and since then it became a model organism for eukaryotic chemotaxis studies (Jin and Hereld 2006). Migrating leukocytes undergo a series of transformations leading to redistribution of chemokine receptors, integrins and cytoskeletal proteins (Mackay 2001). The cell surface becomes irregular with rapid protrusions and retraction of ruffles due to actin polymerization changing the cell morphology to a polarized form with actin concentrated at the leading edge (Wilkinson 1996). A trailing end of the cell is not an essential part but is particularly well seen in lymphocytes (Baggiolini 1998; Rot et al. 2004; Wilkinson 1996).

Significant efforts have been focused on immune system cell migration studies in drug development to determine factors influencing migration. These studies identified numerous elements such as chemoattractants and cell adhesion proteins mediating transmigration of leukocytes in post capillary venules, but also the importance of shear stress (Lawrence et al. 1997; Finger et al. 1996; Toetsch et al. 2009). Development of new drugs relies on *in vitro* model systems to test potent drug candidates and determine their influence on cell migration (Toetsch et al. 2009). Conventionally, migration was studied in an *in vitro* gradient generating assay called a Boyden chamber. It consists of two wells, one inserted into another separated by a porous membrane, which is a static model to study cell transmigration (Boyden 1962). The introduction of a shear flow chamber assay solved the lack of shear flow acting on cells in the transwell assay. It consists of endothelial cells grown on a transparent surface and a system to perfuse leukocytes under different shear flow values. Real time microscopic observation is performed to monitor the sequential adhesive interaction of leukocytes and cell adhesion proteins expressed on endothelial cells. Contrary to nature, where a soft tissue underlies blood vessels, cells are grown on a solid support, which does not enable true transmigration (Hamann and Engelhardt 2005).

The complexity of the cell environment makes it difficult to model *in vitro* (Breckenridge et al. 2010), and the conventional cell migration assays are far from mimicking natural conditions. In nature, leukocytes present in vessels are exposed to a continuous blood flow. Thus, a new *in vitro* migration assay should imitate physiological conditions in the capillaries by mimicking transmigration from blood vessels under flow conditions. The investigation of the entire transmigration process in regards to cell movement analysis is important in drug development. Novel anti-inflammatory drugs are designed to act on different groups of proteins to inhibit either the rolling or the adhesion step (Proudfoot et al. 2000; Pitzalis et al. 1997). The transwell system is an endpoint assay that allows cell quantification after the migration event, with no means to track the transmigration process itself. In contrast, the shear flow chamber is used to observe the sequential adhesive interactions between leukocytes and cell adhesion proteins, but no real transmigration to underlying tissue is possible. Thus, the investigation of the complete transmigration process is impossible to achieve with existing assays. There is therefore a need for a new system enabling real time monitoring of cell migration under physiological flow conditions.

Here we describe a novel cell migration assay based on the principles of both Boyden chamber and flow chamber assays. This device meets the requirements for a novel cell transmigration assay maintaining a constant concentration gradient, introducing shear flow action on migrating cells, as well as imitating the natural environment of cells. The microfluidic system enables studies of cell migration in the context of interactions between chemoattractants, cell adhesion proteins and migrating cells under physiological shear flow conditions. The device facilitates control of shear stress, which is an important factor in regulating expression of cell adhesion proteins that mediate the transmigration. The continuous flow of chemoattractant ensures the stable concentration gradient in time and space. Another unique feature of the demonstrated microfluidic device is its ability to monitor sequential adhesive interactions between leukocytes and proteins coated on a membrane. The role of VLA4 integrin expressed on leukocytes was tested by interactions with fibronectin and VCAM-1 proteins on the membrane. To demonstrate the applicability of the device to monitor steps involved in cell migration in real time, we tested the migration of Jurkat cells and lymphocytes purified from blood towards fetal bovine serum and 50 ng/ml CCL2 chemokine respectively (Carr et al. 1994). The system enables studies of all steps involved in the cell migration process with potential application in basic research and therapeutic drugs screening.

2 Materials and methods

2.1 Device design

The microfluidic device was designed in AutoCad2000i. The design is based on the principles of the Boyden chamber and the shear flow chamber. It consists of two narrow flow channels imitating blood vessels in which shear stress is controlled by a syringe pump. The channels are separated by a porous membrane as shown in Fig. 1. It acts as a physical barrier, separating cells in the upper channel from a chemoattractant solution in the lower channel. The design allows for coating of the membrane after thermal bonding of a complete device to imitate the 3D environment of migrating cells.

2.2 Device fabrication

Two 500 μm wide, 100 μm deep and 2 cm long channels were milled by a high precision milling machine (Folken Industries, Glendale, USA) in a 2-mm poly (methylmethacrylate) (PMMA) sheet (Nordplast) and cut out in the dimensions of a microscope glass slide (75 × 25 mm). The channels contain separate inlets and outlets for cell suspension and chemoattractant solution. The interconnections were milled as described by Sabourin et al. (2010) to fit a 3-mm silicone tubing.

After defining the channels, the device parts were cleaned with MilliQ water, further washed with ethanol, treated with UV (Dymax EC5000, Connecticut) for 1 min and thermally bonded at 85°C, at a pressure of 5 kN for 15 min in a bonding press (P/O/Weber, Remshalden, Germany). During bonding, a 5 μm pore size polycarbonate (PC) membrane (Pieper Filter GmbH, PC50BP02500) was sandwiched between the two parts of the device separating them and ensuring that the membrane covered the overlying channel parts. The three elements of the device are shown in Fig. 2 before and after the bonding process. Silicone and Teflon tubing (VWR) were used to interconnect the device with a syringe pump.

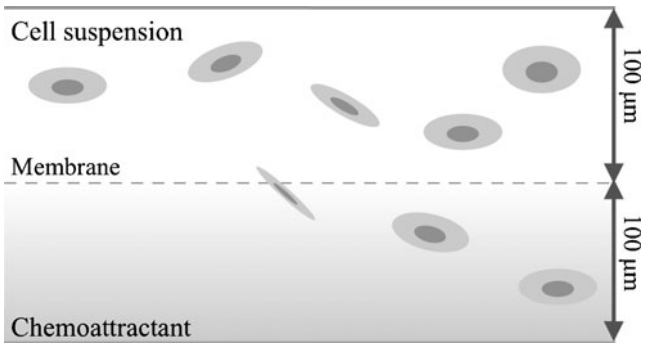

Fig. 1 The principle of migration through a PC membrane in the microfluidic device. Cells flowing in the upper channel can sense a chemoattractant diffusing through pores from the bottom channel and migrate through the membrane

2.3 Cell culture and purification

Jurkat cells were cultured in RPMI media (Invitrogen, 61870) containing 10% Fetal Bovine Serum (FBS) (Sigma Aldrich, F2442) and 1% Penicilin/Streptomycin (Invitrogen, 15140) in a humidified incubator at 37°C in a 5% CO_2 moist atmosphere. The cells were synchronized for 12 h before the migration experiments by FBS starvation.

Buffy coat was isolated from a blood sample obtained from healthy donors (blood bank, Rigshospiltalet, Copenhagen, Denmark) by centrifugation with Ficoll Paque PLUS (GE Healthcare, 17-1440-02) following the manufacturers protocol. Lymphocytes were resuspended in RPMI medium and used for experiments.

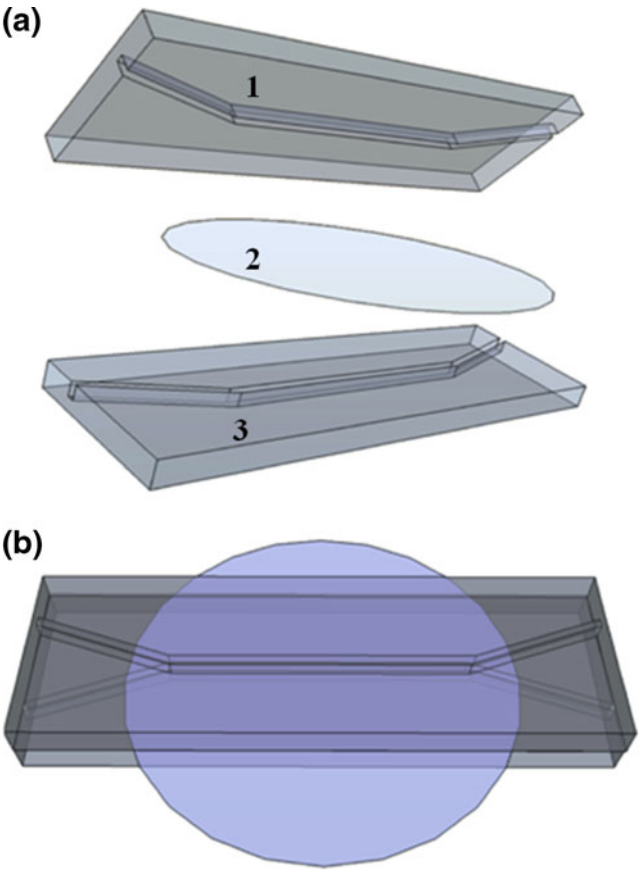

Fig. 2 The schematic drawing of three elements of the device during assembling (**a**) and after thermal bonding (**b**). *1* Cell suspension channel, *2* Membrane, *3* Chemoattractant channel

2.4 Device operation

The device was primed with liquid by flushing 10% ethanol solution, followed by washing with MilliQ water and 1× PBS (Invitrogen, AM9625). The cell suspension channel and the membrane were coated by injecting 10 μg/ml fibronectin (Sigma Aldrich, F0895) or 5 μg/ml VCAM-1 (PeproTech, 150-04) solutions to the cell suspension channel for 1 h at 1.67×10^{-3} m/s flow velocity. Both microfluidic channels were subsequently blocked with 1% Bovine Serum Albumin (BSA) (Sigma Aldrich, B4287) solution to prevent unspecific binding. Medium supplemented with 10% FBS acted as a chemoattractant for Jurkat cells while 50 ng/ml CCL2 (Biosource, PHC1014) solution induced migration of lymphocytes. The cells were stained with DiO dye (Invitrogen Molecular Probes, V22889) as described by the manufacturer just before device testing. Labeled cells at a concentration of 1×10^6 cell/ml in serum free medium were pumped into one channel at 1.67×10^{-3} m/s flow velocity. At the same time the second channel was filled with chemoattractant solution at 1.67×10^{-3} m/s flow velocity. The chemoattractant-induced migration was observed with a fluorescent microscope equipped with a camera (Photometrics Cascade II512, USA). Experiments were performed at a room temperature with a disposable device. Glass syringes were used to ensure a stable flow.

2.5 Simulation of concentration gradient

The concentration gradient across the membrane was simulated in the multiphysics modeling software COMSOL 3.5. In the analysis, a 2D model of the device was created with channel dimensions of 0.1 × 20 mm separated by a porous membrane of thickness 10 μm with a pore size of 5 μm, porosity 0.14 and 20 mm length. For the purpose of the simulation the concentration of chemoattractant in the bottom channel inlet was normalized to 1, while the upper channel is free of chemoattractant at the beginning of the analysis. Fluid dynamics calculations were performed using the Navier-Stokes equation with a flow velocity of 1.67×10^{-3} m/s, and a fluid viscosity of 1×10^{-3} Pa.s. To obtain a concentration profile, Fick's law of diffusion was applied. The diffusion coefficient of CCL2 was calculated to be 1.76×10^{-10} m^2/s taking into account the effective radius of a protein and a molecular weight of CCL2 8 kDa. Diffusion through the membrane was simulated by setting the diffusion coefficient in the membrane to 0.14 of the calculated value for CCL2, to account for the membrane porosity. Similarly, convection through the membrane was simulated considering Darcy law for convection in porous media as described in Dimaki et al. (2008). The flow problem was solved first in steady state and the solution was used afterwards to calculate the time-dependent diffusion. As a control, the same simulation was repeated by using a geometrical representation of the membrane instead of the Darcy law.

2.6 Imaging and analysis

Videos were recorded on an inverted fluorescent microscope (Nikon Eclipse TE2000, Japan) with a EMCCD camera (Photometrics Cascade II512, USA). The sequence of images was further processed with ImageJ and analyzed manually from AVI files (7 frames per second) to obtain coordinate trajectories of locomotive cells in time. The cell coordinates were used to create a scatter plot of the cells' trajectories with changing velocity using Matlab.

3 Results and discussion

3.1 Microfluidic device

The complete device in a shape of a microscope slide is shown in Fig. 3. The channels serving as the migration platform are well defined by micromilling. During thermal bonding the two parts of the device were connected and a PC membrane was incorporated to separate the channels, which can be seen in Fig. 3 as

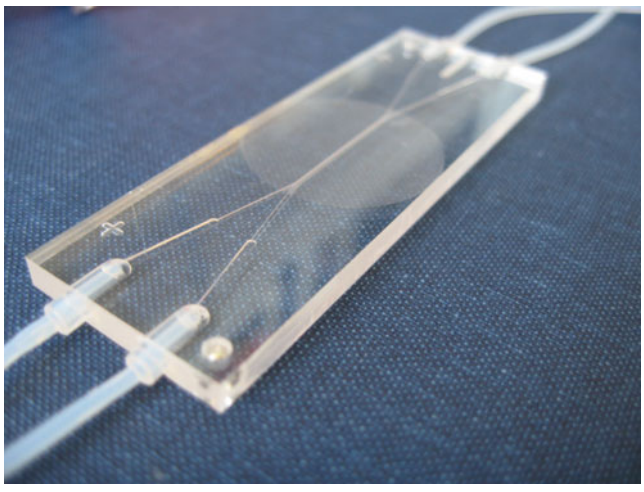

Fig. 3 The microfluidic device for cell transmigration studies fabricated in PMMA. The chip contains separate channels for cell suspension and chemoattractant flow. The middle part of the device consists of channels separated by a PC membrane which serves as a migration site

a circle in the middle part of the chip. The plus sign visible in the corner of the device is an indication of a cell suspension channel inlet for easier device handling.

The microscope slide format was chosen as standard in biological analysis as well as for easy handling during investigation of the cell migration. The placement of interconnections on each side of the slide is crucial for easy operation at a microscope stage. During device fabrication a proper alignment of the membrane in the central part of the device has to be assured, because the membrane separates the overlapping parts of the channels serving as migration point. Misalignment of the membrane would result in mixing of cell suspension and chemoattractant solution. The 2.5 cm membrane diameter was selected to cover the 2 cm long overlapping channels region. Furthermore, the membrane has to be stretched to prevent folding in the channels which could influence the microscopic investigation.

3.2 Gradient simulation

The time evolution of the chemokine concentration gradient in the top channel is plotted in Fig. 4. In the top part of Fig. 4 the channel outline is sketched with a dashed line indicating the membrane position. The concentration change with time and channel length was plotted at 5 μm above the membrane. In Fig. 4(a) the time dependent change in concentration within 25 seconds is plotted. Each line represents the time of the simulation, at the beginning of the assay the concentration of chemokine in the top channel is equal to 0.1 of input concentration. The concentration of chemokine in the top channel increases with time and length of the channel being the highest after 20 seconds of simulation. After this time, the concentration of chemokine in the end of the top channel reaches the highest value of 0.3 of input concentration, with no further change observed, proving that the gradient across the membrane is formed within few seconds of the experiment and remains stable with time. In Fig. 4(b) the simulation using a real geometrical representation of the membrane is shown. The only differences noted are an oscillating concentration profile with the largest concentrations directly above the pores, as can be expected, and the value of the highest concentration in the top channel was 0.25 of the input concentration.

The device consists of two channels with continuous flow applied during experiments. The chemokine diffuses through the membrane from the beginning of the experiments, but because of the flow in the top channel it is moved to the end of the channel. Thus, the simulated concentration in the top channel is the highest in the end of the channel. The observed cell behavior during experiments confirms the correctness of the simulation, as the cell migration was higher in the end of the channel.

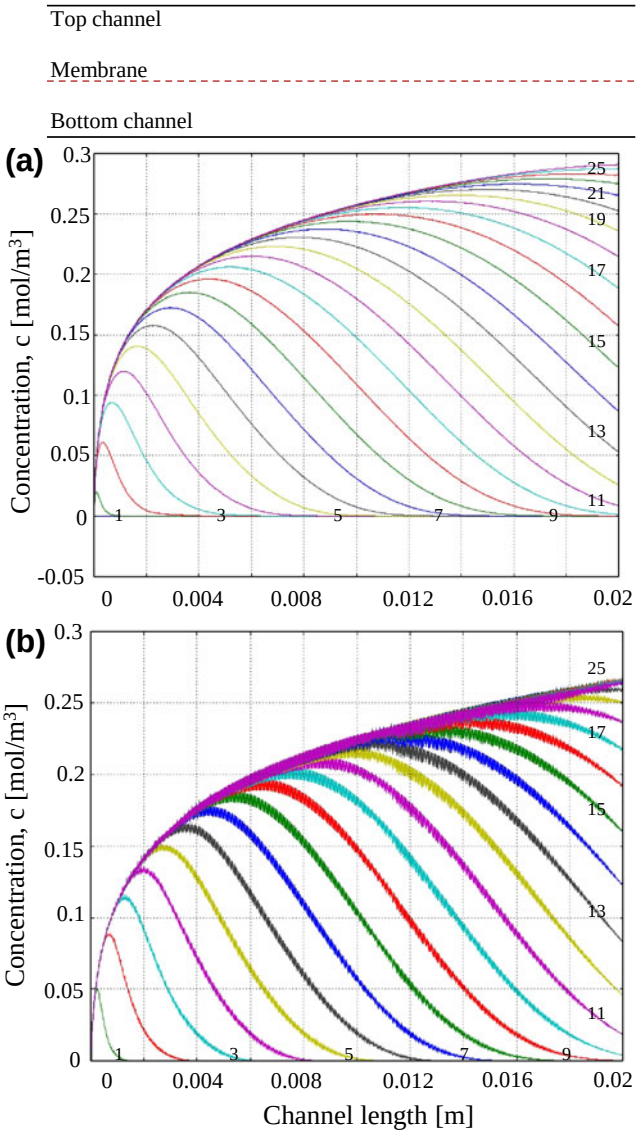

Fig. 4 The simulation of the concentration gradient formation in the microfluidic device. The channels outline is sketched above the graphs, with a dashed line as a membrane. The chemoattractant concentration was measured at 5 μm above the membrane. (**a**) The graph of concentration of chemoattractant in the top channel changing with time and channel length. (**b**) The oscillating concentration profile simulated with a geometrical representation of the membrane

3.3 Migration in the device

The migration in the microfluidic device was recorded with an inverted fluorescent microscope equipped with

a CCD camera. The device was mounted on a microscope stage and the cell movement was recorded looking through the device while focusing on the membrane. The obtained data are movies of cells as they interact with a membrane coated with adhesive substrates under shear flow conditions ($Q = 5$ µl/min and a shear stress of 1 dynes/cm^2). A control experiment was also prepared by observing Jurkat cell behavior on an uncoated membrane in a prototype device with a higher flowrate of $Q = 10$ µl/min and a shear stress of 1 dynes/cm^2. The movies visualize the moment of cell transmigration through the membrane as the cell is out of focus after migration. The cell movement was analyzed manually by means of ImageJ, where the relative position of each cell in time was recorded and used further for calculating the path and cell velocity. The behavior of 4 representative cells for each experimental system is plotted as a change of cell velocity as a function of time of observation. The data were normalized to present a transmigration step at time 0 for all the analyzed cells. Analyzed X and Y cell positions in pixels (one pixel corresponds to 0.8 µm) were also used to plot the cell path before and after transmigration through the pore by means of Matlab.

A control experiment was performed to analyze cell migration without coating of the membrane with cell adhesion proteins. The cell velocity presented in Fig. 5 in the device with an uncoated membrane does not change significantly during observation time and is in the range of the applied flow velocity of 3.3 mm/s. The experiment was performed to check whether transmigration under shear flow will occur due to stimulation with a chemoattractant. As no migrating cell was observed in the movies we concluded that for more effective migration a membrane coating must be applied. All further experiments were thus performed with a membrane coating with cell adhesion proteins.

Among adhesion receptors involved in migration VLA4 plays a major role in the adhesion of leukocytes to endothelial cells (Barreiro et al. 2002). VLA4 interacts with both fibronectin and VCAM-1 proteins that are often used in transwell assays (Alon et al. 1995). Fibronectin is naturally present in the basement membrane underlying endothelial cells (Hamann and Engelhardt 2005). Moreover, it enhances cell adhesion to the membrane due to integrin activation (Pankov et al. 2002). However, the main ligand for VLA4 integrin is the VCAM-1 protein, which is one of the major endothelial receptors that mediates leukocyte rolling (Alon et al. 1995; Butcher and Picker 1996) and adhesion to the vascular endothelium (Barreiro et al. 2002). Parallel experiments were run with a membrane in the device coated with fibronectin and VCAM-1 to test their effect on cell migration of Jurkat cells and lymphocytes.

An example of Jurkat cell migration in the device coated with fibronectin is shown in Fig. 6, presenting changing cell velocity in time. The graph can be divided

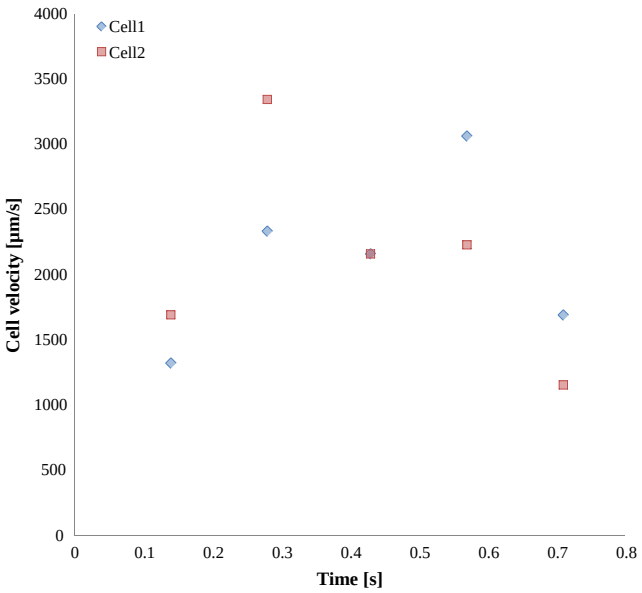

Fig. 5 Jurkat cell velocity change in time in the device with uncoated membrane. Cell velocity does not change during time of observation. Cell moves with a velocity close to flow velocity of 3.3 mm/s

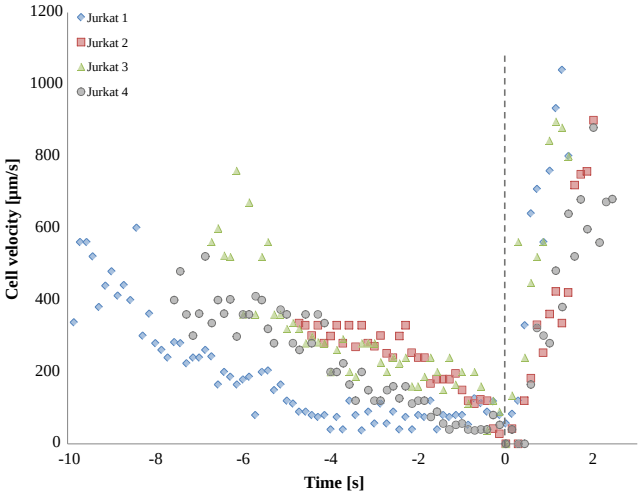

Fig. 6 Jurkat cell migration through the membrane coated with fibronectin. The initial linear drop in cell velocity indicates the adhesive interactions with the fibronectin on a membrane. The short constant cell velocity region occurs due to adhesion to the membrane before the migration through the pore. After transmigration (a *dashed line*) the cell velocity drastically increases as the cell is taken with a constant flow in the chemoattractant channel where no adhesive interactions slow down the cell motion

into three regions—linear decrease, short constant and increase in cell velocity. The decrease in cell velocity occurs due to chemoattractant sensing, which activates the cell surface and results in the cell slowing down and approaching the membrane. The cell velocity is decreasing linearly, however no distinct rolling step was observed. A very short region of constant cell velocity can be observed just before the transmigration through pores for the cells presented as diamonds and circles in Fig. 6. During the time of constant cell velocity the cell is further activated by the diffused chemoattractant and adheres to the membrane due to fibronectin-integrin interactions. The cell is slowly crawling on the membrane to reach a pore and transmigrates. After transmigration, the cell moves with high velocity with the flow in the chemoattractant channel, due to lack of adhesive interactions with the membrane, illustrated in the graph as a linear increase in cell velocity. The cell velocity after transmigration is close to the flow velocity.

In the separate experiment with VCAM-1 coated membrane, we observed that VCAM-1 induced rolling of Jurkat cells on the membrane, followed by adhesion and transmigration through the membrane. The change in velocity of Jurkat cells in time is shown in Fig. 7. The graph can be divided into regions of a linear decrease in velocity, a very short region of a constant velocity and a linear increase in velocity. The initial cell velocity slightly decreases in the observation period due to sensing of the diffused chemoattractant. As the cell is flowing close to the membrane the interaction between VCAM-1 and the cell surface receptors occurs, resulting in a loose attachment of the cell to the membrane. The cell is moving with an average of 150 μm/s which indicates a rolling step as it is much lower than the flow velocity at the distance of 5 μm from the wall (calculated to be 475 μm/s). The shear flow in the channel detaches the cell allowing it to roll on the surface. During rolling the cell surface becomes activated and tight adhesion occurs due to strong interactions between VCAM-1 and integrins on the cell surface, which is presented as the short constant velocity. This constant velocity region, which lasted from 6 s (diamonds) to 1 s (squares), represents the cell arrested on the membrane and slowly moving towards the pore. After transmigration through the pore (dashed line in Fig. 7), similarly to the fibronectin experiment, the cell velocity increases after reaching the chemoattractant channel.

The last experiment prepared to validate the microfluidic device operation was performed with purified lymphocytes migrating on a surface coated with VCAM-1. The movement of four cells was analyzed and is plotted as cell velocity change in time in Fig. 8. Two different cell behaviors can be observed in the graph. Two cells (diamonds and circles in the graph) behave like Jurkat cells on fibronectin surface, with a linear decrease in the cell velocity followed by rapid ve-

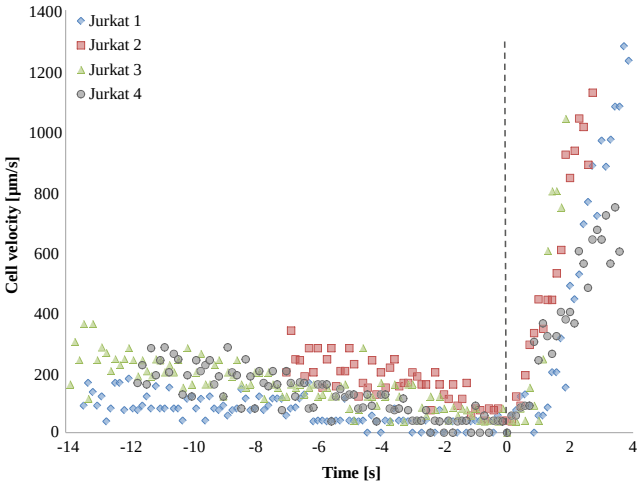

Fig. 7 Jurkat cell migration on the membrane coated with VCAM-1. The initial linear decrease in velocity indicates the rolling step, the cell velocity is further reduced during adhesion step, when cell is crawling to reach the pore. After transmigration (a *dashed line*) cell velocity rapidly increases when the cell joins the flow in the other channel

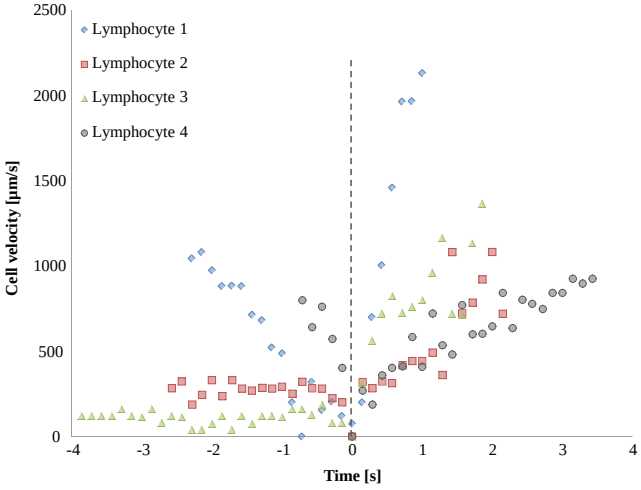

Fig. 8 Lymphocytes migration on the membrane coated with VCAM-1. The four analyzed cells present different behavior before transmigration, *red* (*squares*) and *green* (*triangles*) cells are rolling, while *blue* (*diamonds*) and *grey* (*circles*) represent rapid linear decrease in velocity when approaching the membrane. After transmigration through the pore (a *dashed line*) the cell velocity increases, as the cell starts moving in the chemoattractant channel

locity increase after transmigration. The other two cells (triangles and squares) act as Jurkat cells on VCAM-1 coated membrane. These two cells are rolling on the surface with an average velocity of 110 μm/s and 280 μm/s for triangles and squares, respectively. After transmigration, all four cells experience an increase in cell velocity. No adhesive interactions occur between lymphocyte and the surface after transmigration, thus the observed high cell velocity.

In Fig. 9 the trajectories (in pixels) of the Jurkat cells of Fig. 6 are shown with a color change according to the cell velocity. The cells are moving in the direction of flow; after adhesion to the membrane, they start crawling to reach the nearest pore. Figure 9 also shows the change in cell velocity before and after migration through pores. All cells slow down approaching the membrane; once they reach the membrane, they start to slowly move in the direction of the nearest pore. After migration their velocity increases when they join the flow in the chemoattractant channel. Such behavior of cells is mediated by adhesive interactions with the substrate in response to chemoattractant activation.

Cell migration is a multistep process that starts with an initial rolling step, which involves transient attachment between leukocytes and ligands on endothelial cells. In the proposed microfluidic migration device the ligands naturally present on endothelial cells are coated on the membrane surface. Near the membrane rolling cells are exposed to chemoattractant solution that serves as an activating molecule. The activation of integrins on the leukocyte surface occurs within seconds and leads to firm adhesion to the membrane followed by transmigration directed by the chemoattractant gradient (Roth et al. 1995). The described device, enables studies of the migration process in real time, with cell transmigration occuring as fast as in a natural process.

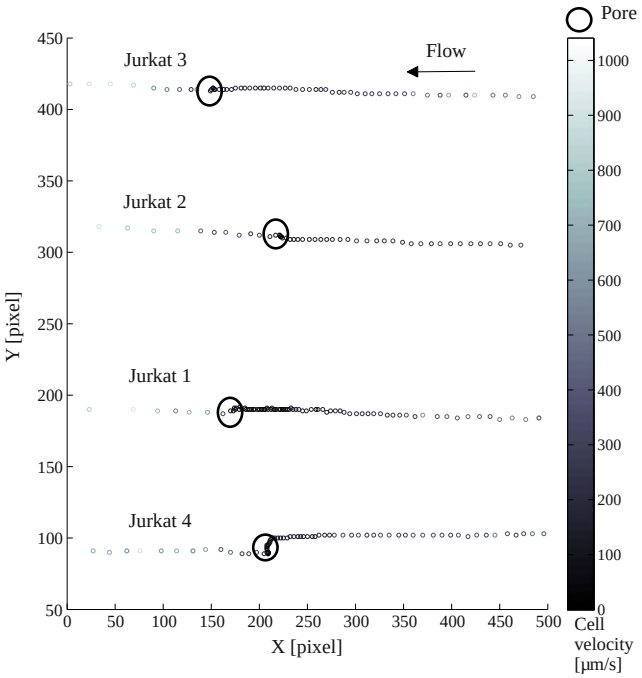

Fig. 9 Jurkat cells movement on the surface coated with fibronectin. The cells moving in the direction of flow slow down when approaching the membrane, once they adhere they start crawling to reach the nearest pore. After transmigration the cell velocity increases as the cells reach the other channel

During the experiments with coated membrane we observed higher cell adhesion and migration at the end of the channel. Due to the diffusing chemoattractant cells were activated more significantly towards the end of the channel. Jurkat cells were seen to strongly adhere on the fibronectin surface, however no distinct rolling step was observed. On the other hand, Jurkat cells were rolling over long distances on the surface coated with VCAM-1. The maximum velocity of a free flowing cell in the device is around 1,500 μm/s, thus the 10 times drop in cell velocity is considered a rolling velocity. The rolling step was followed by firm adhesion and subsequent transmigration through pores. These findings are contrary to those presented by Alon et al. (1995) where no rolling was observed in case of Jurkat cells on VCAM-1. The average velocity of rolling Jurkat cells is around 150 μm/s, the average velocity of the two rolling lymphocytes is around 195 μm/s. The cell velocity of lymphocytes obtained by Campbell et al. (1998) is 100 μm/s, which is close to our results. The difference might arise from manual analysis of our migration data, different chemokines used for cells activation as well as the system used for migration experiments.

Even though some purified lymphocytes were seen to both roll and adhere to the surface coated with VCAM-1, such behavior was not observed for all cells. Lymphocytes were purified from the donors blood and used in the experiments without further steps of synchronization. Cells being in different stages of cell cycle might respond differently to chemoattractant stimulation, hence migrate without an initial rolling step. Furthermore, lymphocytes purification has a yield of around 60% with some other immune system cells also present in the suspension, which may be activated in different ways by chemoattractant and proteins on the membrane. The average rolling velocity of lymphocytes in the experiments was 195 μm/s, which is close to the velocity obtained by Campbell et al. (1998), but far from Alon et al. (1995). Alon et al. found that rolling velocity of lymphocytes on VCAM-1 surface is around 5 μm/s for a shear stress of 1 dyn/cm^2. Such a huge

difference may occur due to different chemokines used for stimulation of cells migration.

The control experiment performed in the device without membrane coating revealed the importance of cell adhesion molecules on cell migration. No cells were seen to slow down and migrate through the membrane with stimulation by chemoattractant only. Thus, we conclude that for migration to occur under shear flow conditions, cell adhesion proteins such as fibronectin or VCAM-1 should be applied (Elices et al. 1990). Both these proteins are naturally present in the blood vessels—fibronectin in the basement membrane underlying endothelial cells and VCAM-1 apically overexpressed on endothelial cells during inflammation. The VLA-4 integrin expressed on the leukocytes surface can bind both these proteins using different mechanism, which is advantageous in the natural process as the cell during inflammation can adhere to both of these substrates (Elices et al. 1990). Both proteins enhanced the cell migration in the microfluidic device, however, their effect was not the same on all migrating cells. Jurkat cells and some lymphocytes experienced a rolling step on the surface coated with VCAM-1. All cells were at some point arrested on the membrane and started crawling to reach the nearest pore, but the time of the arrest step varied from cell to cell. Such a variation could arise from difference in expression of proteins on the cell surface or the vertical distance of the cell from the membrane. We concluded that both fibronectin and VCAM-1 proteins are useful for studying migration, however, to investigate a multistep process it is advantageous to use VCAM-1 as it enables a distinct rolling step to be observed.

4 Conclusions

We have developed a novel microfluidic migration device aiming at imitating physiological conditions of cell transmigration. Combining the principles of a Boyden chamber and a shear flow chamber assay in one microfluidic device we created a system that closely resembles the natural environment of migrating cells. Due to physical separation of channels by a membrane the cells must actively migrate towards a pore, similarly to extravasation from blood vessels to underlying tissue. Moreover, application of a continuous shear flow promotes migration and maintains the concentration gradient in time and space. Coating of both channel and membrane imitates the 3D environment of migrating cells. Furthermore, not only does the described device allow for reduction in sample volume used but is also inexpensive, easy to fabricate, disposable and amenable for high throughput analysis.

References

R. Alon, P.D. Kassner, M. Woldemar-Carr, E.B. Finger, M.E. Hemler, T.A. Springer, J. Cell Biol. **128**, 1243–1253 (1995)

M. Baggiolini, Nature **392**, 565–568 (1998)

O. Barreiro, Yanez-M. Mo, J.M. Serrador, M.C. Montoya, Vicente-M. Manzanares, R. Tejedor, H. Furthmayr, Sanchez-F. Madrid, J. Cell Biol. **157**, 1233–1245 (2002)

S. Boyden, J. Exp. Med. **115**, 453–466 (1962)

M.T. Breckenridge, T.T. Egelhoff, H. Baskaran, Biomedical Microdevices **12**, 543–553 (2010)

E.C. Butcher, L.J. Picker, Science **272**, 60–66 (1996)

J.J. Campbell, J. Hedrick, A. Zlotnik, M.A. Siani, D.A. Thompson, E.C. Butcher, Science **279**, 381–384 (1998)

M.W. Carr, S.J. Roth, E. Luther, S.S. Rose, Proc. Natl. Acad. Sci. USA **91**, 3652–3656 (1994)

M. Dimaki, J.M. Lange, P. Vazquez, P. Shah, F. Okkels, W.E. Svendsen, in *Proceedings of COMSOL conference* (Hannover, 2008)

M.J. Elices, L. Osborne, Y. Takada, C. Crouse, S. Luhowskyj, M.E. Hemler, R.R. Lobb, Cell **60**, 577–584 (1990)

E.B. Finger, K.D. Puri, R. Alon, M.B. Lawrence, U.H. von Andrian, T.A. Springer, Lett. Nature **379**, 266–269 (1996)

E.K. Frow, J. Reckless, D.J. Grainger, Med. Res. Rev. **24**, 267–298 (2004)

R.A. Goldsby, T.J. Kindt, B.A. Osborne, J. Kuby, in *Kuby immunology*, 6th edn. (W.H. Freeman & Company, 2006), Chapter 15

J.-L. Guan, in *Cell migration—developmental methods and protocols* (Humana, Totowa, 2005)

A. Hamann, B. Engelhardt, in *Leukocyte trafficking. Molecular mechanisms therapeutic targets and methods* (Wiley-VCH, Weinheim, 2005), Chapters 19–21

T. Jin, D. Hereld, Eur. J. Cell Biol. **85**, 905–913 (2006)

R.R. Kay, P. Langridge, D. Traymor, O. Hoeller, Nat. Rev., Mol. Cell Biol. **9**, 455–463 (2008)

M.B. Lawrence, G.S. Kansas, E.T. Kunkel, K. Ley, J. Cell Biol. **136**, 717–727 (1997)

C.R. Mackay, Nat. Immunol. **2**, 95–101 (2001)

F.Q. Nie, M. Yamada, J. Kobayashi, M. Yamato, A. Kikuchi, T. Okano, Biomaterials **28**, 4017–4022 (2007)

T.J. Nowak, A.G. Handford, *Pathophysiology: Concepts and Applications for Health Care Professionals* (McGraw Hill, 2004)

R. Pankov, K.M. Yamada, J. Cell Sci. **115**, 3861–3863 (2002)

C. Pitzalis, N. Pipitone, G. Bajocchi, M. Hall, N. Goulding, A. Lee, G. Kingsley, J. Lanchbury, G. Panayi, J. Immunol. **158**, 5007–5016 (1997)

A.E.I. Proudfoot, C.A. Power, T.N.C. Wells, Immunol. Rev. **177**, 246–256 (2000)

A. Rot, U.H. von Andrian, Annu. Rev. Immunol. **22**, 891–928 (2004)

S.J. Roth, M.W. Carr, S.S. Rose, T.A. Springer, J. Immunol. Methods **188**, 97–116 (1995)

D. Sabourin, M. Dufva, T. Jensen, J. Kutter, D. Snakenborg, J. Micromech. Microeng. **20**, 1–7 (2010)

S. Toetsch, P. Olwell, Prina-A. Mello, Y. Volkov, Integr. Biol. **1**, 170–181 (2009)

P.C. Wilkinson, METHODS: A Companion to Methods in Enzymology **10**, 74–81 (1996)

7.2 Concluding Remarks

A thorough understanding of leukocyte recruitment from the circulation to peripheral tissue is important in many medical aspects. We developed an *in vitro* setup to study immune cell transmigration in a three dimensional microenvironment. The system enables studies of all steps involved in the cell migration process with potential application in basic research and therapeutic drugs screening.

Currently, the device is based on microscopic detection, and the next step is to integrate conductive polymer electrodes at the inlet (where cells are introduced) and outlets to obtain a quantitative measure of the cell transmigration by electrochemical impedance spectroscopy.

The physiological conditions of the microenvironment could be further improved by introducing a monolayer of endothelial cells on the membrane that separates the microfluidic channels, and it would also be interesting to use a hydrogel as a model for the soft tissue cells are migrating towards.

Chapter 8

Impedimetric Detection of Cell Migration

8.1 Introduction

Cell migration is an essential feature of life, and the importance of this complex process was broached in Chapter 7. Cell motility is influenced by many different factors in the blood and the surroundings. Some cells are said to be intrinsically motile, whereas others need at least a global stimulation with a chemoattractant to initiate movement [64]. That signal could be introduced by a variety of proteins for instance extracellular matrix components, chemokines or growth factors.

Wound healing is a classical example of a biological process, involving directional migration of cells. Traditionally, this type of cell migration assay was performed by physically wounding cell monolayers in cell culture dishes with a razor blade [77]. Despite the simplicity of this method, physical scraping often damage cells near a wound edge, disrupting biological activities. Moreover, the assay requires large volumes of cell culture medium and additional reagents to examine biological activities, and is unfit for scaling up towards high throughput screening. One way to resolve these shortcomings is by combining novel micro- and polymer technologies to develop a new cell migration assay for studies of wound healing.

The microfluidic technology is increasingly being explored in cell biology for cell sorting [78], cell culture [79–82], and single cell analysis [83]. For cell culture applications some of the more important benefits are a high degree of control of the near cell environment compared to the traditional large scale systems. This includes control of mechanical impact, control of chemical environment by controlled addition and removal of factors, and tailored cell culture substrates by chemical surface engineering and micromachining. Other typical advantages of downscaling are reduced sample consumption, increased throughput and reduced cost. Combined with the option to adjust the conditions over

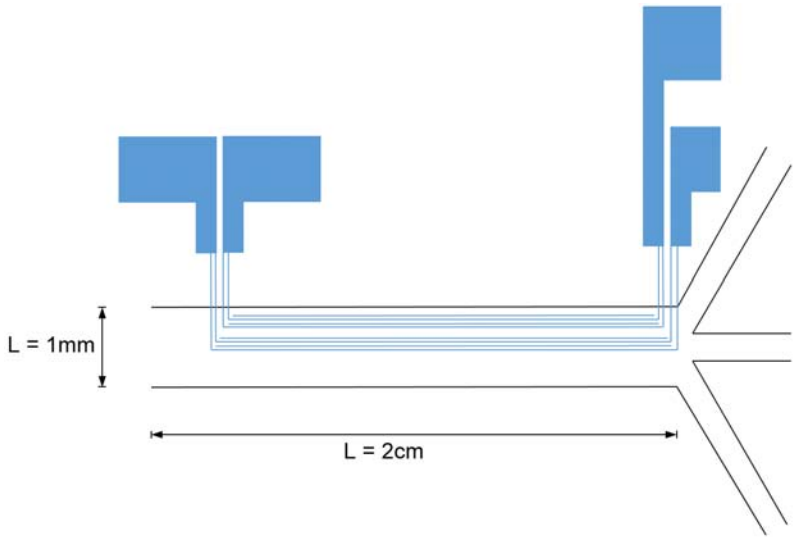

Figure 8.1: Schematic representation of microelectrode design; conductive polymer microelectrode pairs were designed with a width of 20 µm and placed 100 µm apart.

time the spatio-temporal control enables microfluidics to approach *in vivo* scenery.

This chapter presents an overview of the preliminary[1] work on an on-chip cell migration assay. An all polymer microfluidic device with conductive polymer microelectrodes was developed for real time and label free electrochemical detection of directional cell migration. By exploiting laminar fluid flow conditions, a precisely controlled wound edge was formed of a cell monolayer in the main channel of the chip without damaging the cells. The microfluidic device enables quantitative and qualitative studies of cell migration by electrochemical impedance spectroscopy and video time lapse microscopy.

8.2 Microfluidic System

An all polymer microfluidic device was designed with two sets of conductive polymer microelectrodes for impedimetric real time sensing of migrating cells. The microdevice was fabricated in Topas® and PEDOT:TsO by injection molding [11] and standard photolitographic processing techniques in the Danchip Cleanroom (Technical University of Denmark) as described in Chapter 6 [13].

The system features three inlets, converging into a single main channel as depicted in Figure 8.1. Conductive polymer microelectrode pairs were designed with a width of 20 µm, placed 100 µm apart. Taking advantage of the microfluidic flow conditions, laminar flow streams were used to control the distribution of human cells in the microchannel. To

[1]Experiments were partly performed by master student Louise Laursen, supervised by the author of the thesis.

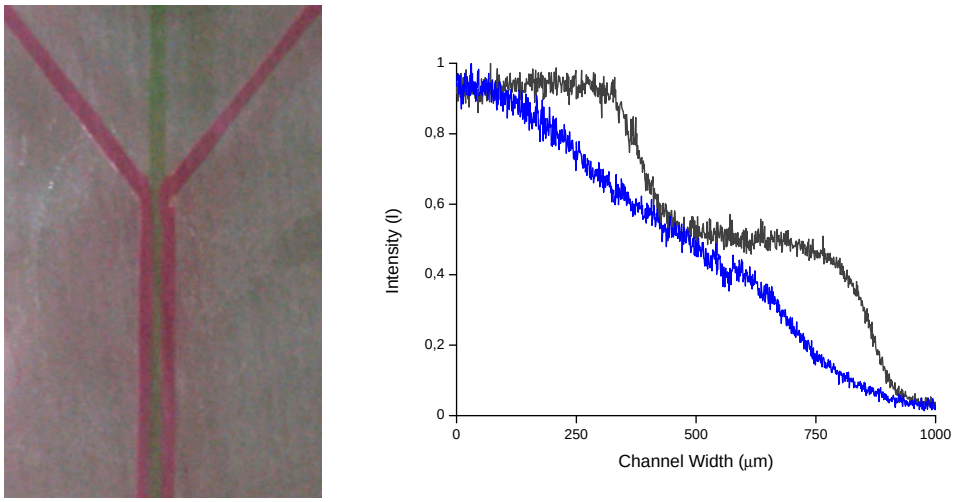

Figure 8.2: Visualization of laminar flow using color, and fluorescence intensity profile near the inlet (gray) and in the middle of the main channel (blue), indicating the formation of a two dimensional fluid phase gradient.

confirm the formation of laminar flow in microchannels, coloring was introduced from different inlet reservoirs, and microscopy was used to visualize the laminar flow. The color flowed with very faint diffusion, and the three streamlines showed clear boundaries (Figure 8.2).

At laminar flow conditions, interfacing streamlines mix by diffusion. A two dimensional fluid phase gradient was established in the main channel of the microfluidic device by introducing a solution of fluorescently labelled biomolecules at separate inlets. The acquired microscopy images were analyzed in MATLAB and the intensity profiles were found to correlate with a simulation in Comsol Multiphysics (data not shown).

The changes in intensity in the width of the channel illustrated changes in the steepness of a concentration gradient. As illustrated in Figure 8.2, the concentration gradient was very steep near the inlets due to little mixing. The slope of the intensity profile decreased continuously along the length of the channel as particles were mixed by diffusion.

8.3 Wound Healing Assay

Healthy human cells were seeded directly in the microfluidic channel of the chip, and allowed to attach and spread on the substrate and acclimatize over night. A wound edge was formed by injecting cell medium and a trypsin-EDTA solution from the three inlets, thereby selectively treating the cell monolayer. Based on the formation of laminar flow in the microchannels, only cells in contact with trypsin-EDTA were detached from the substrate, while untreated cells remained intact and formed a clear wound edge. The

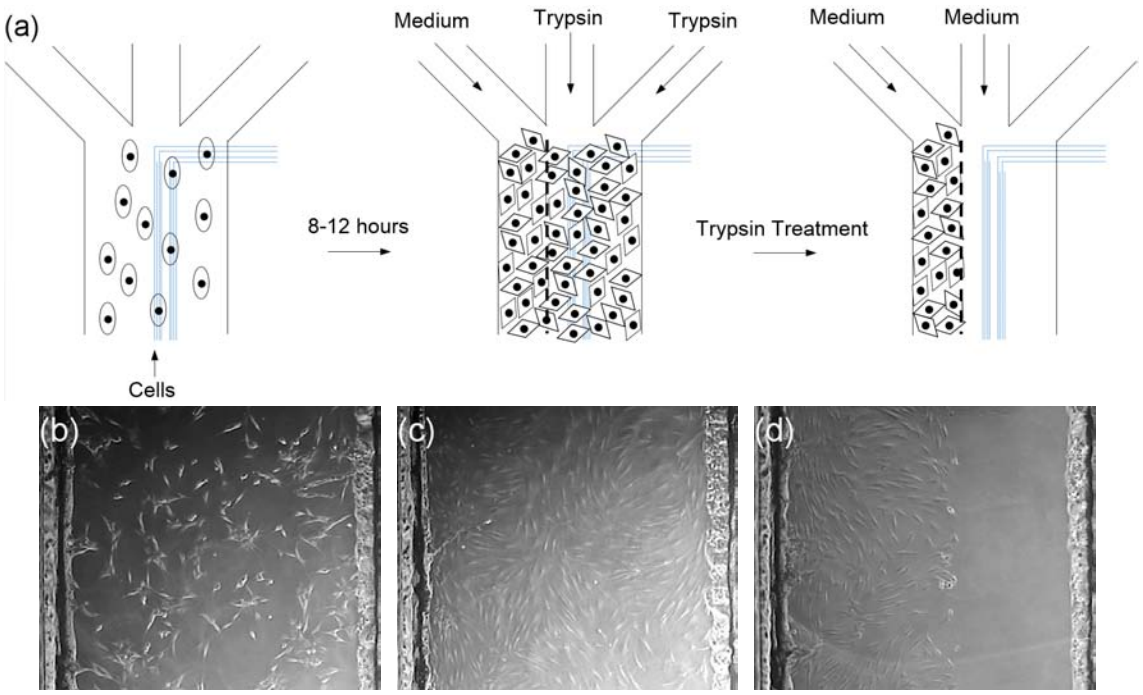

Figure 8.3: Patterning processes to create wound edges for the confluent monolayer of cells in microchannel. (a) Schematic illustration of experimental processes, modified from [84]. (b) Five hours post seeding, (c) confluent cell monolayer, and (c) the formed wound edge after treatment with trypsin-EDTA. Channel width is 1 mm.

patterning procedure is illustrated in Figure 8.3, together with phase contrast microscopy images of the main channel of the device at different steps in the process.

For these preliminary experiments, human foreskin fibroblast cells were employed, and the changes in the distribution of cells in the main channel before and after partial digestion of the cell monolayer was evident. We have examined the cell viability of other established cell lines (HeLa, HT1080, and HUVEC) and primary dendritic cells in the microdevice for potential application in the future. The establishment of a wound edge by selective digestion of the cell monolayer has previously been reported [84, 85].

Following wound edge formation, random cell migration was allowed to proceed in the microchannel for several days, and the fibroblast cells were observed to migrate across the wound edge toward the cell denuded areas (Figure 8.4). Human foreskin fibroblast cells are quite immobile, hence not an ideal choice for cell migration studies, however, the cells are very robust and easy to handle for preliminary experiments. Figure 8.4(b) and (c) display phase contrast microscopy images captured 17 and 41 hours after partial digestion of cell monolayer, respectively. After two days, a noticeable random cell migration across the wound edge was observed and the distribution of cells appeared more evenly in the microfluidic channel.

Based on these preliminary findings, the microelectrode design was optimized, allowing for impedimetric detection of cell migration. Figures 8.5(a) and (b) display phase contrast microscopy images of the main channel in the microfluidic device before and immediately after selective digestion of the cell monolayer, featuring two pairs of conductive polymer microelectrodes for electrical detection of cell migration. For these preliminary experiments, impedance measurements were performed using only one pair of microelectrodes. Cell migration was then allowed to proceed for several hours, monitored by video time lapse microscopy and electrochemical impedance spectroscopy.

Time lapse films illustrated the motility of human foreskin fibroblast cells in the microfluidic channel of the chip, and snapshots captured at different time points (several hours into the experiment) during an assay are shown in Figures 8.5(c)-(f). The change in absolute impedance in response to cell migration is depicted in Figure 8.6. Preliminary results indicate that cells migrate across the wound edge toward cell denuded areas, reaching the first pair of conductive polymer microelectrodes after a couple of hours (the time scale is cell type dependent). This is reflected by a drastic rise in the impedance at 2 -8 hours, because healthy cells act as an insulating layer on the electrode surface [45] by blocking the diffusion of ions to the electrodes. Subsequently, the absolute impedance arrives at a plateau, indicating that the electrode is completely covered with a monolayer of cells. These findings correlate with previously published data [45, 46].

The next step is to measure the impedance on both electrode pairs in parallel to quantify the cell migration, and to direct the cell migration by establishing a two dimensional chemotactic gradient in the main channel of the chip. Based on our findings, we will re-evaluate the design of the microelectrodes and microfluidic channels, and eventually continue directional cell migration studies with another cell type.

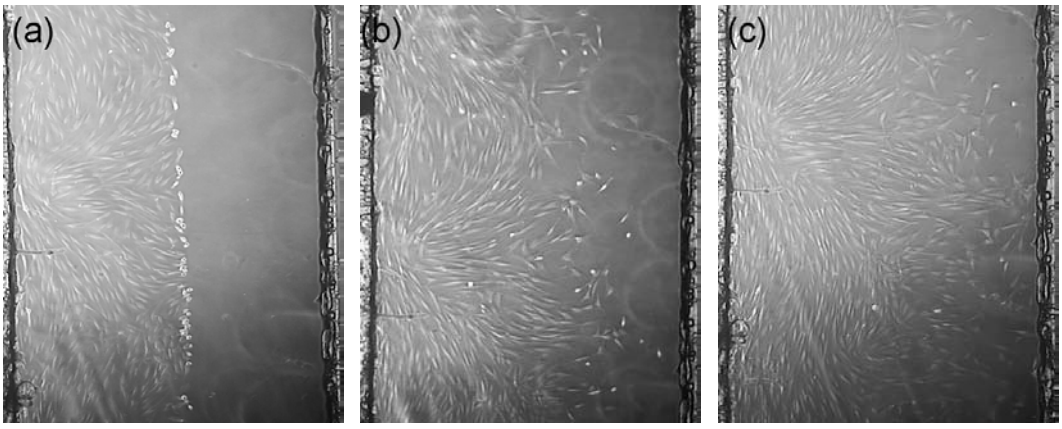

Figure 8.4: Phase contrast microscopy images captured (a) immediately after selective digestion of cell monolayer, (b) 17 hours and (c) 41 hours after after wound edge formation. Cells migrate across the wound edge towards cell denuded areas (from left to right).

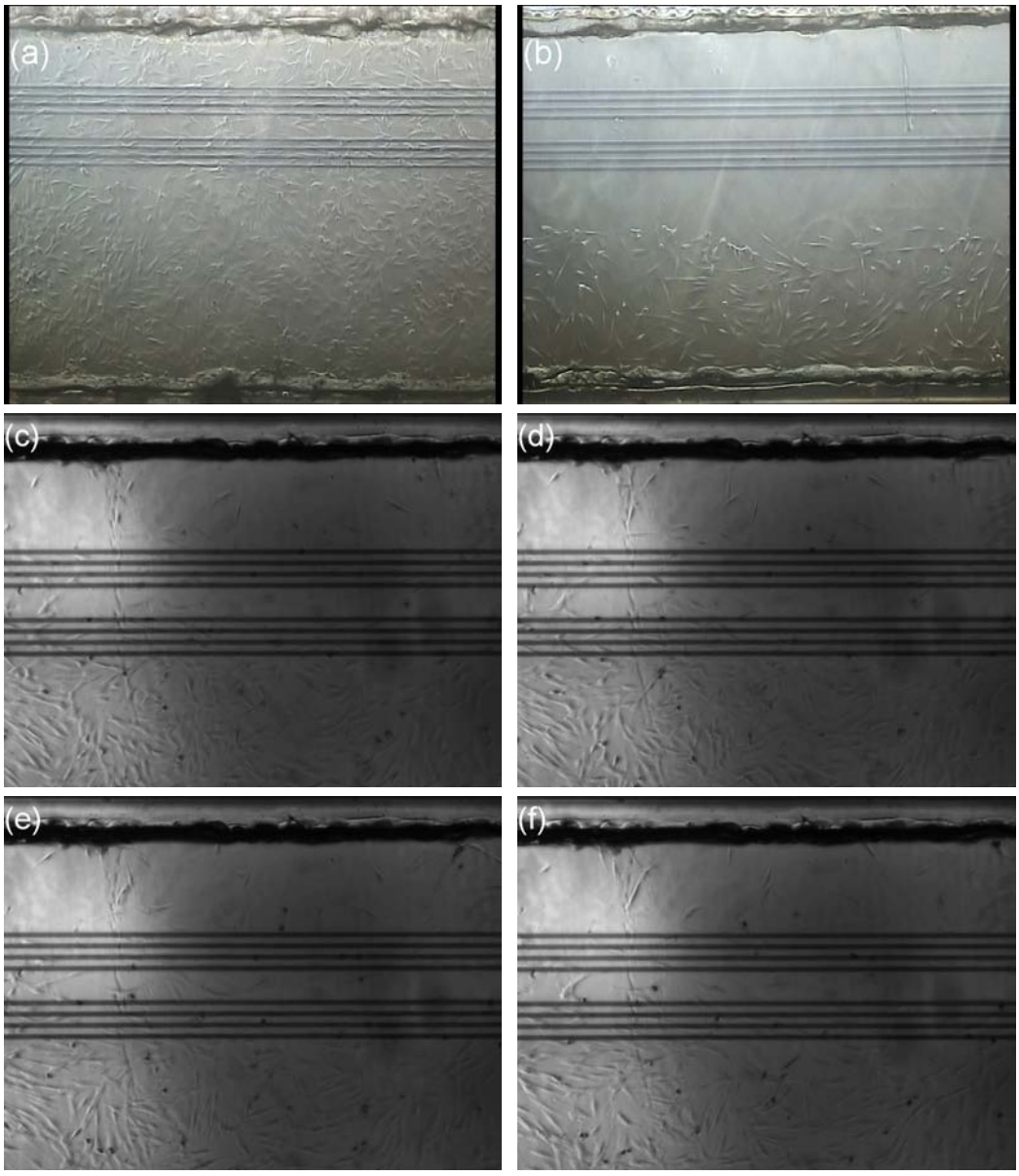

Figure 8.5: Preliminary result. Cell migration in main channel of microdevice; (a) phase contrast microscopy image before selective digestion, (b) phase contrast microscopy image immediately after selective digestion, and (c)-(f) phase contrast microscopy snapshots of motile human foreskin fibroblast cells in the microfluidic channel of the chip. Cells migrate towards the conductive polymer microelectrodes, and cells in contact with an electrode are detected by electrochemical impedance spectroscopy.

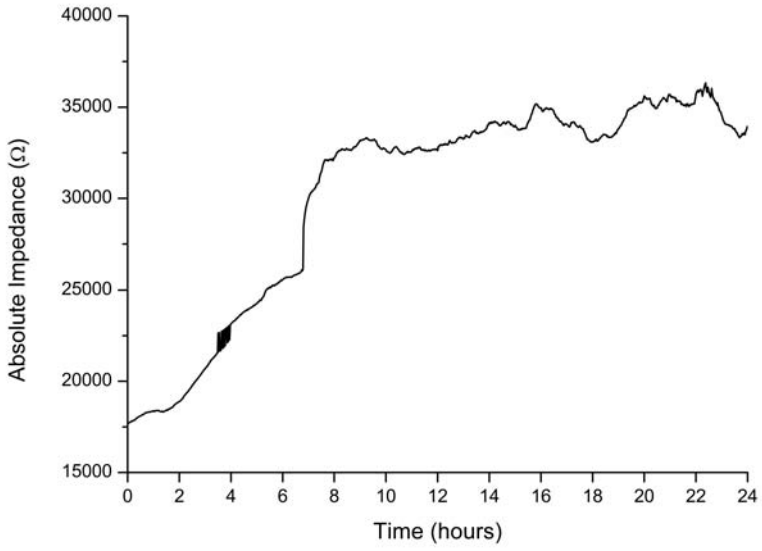

Figure 8.6: Preliminary result. Electrochemical detection of cell migration in microdevice. The absolute impedance was measured at a frequency of 2 Hz and baseline was subtracted.

8.4 Concluding Remarks

In summary, we have developed a prototype of an all polymer microfluidic device for impedimetric cell migration studies of wound healing. The preliminary data suggest that cells migrate across the wound edge towards cell denuded areas. Cell migration was detected by video time lapse microscopy and electrochemical impedance spectroscopy.

In the current experimental setup, cells migrate randomly in the microfluidic channel of the chip. With time, a two dimensional chemotactic or haptotactic gradient should be established in the main channel of the device to enable studies of directional cell migration. It is also essential to measure the impedance on both microelectrode pairs, in order to extract any quantitative data from the experiment. In general, further experimentation is required before any conclusions can be drawn whether or not further device modifications have to be implemented.

The main features of the presented cell migration assay are the easy and delicate handling of cells, combined with visual and electrical detection of migration. Materials were selected with care. To keep the costs and environmental footprint low the entire biosensor was fabricated in plastic; featuring microfluidic channels and an electrode system fabricated from conductive polymers.

Chapter 9

Project Review

The objective of the PhD project was to develop an all plastic biosensor for medical diagnosis of acute viral disease and with potential for miniaturization into a point of care system.

The goal was met and documented in peer reviewed journals. Review, assessments, opportunities for improvement or future work, and general discussions with respect to each of the solutions and the project in general are provided below.

9.1 Aptamer Based Biosenor

A simple, accurate and fast alternative to the commercially available rapid influenza diagnostic tests was developed. In the wake of the 2009 flu pandemic, there has been a strong interest in rapid influenza tests, but these tests are inaccurate and lack sensitivity. Electrochemical impedance spectroscopy is a very sensitive technique for label free biosensing in real time, and the platform is acknowledged for its possibility of miniaturization and use in point of care diagnostic devices.

A plastic microfluidic device, featuring conductive polymer microelectrodes was fabricated by injection molding and out of cleanroom processing techniques. This microelectrode patterning procedure was chosen for economic reasons and agarose stamping is highly suitable for prototyping and low throughput. Since absolute reproducibility of microelectrodes was unattainable, other fabrication methods should be considered for future large scale production of a finalized chip.

High specificity of the polymer biosensor was achieved by functionalization; aptamers with high affinity for influenza virus were covalently linked to the conductive polymer microelectrode surface to selectively fish out virions from an introduced fluid.

The polymer biosensor was exploited for label free, and real time detection of influenza A virus particles. Based on changes in the impedance when virions were captured by

immobilized aptamer probes, clinically relevant concentrations of influenza virus in saliva specimens were directly measured. The disposable microfluidic system is highly sensitive, highly specific, highly stable, and with a very attractive response time of less than fifteen minutes. We used influenza A virus in saliva specimens as an example to demonstrate the usability of the biosensor, and the foundation for a competitive diagnostic tool is at hand. This could become an alternative to current diagnostic techniques.

The biosensing platform was also with success adapted to different tasks and tested against DNA and antibiotics. Throughout the experiments, the sensors demonstrated high sensitivity and were able to detect very low analyte concentrations in both buffered solutions and milk.

Although the biosensor showed promising results, the microdevice could be improved in many aspects: The manufacturing procedure is inappropriate for large scale production, and improved control of the conductive polymer - which is very sensitive to environmental factors - is another necessity for the biosensor to perform well under non laboratory conditions. With improvements, the system has the potential for several marketable applications in health care and other industries.

9.2 Nanowire Based Biosensor

Most recently, we initiated work on conductive polymer nanowires in collaboration with the NaBIS group at DTU Nanotech, employing a novel procedure for fast and cost effective fabrication of nanowires. The goal is to explore the sensitivity of these tiny sensors for impedance based characterization of single cells and detection of single virus particles in body fluids. We are at the stage of learning by doing. So far, we have electrically measured the adhesion of single cells on conductive polymer nanowires in a microdevice. Nanowires could represent a new future in point of care medicine and diagnostics, using minute sample volume and delivering an accurate response within minutes.

9.3 Cell Based Biosensor

An all polymer microfluidic biosensing system for real time detection of acute viral disease in human cell culture was developed. A plastic microfluidic device, featuring conductive polymer microelectrodes was designed and fabricated by injection molding and standard photolitographic processing techniques in cleanroom. This procedure ensured complete reproducibility of all device components, including microelectrodes. During the design process, the cell compatibility of different polymer materials was evaluated by culturing human cells for a full week, and cell viability was also surveyed in microchips. Both separately and united, the materials demonstrated excellent cell compatibility, and human fibroblast cells behaved naturally in the microenvironment for studies of more than a week duration.

The polymer biosensor was exploited for label free and real time electrochemical detection of infectious agents in human cell culture - human fibroblast cells were infected with human cytomegalovirus. Employing electrochemical impedance spectroscopy, we could measure the immediate cell response to virus, and detect an infection within three hours, which are several hours before the cytopathic effect is apparent with conventional imaging techniques. Atomic force microscopy and scanning ion conductance microscopy imaging consolidated the electrochemical measurements by demonstrating early induced changes in cell morphology and apparent programmed cell death.

In conclusion, we developed an impedimetric cell based biosensor for fast and sensitive detection of infectious agents. The sensing platform presents a low cost and competitive alternative to viral culture and other traditional techniques for diagnosis of acute viral disease, and also has the makings of a success in other fields of medicine.

9.4 Cell Migration

Parallel to the main topics of the PhD project, I have been engaged in design and development of microfluidic systems for cell migration studies. This is a fascinating field of research, seeking answers to fundamental questions, as opposed to the more application oriented experimental work associated with biosensors.

The development of new drug therapies relies heavily on cell migration studies *in vitro*. Many years of extensive research has improved the comprehension of immune surveillance and host defence, however there is a shortage of cell migration assays incorporating this knowledge. We developed a novel cell migration assay based on the principles of two conventional systems, yet imitating the natural environment of migrating cells and meeting the requirements for a new transmigration assay.

In another project, we focused on developing a plastic microfluidic system for quantitative and qualitative studies of directional cell migration. Preliminary data indicate that the biosensor - with some adjustments - is operable for visual and electrical detection of cell migration.

9.5 Summary

Plastic sensing platforms for virus detection were developed and evaluated during the PhD project. The microsystems were fabricated solely from polymers, allowing the potential for upscaling for mass production of portable diagnostic point of care devices.

Chapter 10

Conclusion and Perspectives

The presented work demonstrates the development and usability of all polymer microfluidic devices for biosensing applications in medicine and diagnostics. An all polymer microfluidic device formed the basis of the work, and during the project the biosensing unit and microfluidic channel design were continuously modified for improved sensitivity and specificity in accordance with the requirements for specific use.

Different microfluidic sensing platforms for medicine and diagnostics were presented in this thesis. The main focus of the PhD project was development of an impedimetric sensor for diagnosis of acute viral disease, and two sensing platforms have been presented; a cell based biosensor and an aptamer based biosensor. Microfluidic devices for studies of cell migration were developed in parallel projects.

The list below points out the three main results accomplished during this PhD project.

Aptamer based biosensor
Detection of clinically relevant concentrations of influenza virus in saliva within minutes.
Competitive to polymerase chain reaction and immunology based assays.

Cell based biosensor
Identification of virus infection in cell culture within few hours.
Competitive to conventional cell culture.

Cell Migration in Microfluidic Device
Microfluidic device imitating the physiological conditions of cell transmigration.
Competitive to conventional Boyden chamber and shear flow chamber assay.

With some modifications and clinical studies, the diagnostic sensors have the potential to replace conventional assays for virus identification, or be included in the routine screening program in combination with the established assays. Basic research and development of new drug therapies rely heavily on studies of cell migration in *in vitro* systems. The presented devices represent a significant improvement compared to the currently available experimental platforms.

Unlike the traditional diagnostic techniques, simple and disposable impedance based biosensors produce a sensitive and accurate response in minutes rather than hours or days, and the systems have the makings of miniaturization into cheap point of care devices for use in third world countries to identify and diagnose infectious diseases.

In general, electrochemical sensors have played an important role in the move towards simplified testing. The electrical devices are extremely useful for delivering medicinal and diagnostic information in a simple, fast, low cost and accurate fashion.

Bibliography

[1] DM Morens, GK Folkers, and AS Fauci. The challenge of emerging and re-emerging infectious diseases. *Nature*, 430(6996):242–249, 2004.

[2] R Barrett, CW Kuzawa, T McDade, and GJ Armelagos. Emerging and re-emerging infectious diseases: The third epidemiologic transition. *Annual Review of Anthropology*, 27:247–271, 1998.

[3] RA Medina and A Garcia-Sastre. Influenza A viruses: new research developments. *Nature Reviews Microbiology*, 9(8):590–603, 2011.

[4] O Lazcka, FJ Del Campo, and FX Munoz. Pathogen detection: A perspective of traditional methods and biosensors. *Biosensors & Bioelectronics*, 22(7):1205 – 1217, 2007.

[5] J Chen, J Zhang, H Yang, F Fu, and G Chen. A strategy for development of electrochemical DNA biosensor based on site-specific DNA cleavage of restriction endonuclease. *Biosensors & Bioelectronics*, 26(1):144–148, 2010.

[6] E Primiceri, MS Chiriaco, RE Ionescu, E D'Amone, R Cingolani, R Rinaldi, and G Maruccio. Development of EIS cell chips and their application for cell analysis. *Microelectronic Engineering*, 86(4-6):1477–1480, 2009.

[7] MF Diouani, S Helali, I Hafaid, WM Hassen, MA Snoussi, A Ghram, N Jaffrezic-Renault, and A Abdelghani. Miniaturized biosensor for avian influenza virus detection. *Materials Science & Engineering C-Biomimetic and Supramolecular Systems*, 28(5-6, Sp. Iss. SI):580–583, 2008.

[8] M Hnaien, MF Diouani, S Helali, I Hafaid, WM Hassen, NJ Renault, A Ghram, and A Abdelghani. Immobilization of specific antibody on SAM functionalized gold electrode for rabies virus detection by electrochemical impedance spectroscopy. *Biochemical Engineering Journal*, 39(3):443–449, 2008.

[9] JS Daniels and N Pourmand. Label-free impedance biosensors: Opportunities and challenges. *Electroanalysis*, 19(12):1239–1257, 2007.

[10] NS Mathebula, J Pillay, G Toschi, JA Verschoor, and KT Ozoemena. Recognition of anti-mycolic acid antibody at self-assembled mycolic acid antigens on a gold electrode:

a potential impedimetric immunosensing platform for active tuberculosis. *Chemical Communications*, (23):3345–3347, 2009.

[11] TS Hansen, D Selmeczi, and NB Larsen. Fast prototyping of injection molded polymer microfluidic chips. *Journal of Micromechanics and Microengineering*, 20(1), 2010.

[12] TS Hansen, K West, O Hassager, and NB Larsen. Direct fast Patterning of conductive polymers using agarose stamping. *Advanced Materials*, 19(20):3261–3265, 2007.

[13] K Kiilerich-Pedersen, CR Poulsen, T Jain, and N Rozlosnik. Polymer based biosensor for rapid electrochemical detection of virus infection of human cells. *Biosensors & Bioelectronics*, 28(1):386–392, 2011.

[14] N Rozlosnik. New directions in medical biosensors employing poly(3,4-ethylenedioxythiophene) derivative-based electrodes. *Analytical and Bioanalytical Chemistry*, 395(3):637–645, 2009.

[15] H Yamato, M Ohwa, and W Wernet. Stability of polypyrrole and poly(3,4-ethylenedioxythiophene) for Biosensor Application. *Journal of Electroanalytical Chemistry*, 397(1-2):163–170, 1995.

[16] BL Groenendaal, F Jonas, D Freitag, H Pielartzik, and JR Reynolds. Poly(3,4-ethylenedioxythiophene) and its derivatives: Past, present, and future. *Advanced Materials*, 12(7):481–494, 2000.

[17] B Winther-Jensen and K West. Stability of highly conductive poly-3,4-ethylenedioxythiophene. *Reactive & Functional Polymers*, 66(5):479–483, 2006.

[18] B Winther-Jensen, M Forsyth, K West, JW Andreasen, G Wallace, and DR MacFarlane. High current density and drift velocity in templated conducting polymers. *Organic Electronics*, 8(6):796–800, 2007.

[19] M Asplund, T Nyberg, and O Inganas. Electroactive polymers for neural interfaces. *Polymer Chemistry*, 1(9):1374–1391, 2010.

[20] LJ del Valle, D Aradilla, R Oliver, F Sepulcre, A Gamez, E Armelin, C Aleman, and F Estrany. Cellular adhesion and proliferation on poly(3,4-ethylenedioxythiophene): Benefits in the electroactivity of the conducting polymer. *European Polymer Journal*, 43(6):2342–2349, 2007.

[21] LJ del Valle, F Estrany, E Armelin, R Oliver, and C Aleman. Cellular Adhesion, Proliferation and Viability on Conducting Polymer Substrates. *Macromolecular Bioscience*, 8(12):1144–1151, 2008.

[22] SM Richardson-Burns, JL Hendricks, B Foster, LK Povlich, DH Kim, and DC Martin. Polymerization of the conducting polymer poly(3,4-ethylenedioxythiophene) (PEDOT) around living neural cells. *Biomaterials*, 28(8):1539–1552, 2007.

[23] RA Green, NH Lovell, and LA Poole-Warren. Cell attachment functionality of bioactive conducting polymers for neural interfaces. *Biomaterials*, 30(22):3637–3644, AUG 2009.

[24] RA Green, S Baek, LA Poole-Warren, and PJ Martens. Conducting polymer-hydrogels for medical electrode applications. *Science and Technology of Advanced Materials*, 11(1), FEB 2010.

[25] S Sekine, Y Ido, T Miyake, K Nagamine, and M Nishizawa. Conducting Polymer Electrodes Printed on Hydrogel. *Journal of the American Chemical Society*, 132(38):13174–13175, 2010.

[26] K Kiilerich-Pedersen, J Dapra, S Cherre, and N Rozlosnik. High Sensitivity Point-of-Care Device for Direct Virus Diagnostics. *Biosensors & Bioelectronics*, Accepted 2013.

[27] SCB Gopinath. Antiviral aptamers. *Archives of Virology*, 152(12):2137–2157, 2007.

[28] DHJ Bunka and PG Stockley. Aptamers come of age - at last. *Nature Reviews Microbiology*, 4(8):588–596, 2006.

[29] SCB Gopinath, TS Misono, K Kawasaki, T Mizuno, M Imai, T Odagiri, and PKR Kumar. An RNA aptamer that distinguishes between closely related human influenza viruses and inhibits haemagglutinin-mediated membrane fusion. *Journal of General Virology*, 87(Part 3):479–487, 2006.

[30] KB Andersen, NO Christiansen, J Castillo-Leon, N Rozlosnik, and WE Svendsen. Fabrication and Characterization of PEDOT Nanowires Based on Self-Assembled Peptite Nanotube Litography. *Organic Electronics*, Accepted 2013.

[31] F Patolsky, BP Timko, G Yu, Y Fang, AB Greytak, G Zheng, and CM Lieber. Detection, stimulation, and inhibition of neuronal signals with high-density nanowire transistor arrays. *Science*, 313(5790):1100–1104, 2006.

[32] Y Cui, QQ Wei, HK Park, and CM Lieber. Nanowire nanosensors for highly sensitive and selective detection of biological and chemical species. *Science*, 293(5533):1289–1292, 2001.

[33] B Kannan, DE Williams, C Laslau, and J Travas-Sejdic. A highly sensitive, label-free gene sensor based on a single conducting polymer nanowire. *Biosensors & Bioelectronics*, 35(1):258–264, 2012.

[34] A Das, CH Lei, M Elliott, JE Macdonald, and ML Turner. Non-lithographic fabrication of PEDOT nano-wires between fixed Au electrodes. *Organic Electronics*, 7(4):181–187, 2006.

[35] L Yun-Ze, D Jean-Luc, C Zhao-Jia, J Ai-Zi, and G Chang-Zhi. Electrical conductivity and current-voltage characteristics of individual conducting polymer PEDOT nanowires. *Chinese Physics Letters*, 25(9):3474–3477, 2008.

[36] YZ Long, JL Duvail, ZJ Chen, AZ Jin, and CZ Gu. Electrical properties of isolated poly(3,4-ethylenedioxythiophene) nanowires prepared by template synthesis. *Polymers for Advanced Technologies*, 20(6):541–544, 2009.

[37] SN Krylov and NJ Dovichi. Single-cell analysis using capillary electrophoresis: Influence of surface support properties on cell injection into the capillary. *Electrophoresis*, 21(4):767–773, 2000.

[38] SJ Chen and SJ Lillard. Continuous cell introduction for the analysis of individual cells by capillary electrophoresis. *Analytical Chemistry*, 73(1):111–118, 2001.

[39] HM Davey and DB Kell. Flow cytometry and cell sorting of heterogeneous microbial populations: The importance of single-cell analyses. *Microbiological Reviews*, 60(4):641–696, 1996.

[40] I Vermes, C Haanen, and C Reutelingsperger. Flow cytometry of apoptotic cell death. *Journal of Immunological Methods*, 243(1-2):167–190, 2000.

[41] T Cohen-Karni, BP Timko, LE Weiss, and CM Lieber. Flexible electrical recording from cells using nanowire transistor arrays. *Proceedings of the National Academy of Sciences of the United States of America*, 106(18):7309–7313, 2009.

[42] LR Arias, CA Perry, and L Yang. Real-time electrical impedance detection of cellular activities of oral cancer cells. *Biosensors & Bioelectronics*, 25(10):2225 – 2231, 2010.

[43] T Ona and J Shibata. Advanced dynamic monitoring of cellular status using label-free and non-invasive cell-based sensing technology for the prediction of anticancer drug efficacy. *Analytical and Bioanalytical Chemistry*, 398(6):2505–2533, 2010.

[44] K Cheung, S Gawad, and R Renaud. Impedance spectroscopy flow cytometry: On-chip label-free cell differentiation. *Cytometry Part A*, 65A(2):124–132, 2005.

[45] I Giaever and CR Keese. Use of electric-fields to monitor the dynamic aspect of cell behavior in tissue-culture. *IEEE Transactions on Biomedical Engineering*, 33(2):242–247, 1986.

[46] CR Keese and I Giaever. A Biosensor That Monitors Cell Morphology with Electrical Fields. *IEEE Engineering in Medicine and Biology Magazine*, 13(3):402–408, 1994.

[47] MH McCoy and E Wang. Use of electric cell-substrate impedance sensing as a tool for quantifying cytopathic effect in influenza A virus infected MDCK cells in real-time. *Journal of Virological Methods*, 130(1-2):157–161, 2005.

[48] CE Campbell, MM Laane, E Haugarvoll, and I Giaever. Monitoring viral-induced cell death using electric cell-substrate impedance sensing. *Biosensors & Bioelectronics*, 23(4):536–542, 2007.

[49] Writing Committee of the WHO Consultation on Clinical Aspects of Pandemic (H1N1) 2009 Influenza. Clinical aspects of pandemic 2009 influenza a (h1n1) virus infection. *New England Journal of Medicine*, 362(18):1708–1719, 2010.

[50] PJ Gavin and RB Thomson. Review of rapid diagnostic tests for influenza. *Clinical and Applied Immunology Reviews*, 4(3):151 – 172, 2004.

[51] J Daprà, LH Lauridsen, AT Nielsen, and N Rozlosnik. Comparative study on aptamers as recognition elements for antibiotics in a label-free all-polymer biosensor. *Biosensors & Bioelectronics*, 43(0):315–320, 2013.

[52] MA Bangar, DJ Shirale, W Chen, NV Myung, and A Mulchandani. Single Conducting Polymer Nanowire Chemiresistive Label-Free Immunosensor for Cancer Biomarker. *Analytical Chemistry*, 81(6):2168–2175, 2009.

[53] I Lee, X Luo, XT Cui, and M Yun. Highly sensitive single polyaniline nanowire biosensor for the detection of immunoglobulin G and myoglobin. *Biosensors & Bioelectronics*, 26(7):3297–3302, 2011.

[54] X Luo, I Lee, J Huang, M Yun, and XT Cui. Ultrasensitive protein detection using an aptamer-functionalized single polyaniline nanowire. *Chemical Communications*, 47(22):6368–6370, 2011.

[55] Y Chen and Y Luo. Precisely Defined Heterogeneous Conducting Polymer Nanowire Arrays - Fabrication and Chemical Sensing Applications. *Advanced Materials*, 21(20):2040–2044, 2009.

[56] CM Hangarter, SC Hernandez, X He, N Chartuprayoon, YH Choa, and NV Myung. Tuning the gas sensing performance of single PEDOT nanowire devices. *Analyst*, 136(11):2350–2358, 2011.

[57] YZ Long, JL Duvail, MM Li, C Gu, Z Liu, and SP Ringer. Electrical Conductivity Studies on Individual Conjugated Polymer Nanowires: Two-Probe and Four-Probe Results. *Nanoscale Research Letters*, 5(1):237–242, 2010.

[58] JA Arter, DK Taggart, TM McIntire, RM Penner, and GA Weiss. Virus-PEDOT Nanowires for Biosensing. *Nano Letters*, 10(12):4858–4862, 2010.

[59] J Arter, JE Diaz, KC Donavan, T Yuan, RM Penner, and GA Weiss. Virus-Polymer Hybrid Nanowires Tailored to Detect Prostate-Specific Membrane Antigen. *Analytical Chemistry*, 84(6):2776–2783, 2012.

[60] J KB Andersen, Castillo-Leon, T Bakmand, and WE Svendsen. Alignment and Use of Self-Assembled Peptide Nanotubes as Dry-Etching Mask. *Japanese Journal of Applied Physics*, 51(6, Part 2, SI), 2012.

[61] K Fujita and NI Smith. Label-Free Molecular Imaging of Living Cells. *Molecules and Cells*, 26(6):530–535, 2008.

[62] SL Stott, CH Hsu, DI Tsukrov, M Yu, DT Miyamoto, BA Waltman, SM Rothenberg, AM Shah, ME Smas, GK Korir, JFP Floyd, AJ Gilman, JB Lord, D Winokur, S Springer, D Irimia, S Nagrath, LV Sequist, RJ Lee, KJ Isselbacher, S Maheswaran, DA Haber, and M Toner. Isolation of circulating tumor cells using a microvortex-

generating herringbone-chip. *Proceesings of the National Academy of Sciences of the United States of America*, 107(43):18392–18397, 2010.

[63] SA Bustin and R Mueller. Real-time reverse transcription PCR (qRT-PCR) and its potential use in clinical diagnosis. *Clinical Science*, 109(4):365–379, 2005.

[64] RR Kay, P Langridge, D Traynor, and O Hoeller. Changing directions in the study of chemotaxis. *Nature Reviews Molecular Cell Biology*, 9(6):455–463, 2008.

[65] TJ Nowak and AG Handford. *Pathophysiology; Concepts and Applications for Health Care Professionals*, chapter 2. McGraw Hill, 3rd edition, 2004.

[66] EK Frow, J Reckless, and DJ Grainger. Tools for anti-inflammatory drug design: In vitro models of leukocyte migration. *Medicinal Research Reviews*, 24(3):267–298, 2004.

[67] RA Goldsby, TJ Kindt, BA Osborne, and J Kuby. *Immunology*, chapter 12 and 15. Freeman, 5th edition, 2003.

[68] H Umehara and T Imai. Role of fractalkine in leukocyte adhesion and migration and in vascular injury. *Drug News & Perspectives*, 14(8):460–464, 2001.

[69] F Lin and EC Butcher. T cell chemotaxis in a simple microfluidic device. *Lab on a Chip*, 6(11):1462–1469, 2006.

[70] Y Liu, J Sai, A Richmond, and JP Wikswo. Microfluidic switching system for analyzing chemotaxis responses of wortmannin-inhibited HL-60 cells. *Biomedical Microdevices*, 10(4):499–507, 2008.

[71] J Pihl, J Sinclair, M Karlsson, and O Orwar. Microfluidics for cell-based assays. *Materials Today*, 8(12):46 – 51, 2005.

[72] W Georgescu, J Jourquin, L Estrada, ARA Anderson, V Quaranta, and JP Wikswo. Model-controlled hydrodynamic focusing to generate multiple overlapping gradients of surface-immobilized proteins in microfluidic devices. *Lab on a Chip*, 8(2):238–244, 2008.

[73] N Li, A Tourovskaia, and A Folch. Biology on a chip: Microfabrication for studying the behaviour of cultured cells. *Critical Reviews in Biomedical Engineering*, 31:423–488, 2003.

[74] TM Keenan and A Folch. Biomolecular gradients in cell culture systems. *Lab on a Chip*, 8(1):34–57, 2008.

[75] S Boyden. Chemotactic Effect of Mixtures of Antibody and Antigen on Polymorphonuclear Leukocytes. *Journal of Experimental Medicine*, 115(3):453–466, 1962.

[76] S Usami, HH Chen, Y Zhao, S Chien, and R Skalak. Design and Construction of a Linear Shear-Stress Flow Chamber. *Annuals of Biomedical Engineering*, 21(1):77–83, 1993.

[77] Y Sato and DB Rifkin. Inhibition of endothelial-cell movement by pericytes and smooth-muscle cells - activation of a latent transforming growth factor-beta-1-like molecule by plasmin during co-culture. *Journal of Cell Biology*, 109(1):309–315, 1989.

[78] P Chen, X Feng, W Du, and BF Liu. Microfluidic chips for cell sorting. *Frontiers in Bioscience-Landmark*, 13:2464–2483, 2008.

[79] EWK Young and DJ Beebe. Fundamentals of microfluidic cell culture in controlled microenvironments. *Chemical Society Reviews*, 39(3):1036–1048, 2010.

[80] MH Wu, SB Huang, and GB Lee. Microfluidic cell culture systems for drug research. *Lab on a Chip*, 10(8):939–956, 2010.

[81] EWK Young and CA Simmons. Macro- and microscale fluid flow systems for endothelial cell biology. *Lab on a Chip*, 10(2):143–160, 2010.

[82] JH Yeon and JK Park. Microfluidic cell culture systems for cellular analysis. *Biochip Journal*, 1(1):17–27, 2007.

[83] RJ Taylor, D Falconnet, A Niemisto, SA Ramsey, S Prinz, I Shmulevich, T Galitski, and CL Hansen. Dynamic analysis of mapk signaling using a high-throughput microfluidic single-cell imaging platform. *Proceedings of the National Academy of Sciences*, 106(10):3758–3763, 2009.

[84] FQ Nie, M Yamada, J Kobayashi, M Yamato, A Kikuchi, and T Okano. On-chip cell migration assay using microfluidic channels. *Biomaterials*, 28(27):4017 – 4022, 2007.

[85] S Takayama, JC McDonald, E Ostuni, MN Liang, PJA Kenis, RF Ismagilov, and GM Whitesides. Patterning cells and their environments using multiple laminar fluid flows in capillary networks. *Proceedings of the National Academy of Sciences of the United States of America*, 96(10):5545–5548, 1999.